1962

A preliminary study of the effect of heat treatment on the strength and microstructure of a glass-ceramic material

P. D. Ownby
Missouri University of Science and Technology, ownby@mst.edu

A PRELIMINARY STUDY OF THE EFFECT OF HEAT TREATMENT ON THE STRENGTH AND MICROSTRUCTURE OF A GLASS-CERAMIC MATERIAL

by

P. DARRELL OWNBY

A

THESIS

submitted to the faculty of the

SCHOOL OF MINES AND METALLURGY OF THE UNIVERSITY OF MISSOURI

in partial fulfillment of the work required for the

Degree of

MASTER OF SCIENCE IN CERAMIC ENGINEERING

Rolla, Missouri

1962

Approved by

R. E. Moore (Advisor)

E. D. Fisher

J. D. Clegg

R. F. Davidson

ABSTRACT

The strength and microstructure of a glass-ceramic material of the composition 53 percent SiO_2, 19 percent Al_2O_3, 15 percent MgO, and 13 percent Li_2O were studied. Cylindrical specimens of glass were formed and heat-treated to six different temperature levels for various time periods. The method of strength testing used was a diametral compression loading technique.

It was found that the strength of this material increased initially with heat-treatment but then decreased. The strength characteristics of the completely crystallized glass-ceramic material were found to be dependent on the initial nucleation period. Some factors which influenced anomalous crystal growth are described. The relationship of stress and nucleation in this study is discussed. Mechanisms of nucleation and crystallization were observed by transmitted and reflected light microscopy. The phases at various time periods were determined by X-ray diffraction, and the changes in softening characteristics were recorded by means of thermal dilatometer tests.

ACKNOWLEDGMENTS

The author wishes to express his gratitude to his advisors, Dr. Delbert E. Day and Dr. Robert E. Moore, for their support and encouragement, and also to Dr. T. J. Planje and Professor G. E. Lorey for their valuable suggestions

The financial assistance of the Kaiser Aluminum and Chemical Corporation in the form of a fellowship and research fund is also deeply appreciated and gratefully acknowledged.

Finally, thank you my dear wife Nina for your untiring efforts in assisting in the laboratory work, typing the manuscript, drawing the figures, and in giving your continued support and encouragement

TABLE OF CONTENTS

LIST OF FIGURES

Figure Page

LIST OF TABLES

I. INTRODUCTION

When dealing with concepts of the strength of solids, it is apparent that the theoretical limiting strength must be closely identified with the forces necessary to break atomic bonds. Although this bond strength has been calculated to be of the order of 10^6 psi, and experiments on very carefully prepared specimens of glass confirm these calculations, common experience has shown that most samples of solid materials rupture at elastic strains much smaller than the theoretical limit. In many cases the reduced strength of these samples is known to be caused by imperfections within the sample.

Crystals and crystalline materials contain imperfections in the form of dislocations (line defects which form a boundary between slipped and unslipped regions of a crystal, therefore allowing inelastic deformation to occur locally an atomic row at a time while moving through the crystal) internal cavities, grain boundaries, included foreign particles, and surface notches. The important imperfections in glasses and other amorphous solids are cracks or other flaws that grow under the influence of stress and chemical attack, the most important ones from a strength standpoint being those existing in the surface.

A variety of methods have been employed to test the strength of glass including twisting, bending, crushing, and impact. Regardless of the method used, it is well-known that the actual fracture of solids is due to the tensile component of the applied force. Failure in uniform compression is unimaginable.

A bending method is one of the most common used for strength testing of glass rods. In this method the maximum stress occurs on the outside surface of the bending rod. Since the flaws existing in

the surface of a glass sample are of paramount importance to its strength, and bending tests tend to accent the effect of these flaws, this method doesn't seem ideal if effects on strength other than surface flaws are to be studied. This being the purpose of the present study, a technique which allows for a minimum or no tension at the surface of the specimen to be tested seems desirable. A diametral loading technique was chosen which has been demonstrated to be successful in the strength studies of concrete and porcelain cylinders, and seemed to meet the desired requirement of no tension at the surface.

In choosing a glass composition for this study, the following requirements were considered:

1. The need of a glass with a practical melting range and melt viscosity.
2. A glass whose internal structure is changeable, which change must be reasonably controllable and relatively independent of the surface. This change must also be easily observable by available means.
3. A glass which can be formed into cylinders without the occurence of devitrification during the forming process.

The recent work done on controlled nucleation and crystallization of glass-ceramics, i.e., certain glasses containing nucleating agents which could first be formed and cooled as glasses and later crystallized into fine-grained glass-ceramics such as the well-known new product of the Corning Glass Co., Pyroceram, seems to furnish a plentiful number of compositions from which to choose.

The system that was chosen, Li_2O-MgO-Al_2O_3-SiO_2, provides a glass which reportedly could be easily formed and uniformly devitrified by

an internal nucleation process. The particular composition, 53 percent SiO_2, 19 percent Al_2O_3, 15 percent MgO, and 13 percent Li_2O, is of fundamental interest because a glass-in-glass separation can be observed with an ordinary light microscope. The immiscible glass droplets which form in the glass matrix on careful heat-treating form the nuclei for later internal crystallization. Although other glass compositions have been studied which also exhibited this glass-in-glass separation phenomenon, most of them cannot be observed except by electron microscope shadowing techniques.

The purpose of this investigation was, therefore, to compare the degree of heat-treatment of prepared glass cylinders of the desired composition with the strength, the melting range, the phase composition, and the microstructure of the resulting glass-ceramic.

II. REVIEW OF LITERATURE

A. Structure and Strength of Glass

1. Atomic structure of glass

When seeking to understand the factors which control the strength of solids, the binding between atoms and the spatial arrangements of these atoms must be considered.

Most silicates are made up of building blocks of tetrahedra of oxygen atoms centered with a silicon atom. Each of these oxygen atoms shares a partially covalent and relatively strong bond with the enclosed silicon atom. By sharing oxygen atoms, each of the tetrahedra has a strong tendency to join with others setting up an excellent mechanism for building chains of oxygen tetrahedra. The characteristic Si-O-Si angle between tetrahedra differs from 180° in most crystalline silicate minerals and allows ordered and relatively close packing of the individual units. Most of these minerals, however, still show characteristic chains which are oriented in specific crystallographic directions.

In the cooling of a molten silica mass, if insufficient time is allowed or if the chains are insufficiently segmented by other charged ions, which compete for association with oxygen atoms, then arranging the silica chains in a definite pattern may be very difficult as the viscosity rapidly increases. When the melt becomes solid, the same degree of long-range disorder and very short-range order may still exist characterizing a glass.

The relatively low densities of glasses are indicative of the insufficient packing of tetrahedra, and the Si-O-Si angles formed at the junctions of the tetrahedra are very close to 180°, as shown by Warren, Krutter, and Morningstar.[1]

The network structure proposed by Zachariasen,[2] a two-dimensional representation of which is shown in Figure 1(b), illustrates the high degree of long-ranged disorder which may be introduced into a substance that readily forms chains such as has been described. It can be compared to the long-range crystalline structure of (a) of Figure 1. In this illustration the silicon atoms are shown bonded to 3 oxygens. The fourth, being directly above or below the silicon atoms, therefore completing the tetrahedra, is not shown. The network may be modified by alkali and alkaline earth cations which effectively break the Si-O bonds, as shown in Figure 2,[3] resulting in some of the oxygen atoms being referred to as "non-bridging". These "non-bridging" cation-oxygen assemblies are called terminal structures.

It has logically been suggested that the ratio of network structure to terminal structure in a glass might control many of its physical properties, including its strength. (Many properties such as density, refractive index, dispersion, expansion, and heat capacity can be calculated on an additivity basis with some degree of accuracy.[3]) Therefore, since it is apparent that the network structure supplies the major resistance to applied stress and since the Si-O bond is partly covalent, the cohesive energy of this bond would be expected to far outweigh that of the ionic bond of a terminal structure. If the theoretical mechanical strength of fused silica glass is estimated on the basis of stretching an Si-O-Si bond linkage to failure, then following the concept of additivity, it is interesting to consider how this theoretical strength might be altered as terminal structure is added to network structure by the addition of alkalies.

2. Theoretical estimates of bond strength

Approaches utilized by many investigators[4,5,6] for estimating the theoretical strength of solids have begun with the familiar two-atom

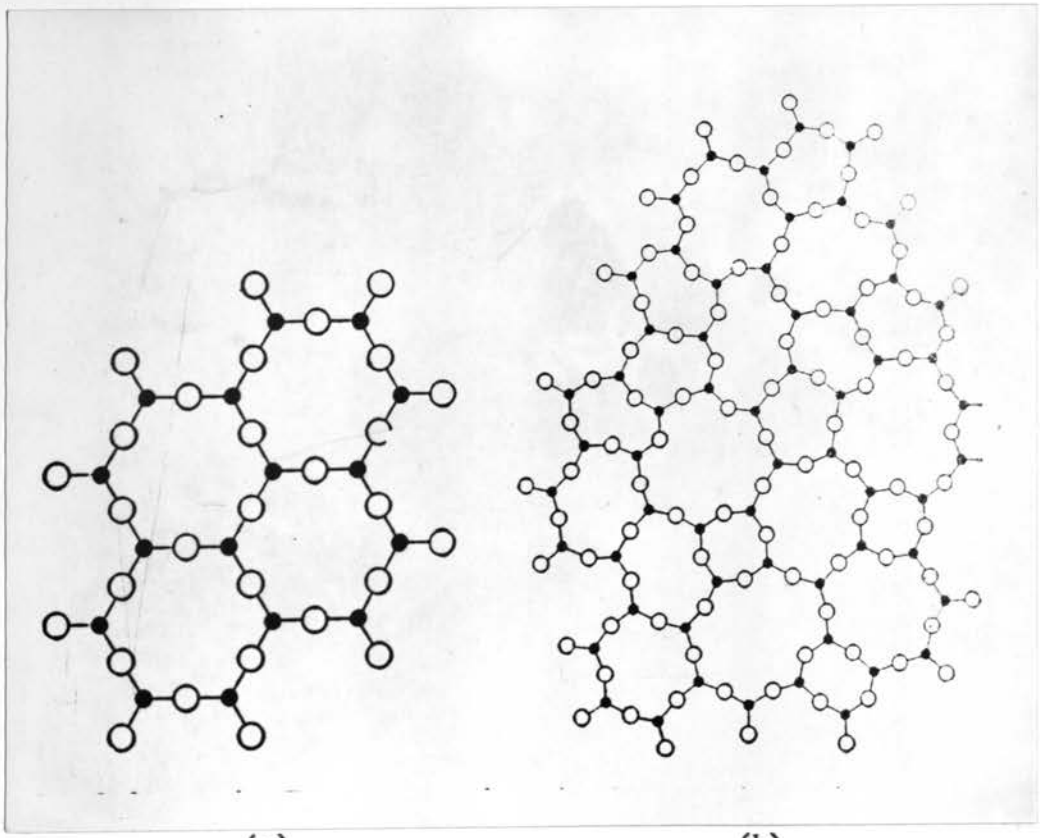

Figure 1. A two-dimensional representation of the structure of (a) a crystal, and (b) a glass as proposed by Zachariasen.[2] (After Morey[3])

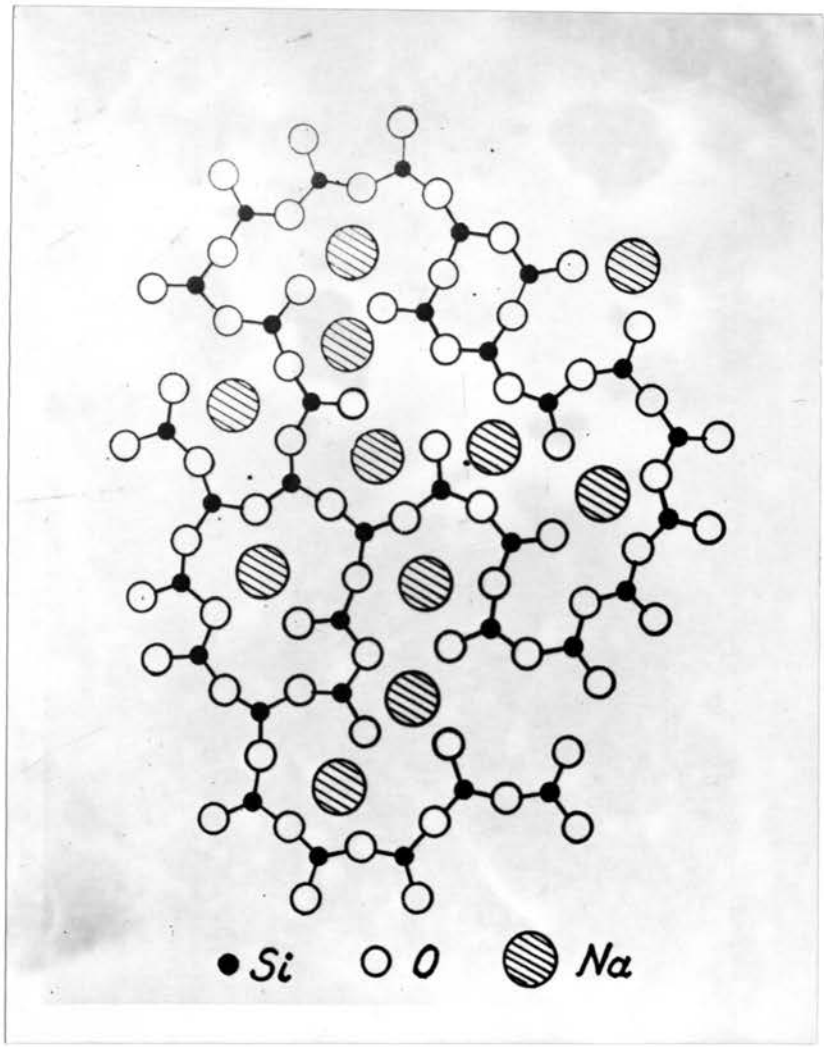

Figure 2. A two-dimensional representation of the structure of soda-silica glass, according to Warren.[1] (After Morey[3])

force-separation diagram shown in Figure 3. A sine function can be used to approximate the initial part of the curve,

$$\sigma = \sigma_{th} \sin \frac{2\pi x}{\lambda} \tag{1}$$

where σ_{th} = the maximum stress required to pull the silicon and oxygen atoms apart,

λ = a separation parameter in the x direction, and

a = the equilibrium separation (Figure 3).

Applying Hooke's law and realizing that for small deformations (as x approaches zero) $\sin\theta \approx \theta$, equation (1) becomes,

$$\sigma = \frac{\sigma_{th} 2\pi x}{\lambda} \qquad \frac{E}{a/x} \tag{2}$$

$$\lambda = \frac{\sigma_{th} 2\pi a}{E} \tag{3}$$

Using equation (1) an energy balance of the separation process may be written realizing that the work of fracture appears as the surface energy 2α of the two newly created surfaces. Thus,

$$2\alpha = \int_0^{\frac{\lambda}{2}} \sigma dx = \frac{\lambda \sigma_{th}}{\pi} \tag{4}$$

Solving for σ_{th},

$$\sigma_{th} = \frac{2\pi\alpha}{\lambda} \tag{5}$$

Substituting in equation (3),

$$(\sigma_{th})^2 = \frac{\alpha E}{a} \tag{6}$$

$$\sigma_{th} = \sqrt{\frac{\alpha E}{a}} \approx 10^6 \text{ psi} \tag{7}$$

It is interesting that a number of investigators have shown fine glass fibers to possess strengths in excess of 10^6 psi[7,8] with Anderegg reporting the highest value of these. He obtained a strength of 3.5 x 10^6 psi on a 4μ diameter fused silica fiber.

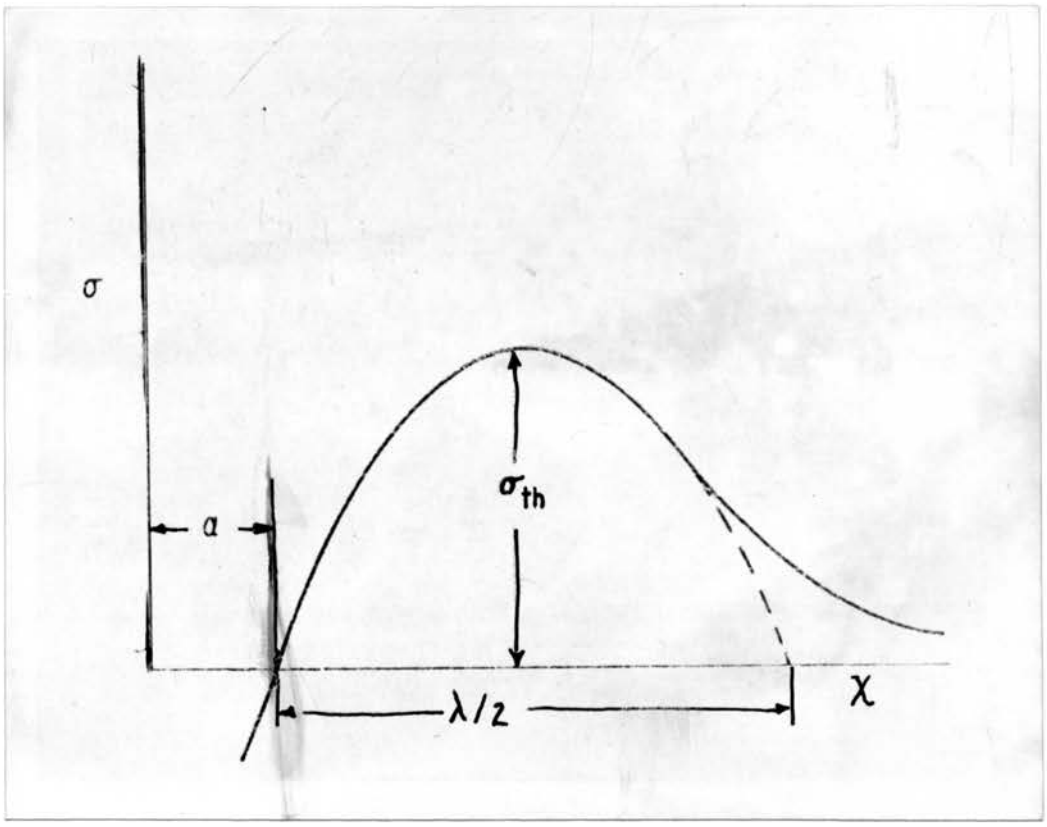

Figure 3. Interatomic force as a function of interatomic spacing.

3. Observed strengths of bulk glass

Common experience regarding glass strength presents a markedly different picture than the foregoing theory and exceptional results just described. In fact, the observation that the normal strength levels of all silicate glasses are approximately equivalent and of very low levels has been the stimulus for numerous investigations of glass strength.

4. Griffith and Inglis theories

A major step in relating practical failure stress to theoretical strength in engineering materials was made by Inglis.[9] He concluded that irregularities or flaws within the bulk or on the surface of specimens acted to concentrate applied stresses to values exceeding the theoretical strength of the material, thus permitting crack propagation.

Griffith[7] extended this theory and proposed his well-known relationship that established the conditions that would lead to the instability of a crack or flaw in an elastic medium. Using Inglis' calculation of the stress distribution around a very flat confocal-orthogonal conic section (elliptical hole) to represent the stress concentration at a crack tip, he obtained the following equation for the highest stress existing at the crack tip:

$$\sigma_m = 2\,\sigma_{av}\sqrt{\frac{c}{\rho}} \tag{8}$$

where $2c$ = the major axis of the crack,

σ_{av} = the tensile stress normal to the crack, and

ρ = the radius of curvature at the crack tip.

The virtual equivalence of the Inglis and Griffith concepts was shown by Orowan[5] when applied to flaws of atomic dimensions.

This stress concentration concept provides a logical reason for the discrepancy between observed and theoretical strengths of materials and

also provides a sound basis for describing the variability of rupture strengths of seemingly identical specimens. Since glasses generally fail by the propagation of cracks from the surface of the specimen, a knowledge of how many and how big the initial flaws have to be in order to result in the levels and variabilities of rupture strengths observed is important. The answer to these questions can only be given in statistical terms based on the assumption that there is an a priori probability of finding a flaw of given severity in each element of the specimen surface. If the probability of finding each kind of flaw in each part of the surface is known, the probable strength of the object can be deduced.

5. Statistical theories of fracture

Statistical theories are based on the weakest link concept of the strength of solids. According to this theory, rupture occurs when a stress sufficient to cause propagation of the largest flaw or crack (the weakest link) is reached. Because this concept is common to all statistical theories, they have a common mathematical basis, which has been summarized by Epstein[10,11] and appears in Appendix A.

6. The glassy microphase theory of glass structure

a. Basic theory. According to Watanabe and Moriya[12] recent electron microscope studies have done a great deal to elucidate the internal structure of glasses. A summary of the conclusions reached follows:

(1) Glass, although seemingly transparent and homogeneous, is, in fact, heterogeneous in the sense of microstructure. A glassy matrix and glassy microstructures which these authors call "glassy-microphases" make up the heterogeneity.

(2) Certain average chemical compositions make up these glass microphases, i.e., in borosilicate glasses, sodium borate and silica-rich phases.

(3) These glassy microphases are not crystalline but amorphous.

(4) These glassy microphases grow with increasing heat-treating time at a constant temperature at a given point within the transformation range.

(5) With different heat-treating temperatures for a constant heat-treating time, they vary in size. Their size is larger in a heat-treated specimen than it is in a quenched specimen.

A schematic representation of these conclusions is shown in Figure 4. It can be seen how the size and shape of the glassy microphases of two different chemical compositions changes with heat-treating time for constant heat-treating temperature. Similarly, if the temperature varies and the heat-treating time is constant, a like pattern results.

This theory seems to be supported in the studies of a number of specific glass compositions related to "glass-ceramics"[13] and will be discussed in detail in part C of this review. It is well to note here that some of these studies make no reference to the work or theories of Moriya or Watanabe, and, therefore, seem to have been done independently. They refer to what has, in this section, been called "glassy-microphases" as "glass-in-glass separation".

In order to substantiate that the leachable spots observed in this study, as well as the silica-rich structure which remains, were not crystalline, X-ray diffraction patterns were run and found to exhibit no definite pattern. In addition, it was pointed out that the crystalline product of devitrification of the W-glass and V-glass used in this study would be α-cristobalite at the temperatures used, and that this crystalline phase gives an entirely different electron micrograph than those obtained by Watanabe, et. al.[14]

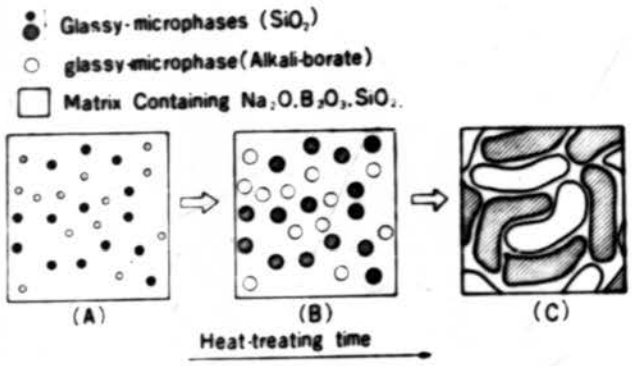

Figure 4. A schematic representation of the change of the internal structure of a glass with heat-treatment.[12] (After Moriya[15])

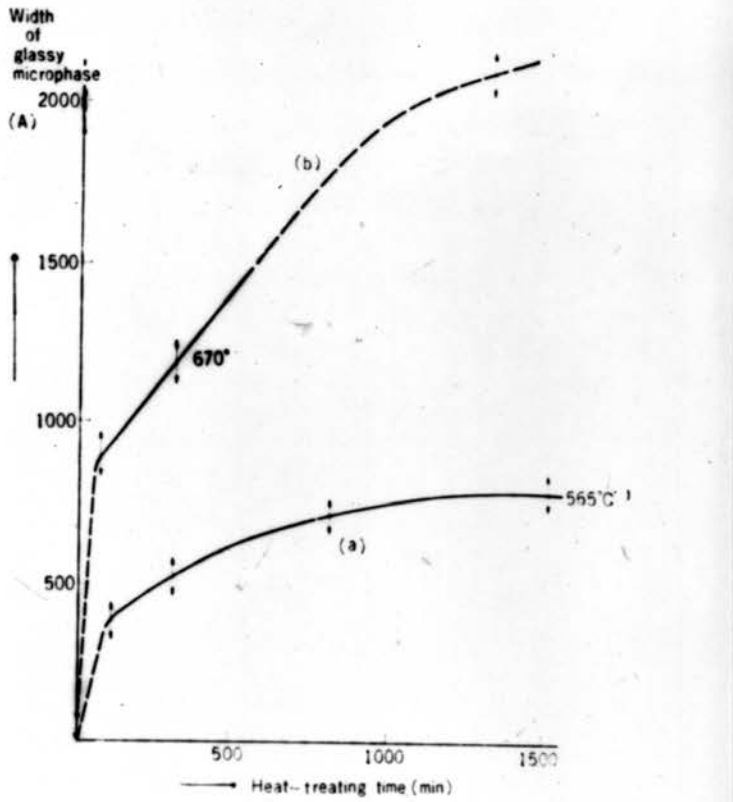

Figure 5. Growth of the "glassy microphase" versus heat-treating time and temperature. (After Watanabe[14])

Watanabe[14] gave Moriya's original theory quantitative expression as shown in Figure 5. This figure shows how the size of the SiO_2 glassy microphases changes with heat-treating time for two different temperatures. The term "width" (Figure 5) stands for the diameter of the spherical glassy microphases when they are isolated from each other (A and B of Figure 4), but for the shorter width of the structures when they grow into non-spherical forms (C of Figure 4), the latter shorter width has the same "width" as an isolated spherical microphase produced under the same heat-treating conditions and, therefore, consistency in definition exists. These authors theorize that although the microphase patterns may not be at all identical to those illustrated in Figure 4, and may differ in size, shape, and chemical composition, glassy microphases exist in every kind of glass.

Even though the specimens used in Watanabe's work were prepared with extreme care[16] so as to avoid any possible damage before their strength was measured, the values of the strength of the unabraded specimens tested in liquid nitrogen were still much lower (150,000 - 180,000 psi) than the theoretical values discussed in A-2 of this section. Deviations from theoretical strength have been attributed to latent Griffith flaws, but the origin of such flaws in virgin specimens which have neither been abraded nor touched is not completely understood. Watanabe and Moriya[12] assume that the latent Griffith flaw is itself the boundary line of the glassy microphases in the glass specimen. This assumption is illustrated in Figure 6 (refer to equation (7) of part A-2 of this section). It can be seen that the size of the glassy microphase in a quenched specimen is small, whereas that in a heat-treated specimen is large. The assumption that there is a weaker boundary layer between a glassy microphase and the matrix that can be considered a latent flaw implies that all specimens

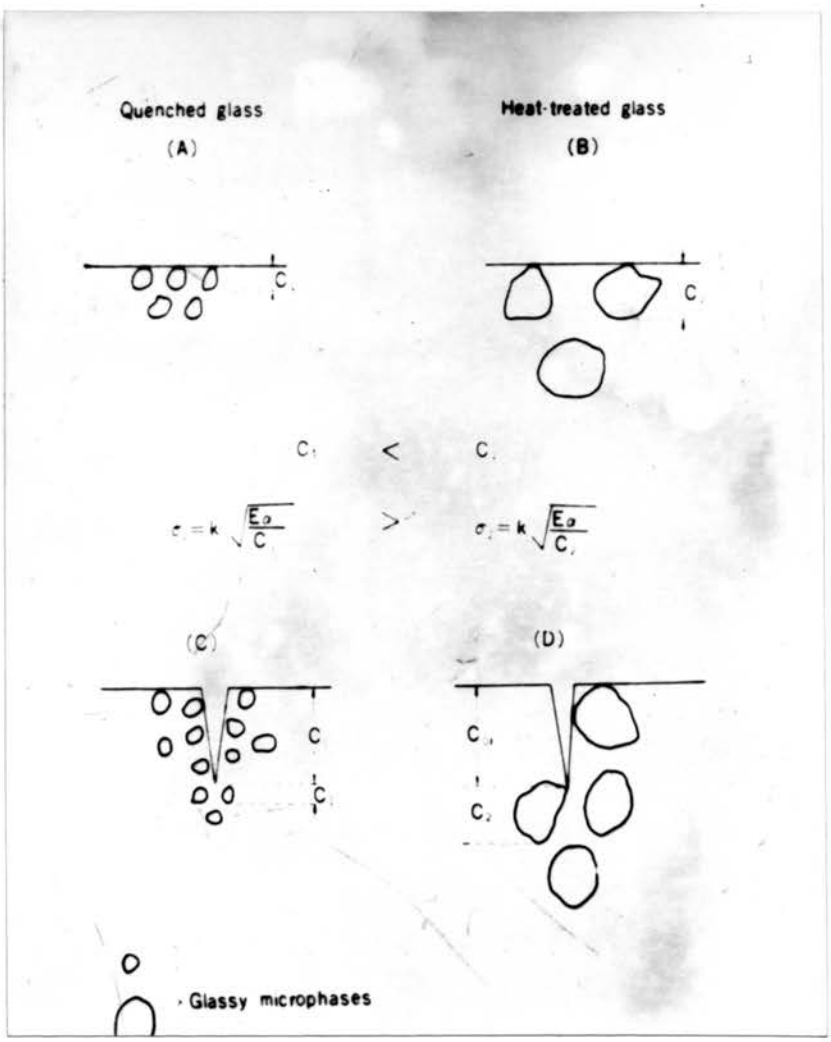

Figure 6. A schematic representation of the effect of "glassy microphase" growth on strength.[12]

σ = theoretical stress
E = Young's modulus
k = constant
α = surface energy
C = "glassy microphase" diameter

(Compare with equation 7)

have latent flaws corresponding in size to C_1 in Figure 6-A, or to C_2 in Figure 6-B. The strength σ of a quenched specimen is greater, therefore, than the strength σ_2 of a heat-treated specimen as can be seen from equation (7) since $C_1<C_2$. Using the experimental data of Spinner and others,[17] as well as their own experimental results, Watanabe and Moriya calculated, from equation (7), the depth of the latent flaws in their unabraded specimens, heat-treated to 500° C for 1 hour, to be 400 Å. The width of the glassy microphase of a specimen heat-treated to 565° C for 1 hour was found by the electron microscope to be 500 Å, which correlates well with the calculated value considering the difference in heat-treating temperatures.

The same thinking can be applied to abraded specimens as shown in C and D of Figure 6. The abrasion depth C_0 is constant in both specimens. Here, $a = C_0 + C_1$ and $C_0 + C_2$ in the quenched and heat-treated specimens, respectively. The strength of the quenched glass would still be greater than the unquenched, but the relative difference would be less than in the unabraded samples.

b. Glassy microphase theory explains fatigue. These authors also supported the glassy microphase theory with experimental evidence and explanations from the theory concerning fatigue phenomena, which is only mentioned here to indicate further support of their theory.

B. Strength Testing Procedures

1. Direct tension method

In applying this method to brittle materials, some means must be used to securely hold the specimen on each end before much tensile stress can be applied. Almost every attempt to use this method has shown the results of local stress concentrations caused by gripping the specimen. Statistically, the points of fracture on a number of bars of uniform size

throughout their length should be distributed evenly along the bar lengths between the grips. In practice, the majority of the fractures occur near the grips. Because of this, the direct tension method hasn't been the most successful strength testing method and wasn't used in this study.

2. Bending method

A three or four point loading technique of bending cylindrical bars to failure is probably the most common method of strength testing glass and ceramic materials. In the three-point loading technique the maximum stress occurs on the surface of the specimen just opposite the point of the applied load. Since the largest flaw (weakest link) is not always right at this point, the fracture locations are merely grouped around this point, most of them being at least some distance removed. The outer stresses fall off linearly with the distance from the central load point to the end of the test bar and, therefore, each test value should be corrected according to the distance the break occurs from point of maximum stress. Another important disadvantage of the use of this method for this study is the emphasis it gives to the surface flaws, whereas in this study the effect of the internal flaws and structure are those to be studied.

3. Diametral loading method

This method is a relatively new one although the stress patterns of diametrally loaded discs have been studied classically by photoelastic means[18] (see Figure 7). It has just recently been used as a strength testing method for use on concrete,[19] porcelain whiteware bodies,[20] and glass.[21] The method involves diametrally loading a relatively short cylinder with the compressive load applied along two opposite generators. The test is carried out in a compression testing machine with strips of a cushioning material normally being placed between the specimen and the

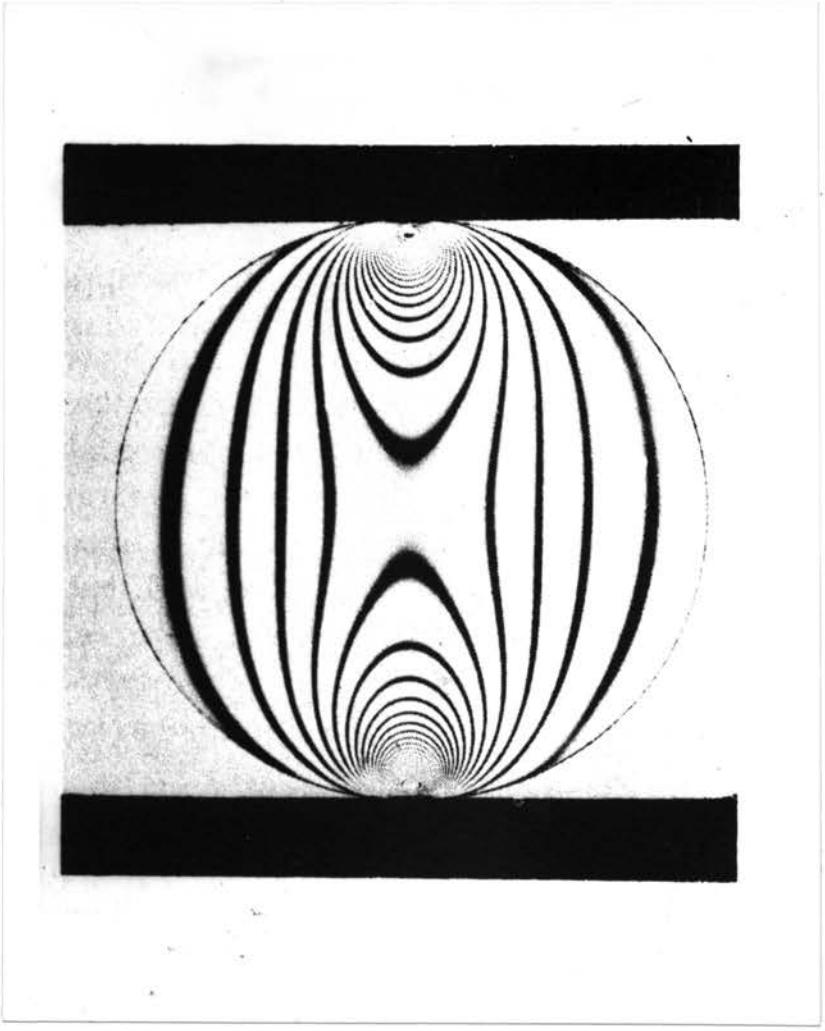

Figure 7. Circular disc under diametral thrust.

Material of model - C.R. 39
Fringe value of material - 100 lb./sq. in. per fringe per inch thickness. (Stress difference)
Dimensions of model - 1.5 in. diam., 3/8-in. thick
Fringe value of model - $\frac{800}{3}$ lb./sq. in. per fringe
Load - 260 lb. applied through flat plates.

Photograph taken by mercury green light with Nicols parallel and quarter-wave plates crossed.

platens of the machine. A uniform tensile stress is set up over the diametral plane containing the applied load at which plane fracture occurs. Materials which behave very nearly elastically to the point of fracture (brittle materials) are the only ones suited to this method. The diametral loading technique was chosen for this study since many disadvantages of other methods did not apply to this one, and in this method the maximum tension occurs internally rather than externally. Particular interest is stimulated in this technique since the application of this method to ceramics was pioneered here in the Missouri School of Mines Ceramic Department.[20]

F. Carneiro[22] introduced the diametral loading method as a strength testing technique in Brazil in 1947. In 1955 Wright[19] used the technique in testing concrete cylinders. He published his results with a review of the theory and a comparison with other strength tests. He studied the effects of the type and dimensions of the cushioning material (called the loading strip) and effects of specimen dimensions. His summary of the theory is given in Appendix B. The resulting equation for the horizontal tensile stress is seen to be,

$$\sigma = \frac{2P}{\pi DL} \tag{9}$$

where P = the applied load,

D = the specimen diameter, and

L = the specimen length.

The practical strength test as is used deviates somewhat from the ideal case considered by the theory. These deviations, as given by Wright, follow:

(a) All real materials deviate somewhat from the idealized homogeneous material assumed in the theory; however, even on concrete Wright

suggests that the stress distribution is changed but little. This can also be assumed for the more nearly homogeneous glass and ceramic body.

(b) Real materials also deviate from Hooke's law which was assumed to hold in the theory, but, as in the above, for this study proportionality of stress and strain can be assumed to a very good approximation.

(c) The theory assumes a state of plane stress which is approximated in loading a thin disc, but when loading a long cylinder, a state of plane strain is more nearly the case. The theory has not yet been developed for plane strain conditions.

(d) The load, rather than being distributed over a line loading along a generator of a cylinder (corresponding to a point load on a thin disc) is distributed over a band, the width of which is equal to the width of the loading strip in contact with the cylinder. If the load is assumed to be uniformly distributed over this width, it can be shown that if this width is less than $\frac{d}{10}$, the stresses on the vertical diameter approximate the following values with sufficient accuracy:

$$\text{Vertically} \qquad \sigma_r = \frac{2P}{\pi DL}\left[\frac{d}{2a}(\alpha + \sin\alpha) + \frac{d}{d-r} - 1\right] \tag{10}$$

$$\text{Horizontally} \qquad \sigma_\theta = \frac{2P}{\pi DL}\left[1 - \frac{d}{2a}(\alpha - \sin\alpha)\right] \tag{11}$$

(See Figure 8.)

The effect of this load distribution is shown in Figure 9. It can be seen that the tensile stress is nearly constant over three-quarters of the vertical plane, but reverses to a high compressive stress at each end. Although the maximum compressive stress is about 18 times the maximum tensile stress, failure always occurs in tension.

Kenny[21,23] studied the elastic energy stored in glass cylinders by crushing them along a diametral plane by slow compression in a hydraulic press. Although he was apparently unfamiliar with the diametral loading

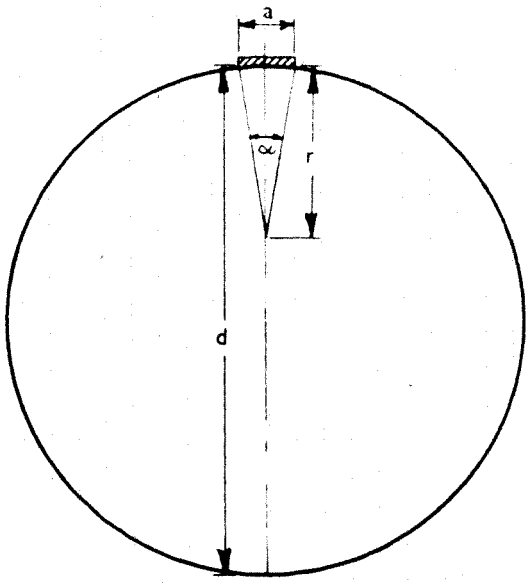

Figure 8. Concentrated force replaced by a force distributed over width a, after Wright.[19]

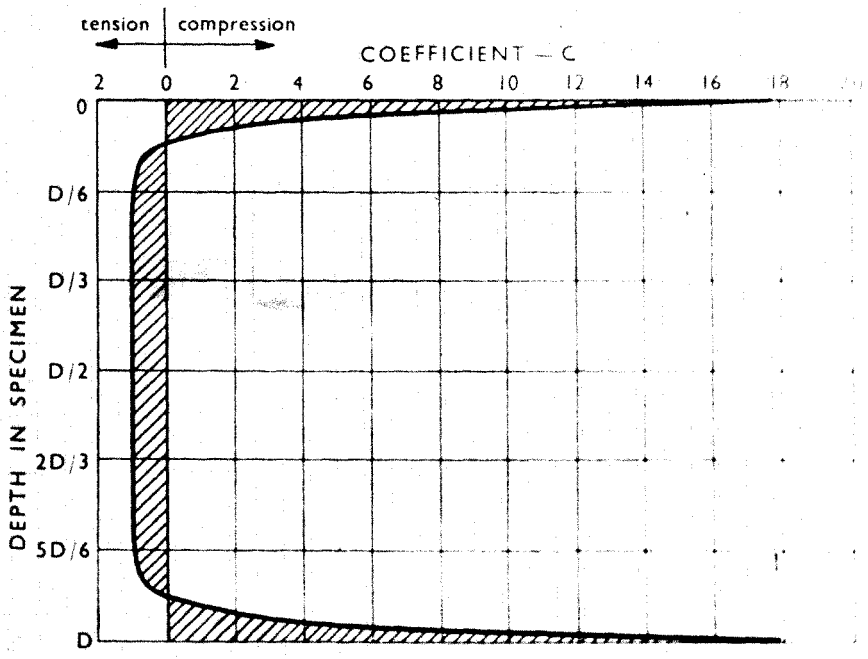

Figure 9. Stress distribution in-cylinder loaded over a width $\frac{D}{12}$. Horizontal stress component $\sigma = \frac{2P}{\pi DL} \times C$.

technique for strength testing as previously described, his results have proven valuable and will be correlated with this study.

He used Pyrex brand glass fabricated into small cylinders by the J. R. Kilburn Glass Co. of Chartly, Mass. The cylinders were of two sizes - 0.5-inch high by 0.5-inch in diameter, and 0.355-inch high by 0.365-inch in diameter. The flat surfaces were finely ground and the round surfaces were fire polished. Annealing was accomplished to the point of showing no strains under polarized light. The jaws of Kenny's loading press were described as being made of "tool steel hardened to maximum hardness and finally ground smooth".[21] His loading procedure was slow, usually taking 2 to 5 minutes from start of loading until fracture occurred.

Products of crushing ranged from large fragments to powder. Kenny[23] observed that the first step in the slow compression crushing process was the splitting of the specimen parallel to the applied load direction and that "these large fragments were always from portions of the specimen outside the region having the highest strain energy content prior to fracture, that is, outside the regions of jaw contact".[21] It is interesting to compare this observation with those of Moore[20] in Figure 10.

> Moore explains that "the secondary fracture shown ... results from the compression of the two halves of the specimen as the initial strain is released upon primary fracture. In diametral loading tests of very weak, brittle materials, the low strains at fracture do not result in a secondary break of this type. For example, in the testing of highly porous, unfired porcelains, no secondary fracture occurred. At the other extreme, for very strong porcelains, fracture under diametral load results in explosive breaks with loss of the specimen."[21]
>
> Kenny observed, "Preliminary crushing experiments showed that a failure of a compressed glass specimen occurred suddenly with a loud report. The initiation of failure in most cases corresponded to an immediate and almost completely disintegration of the specimen to a fine powder. It was believed that the use of the rather uniformly distributed strain energy occurring from

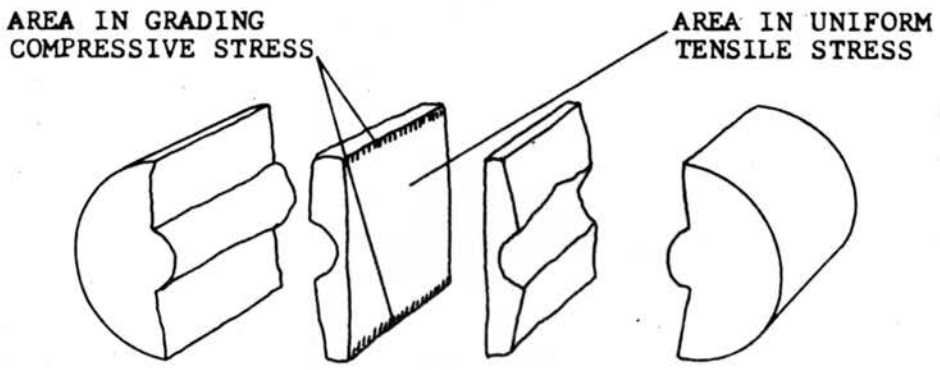

EXPANDED VIEW OF FRACTURED
CYLINDER OF PORCELAIN

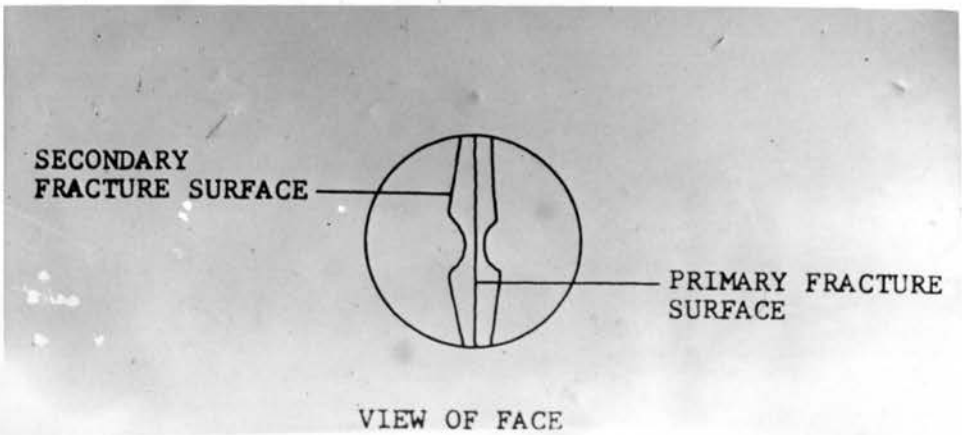

VIEW OF FACE

Figure 10. Characteristic fractures occurring in cylinders diametrally loaded to failure, after Moore.[20]

> the first cracks would cause tension and compression waves, which by reflection from surfaces and by interactions would initiate new fractures at other positions in the specimen. These new fractures would, in turn, release new waves and so lead to a multiplication process of rapidly successive fractures similar to a chain reaction."[23]

It should be noted that the following differences existed between Moore's and Kenny's work in this respect:

(a) Since Kenny's work dealt with surface energy of the powder and fragments resulting in crushing, he employed a retainer around the specimen to be crushed and, therefore, kept all of the products regardless of the explosive nature of the fracture, whereas Moore did not, resulting in "loss of the specimen".

(b) Moore used loading strips which tended to keep the fragments intact more, by distributing the compressive load, while Kenny did not. Kenny's samples, therefore, broke up more in the region of contact with the hard platens.

(c) Generally, the tensile stresses (psi) attained by Kenny were higher than those of Moore's by virtue of the difference in modulus of rupture between Pyrex glass and porcelain. This accounts for the large fragments obtained by Moore as he explained in the foregoing quotation.

C. Glass-Ceramics

1. Definition

Since the coining of the term "glass-ceramics" by Stookey[24] which refers to materials which have been melted and fabricated as glasses and then converted into an essentially crystalline body by special heat-treatment, this term has become widely accepted in the literature.[13,24,25] Glass-ceramics must contain nucleating agents, uniformly distributed throughout the body, which can be converted into tiny crystallites by heat, X-radiation, or ultra-violet radiation. At temperatures in the nucleating range billions of nuclei per cubic centimeter will form and

grow to tiny crystals, even though no perceptible crystallization seems to have taken place. When the temperature is then raised to a higher value the glassy body crystallizes around the nucleating crystals. In some instances, the nucleating process is accomplished by exposing the glass body to X-rays or ultra-violet rays, followed by heat-treatment.

2. History

The first attempt to alter a true glass to an almost completely crystalline object appears to have been made by M. Reaumur, a French chemist about 1735.[26] By packing glass bottles in a mixture of sand and gypsum, and heating them in a potter's kiln at "red heat" for several days, he obtained a "porcelain" article which was completely crystallized and would stand high temperatures without deforming. He described the crystals as being needles which extended inwardly from the surface and met in the center of the glass wall.

A number of researchers in various countries have been reported to have melted and cast mixtures of silicates and fluorides, or natural minerals like basalt, that crystallize during cooling.[27] Historically, these materials have found only very limited usage due to the difficulties involved in forming them into usable objects and of controlling the nucleation and crystallization processes. The recent discovery of glass-ceramics, as defined, that can be crystallized into fine-grained, useful ceramics with desirable properties has stimulated a great deal of research interest in nucleation and crystallization fundamentals and applications.[24] In theory, at least, ceramics can now be produced with an almost ideal polycrystalline structure, and which are fine grained, uniform in size, and randomly oriented, free from pores and many imperfections. Also, new combinations of crystal composition and microstructure with new and useful properties are possible.

3. Manufacturing process affects properties

From a given batch formula of various oxides it is possible, in many cases, to make a glass, a glass-ceramic, or a sintered ceramic, all with the same chemical composition.

A glass is easily formed by mixing and melting the batch. The details of these procedures do not greatly affect the glass structure and properties. Its properties depend mainly upon its thermal history, its composition, and the condition of its surface (which is especially important where strength is concerned).

The crystalline phases present in a sintered ceramic partly determine its microstructure and properties as also do a whole collection of factors such as the shape and size of the grains in the starting materials and their chemical and crystalline forms, the degree with which the separate grains react and bond with each other without melting, and the voids and pores which remain and/or might be produced. The sintering process rarely produces articles that make full use of the crystalline state. Not infrequently, voids and imperfections determine the properties such as strength, optical properties, thermal properties, and electrical properties to as large a degree as the crystalline phases present or larger.

The nucleation and crystallization of glass process is a third way of using the same batch composition, and appears to be the most practical way to mass-produce products approaching the ideal polycrystalline structure. Although it cannot be applied to all ceramic compositions and has new problems of its own, the horizons it reveals to the ceramic industry look very promising.

4. Advantages of glass-ceramics

Many advantages of this new process can be listed, including:

(a) There are practically no limitations on the size and shape of

products other than those imposed by normal glassmaking techniques. Already glass-ceramic cookware, laboratory ware, rod and tubing, cylinders, radomes, ball bearings, and glass-ceramic cement used for glass-to-glass and glass-to-metal seals are appearing on the market.[13]

(b) It is possible to produce grain sizes of crystals smaller with this method than by any other (as small as a few angstroms in size). It has been reported that essentially complete crystallization is possible with an average crystal size down to 200 to 300 angstroms.[27] This is one of the most important advantages.

(c) First making the desired article of a homogeneous glass solves the problems of porosity, uniformity of product, and dependence of the microstructure on the early stages of processing and upon the state of the starting materials.

(d) Orientation of crystals in well-nucleated glass-ceramics is completely random except where the internal nucleating agent is less efficient than the surface.

(e) It is not uncommon to discover crystal phases not found in other ceramics, even new and unknown ones, some of them being metastable phases whose nucleation and crystallization rates are faster than those of the equilibrium phases.

(f) A number of glass-ceramics have been developed which are completely transparent, even though they are highly crystalline and contain at least two phases. They owe their transparency to (1) their small crystal size, (2) the absence of light-scattering crystal boundaries, and (3) the absence of bubbles and voids. The refractive indices of the phases present must be closely matched.

(g) Young's moduli for glass-ceramics are distinctly higher than that of a glass of the same compositions.

(h) In glass the coefficients of thermal expansion vary in a regular manner with chemical composition. The major crystalline phase present is the important factor governing thermal expansion coefficients in glass-ceramics and sintered ceramics. An advantage of the small crystals of glass-ceramics is that they make the use of highly anisotropic crystals such as β-eucryptite possible, which in larger grained sintered ceramics cause porosity and weakness.

(i) Since porosity decreases thermal conductivity, a non-porous glass-ceramic would be more conductive than a porous sintered ceramic of the same composition. The thermal conductivity of glass is relatively low and increases slightly with temperature. That of non-porous crystalline sintered ceramics decreases with increasing temperature, while those that have been determined for glass-ceramics are nearly constant with temperature.

(j) Because of the porosity difference again, the chemical durability of non-porous glass-ceramics is better than that of porous sintered ceramics.

5. Strength studies of glass-ceramics

a. Comparison of strengths of glass-ceramics with those of glass and sintered ceramics. It is of interest to look at the effect of grain size on the strength of sintered ceramics and on the strength of glass to come to grips with its two-fold effect on glass-ceramics. From studies of sintered ceramics with grain sizes over 20μ the strength seems to be inversely proportional to the grain size,[28] and presumably independent of surface flaws. Glass, on the other hand, which may be thought of as having zero crystal size, was shown to have intrinsic strength above 10^6 psi, which was calculated to be of the order of atomic bond strengths. Surface flaws, however, reduce the strength of glass to the order of

10^4 psi. Since glass-ceramics essentially bridge the gap between glass and sintered ceramics with respect to grain size, quantitative studies of the effect of grain size should be possible which may lead to ceramics of maximum strength. Generally, the strength of glass-ceramics is higher than sintered ceramics of the same composition.

b. The effect of heat-treatment on the strength of another glass-ceramic material. Watanabe, et. al.,[25] studied the strength of a heterogeneously nucleated glass-ceramic in the system SiO_2-Al_2O_3-Li_2O-K_2O both in the as-formed, glassy state, and after various stages of heat-treatment. These authors had previously done a great deal of work perfecting the techniques and the elaborate equipment for producing glass in its pristine condition and testing its pristine strength.[16,29,30,31,32] This equipment and technique was used in their study of the strength of this glass-ceramic material.

Very briefly, the experimental procedure was as follows:

(1) A 3-lb. batch of the composition 80 percent SiO_2, 4.0 percent Al_2O_3, 12.4 percent Li_2O, 2.5 percent K_2O, .025 percent CeO_2, .015 percent SnO_2, .18 percent AgCl (weight percent) was mixed in a ball mill for 10 hours according to Stookey's Japanese patent.[33]

(2) The batch was melted in preheated fireclay crucibles in a globar furnace at 1450° C for 4 hours.

(3) A continuous drawing machine[19] was used to draw the glass into cane 0.050 to 0.075-inch in diameter. The machine only touched the cane at 3-inch intervals at which intervals the cane was cut into 3-inch lengths and beaded on one end in a gas flame. The beads served to hold the specimens during heat-treatment to avoid deformation.

(4) Heat-treating the specimens was accomplished according to Figure 11. The N series samples were allowed to nucleate for one hour

at 500° C and begin initial growth of the small crystallites which form during the glass-to-ceramic transition for 1 hour at 600° C. The H series were heated at a constant rate to 900° C. At various stages during the treatment, samples were quenched to room temperature as indicated by the arrows pointing down (Figure 11).

(5) Some of the treated specimens were subsequently abraded in a specially designed grit blaster,[29] aged in an H_2O atmosphere for 20 hours,[31] and tested in a universal tester[29,30] while immersed in distilled water. Abrasion was omitted on other specimens. Figure 12 shows the strength results.

The standard deviation of the strength values for the abraded specimens was between 5 and 15 percent of the mean, while that for the unabraded specimens was 15 to 25 percent of that of the mean value.

It can be seen that for this composition, the strength of the completely converted ceramic in the abraded condition was about 27,000 psi, whereas the glassy, as-formed state had a strength of only about 11,000 psi. In the unabraded condition the glassy state strength exceeded 80,000 psi and 38,000 psi after heat-treatment. The heat-treated glass-ceramic is, thus, stronger than the glass after abrasion, but considerably weaker when both are unabraded. Although the strength in the abraded samples decreased slightly upon heating up to the nucleation temperature (600° C), it gradually increased from there to complete crystallization (900° C). The development of optimum mechanical properties was not highly dependent on the detailed heating schedule above the nucleation temperature.

6. Nucleation and crystallization of glass-ceramics

When a new phase forms and grows it is usually thought of as occurring in two steps. First must occur the formation of small, stable nuclei

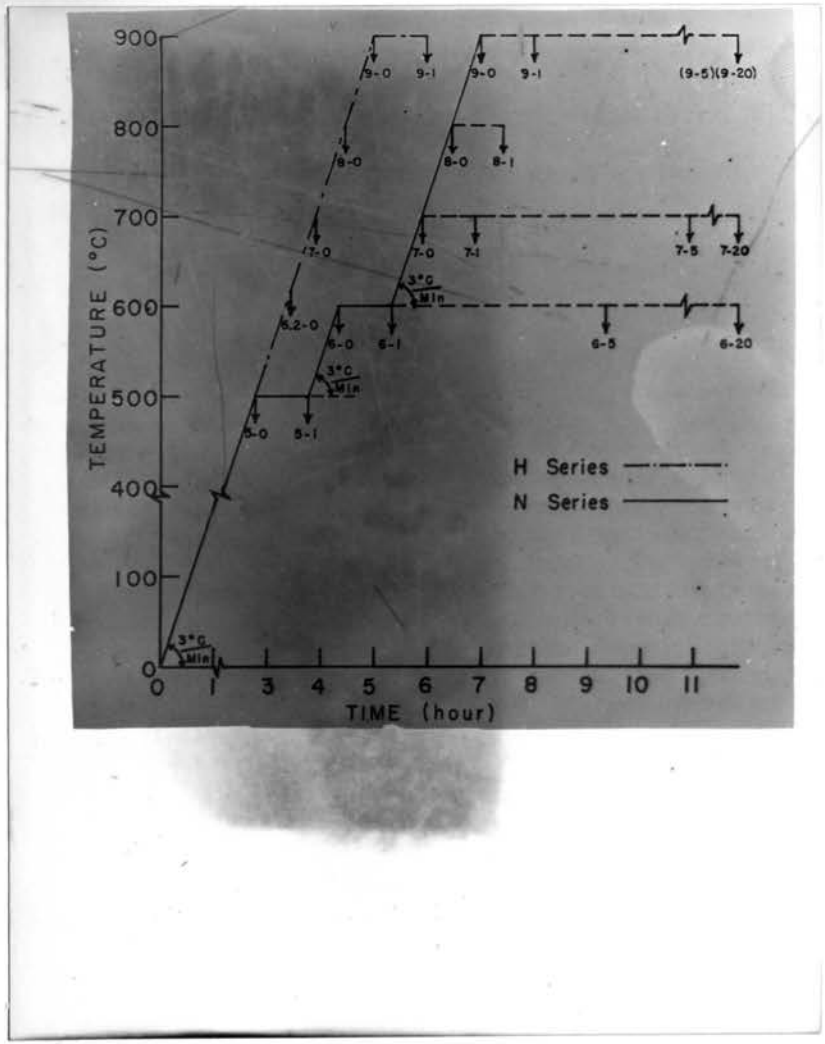

Figure 11. Heat-treatment schedule for glass-ceramic specimens, after Watanabe.[25]

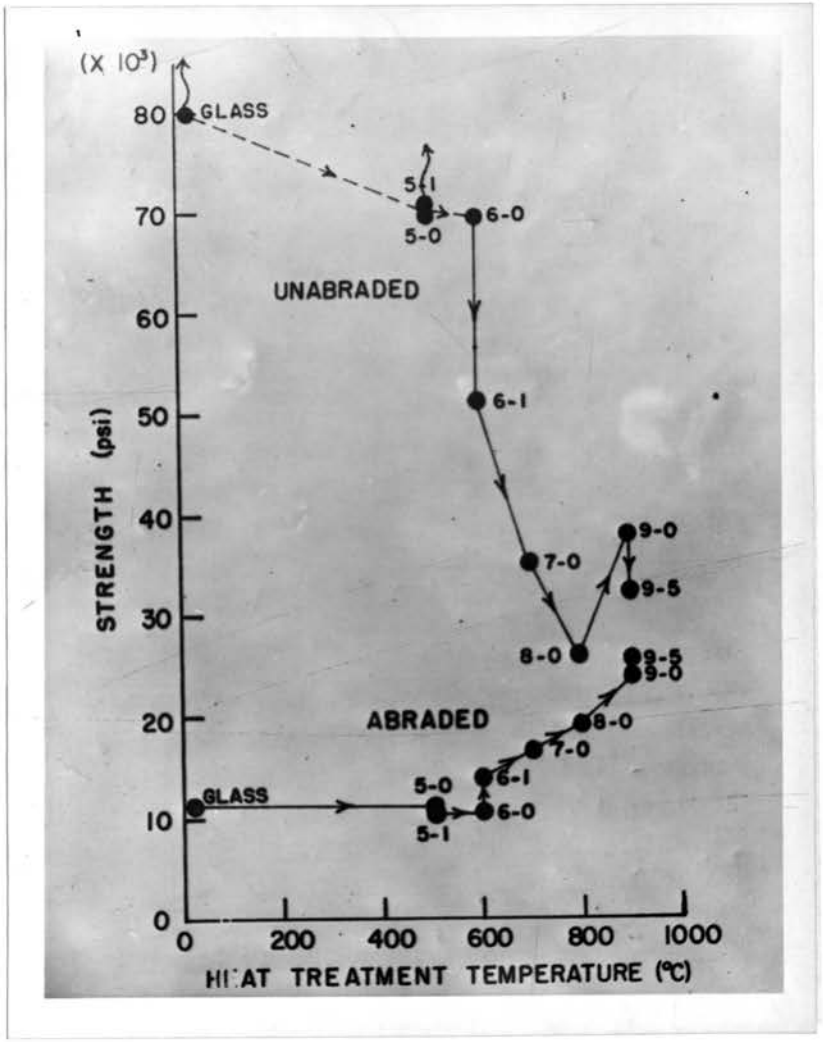

Figure 12. Strength of abraded and unabraded glass-ceramic versus heat-treatment. Tested wet with load duration of 0.820 seconds. (After Watanabe[25])

which must then grow until an equilibrium condition is reached. This equilibrium condition is not always easily reached because either the nucleation process or the growth process acts as the rate controlling step. This is tantamount to saying that either the formation of nuclei or the growth of the nuclei may be so slow that equilibrium is not reached within a reasonable time. For this reason "seeding" melts with nuclei when the nucleation rate is the limiting factor and reheating cooled melts with existing nuclei to allow them to grow more rapidly are both in common practice.

In the glass industry, most of the research efforts have traditionally been directed at preventing nucleation and crystallization (devitrification). This undesirable devitrification was usually surface-nucleated and resulted in a weak, coarse-grained structure. Since the discovery of glass-ceramics a great amount of research effort has been turned on the positive aspects of nucleation and crystallization. Glass-ceramics display an ultrafine grain size and therefore have a high degree of homogeneity. Their formation has been assumed to depend upon nucleating agents or catalysts which are distributed in sufficient concentration and uniformity to produce the fine-grain structure. These nucleating catalysts "dissolve in the melt and precipitate as the glass cools to form nucleation sites for crystallization on subsequent heat-treatment".[34]

Although the theory of nucleation catalysis has been perhaps the most widely recognized, other mechanisms of merit have recently been suggested. One such mechanism is that a "glass-in-glass separation"[35] occurs in the solidified glass melt which initiates crystallization.[35,36,37,38,39] For many years the liquid immiscibility of silicate melts has been recognized. In 1927 Greig[40] made a summary of the immiscibility data that had been obtained to that point. Warren and

Pincus[41] applied the ideas of crystal chemistry to the immiscibility in glass systems and explained it qualitatively and semi-quantitatively on the basis of the effect of various ions on the network structure. Roy[37] called attention to subsolidus nucleation which may be due to liquid immiscibility existing metastably below the solidus line of the phase diagram. The immiscible glass droplets can be formed either during quenching from a melt (Figure 13, composition 1), or after heat-treating a clear glass from room temperature (Figure 13, composition 2), depending on the composition. In reference to these metastable glass droplets Roy explains that,

> "The nucleation of a second liquid phase is in many ways different from the nucleation of a crystalline phase, beyond the obvious distinction of short-range versus long-range order in the nucleus. The composition of such a liquid may be radically different from the crystals one might expect; the rate of nucleation of the liquid nuclei may be very much higher since it could be accomplished by the movement of entire blocs of the same composition rather than the high-activation-energy process of separating out certain cations after breaking many metal-oxygen bonds. Thus, one is provided with a possible method of nucleating and subsequently crystallizing certain glasses at much lower temperatures than might otherwise be possible. For the same reason, a very fine dispersion of the nuclei is not only possible, but likely."[37]

It is noted here that when Roy spoke of "entire blocs of the same composition" he had reference to what has previously been referred to in this thesis as "glassy-microphases", i.e., small units of one type of glass (SiO_2-rich) in a matrix of another glass (richer in modifier cations). Further work in this area has also been done recently by Roy.[42]

Recent experimental evidence in support of this glass-in-glass separation concept has been produced.[39,40] Vogel and Gerth[39] have concluded from their experimental evidence that on cooling a glass melt, clusters of homogeneous ions will aggregate in certain areas. These clusters form in a state intermediate between ideal disorder of the components in the

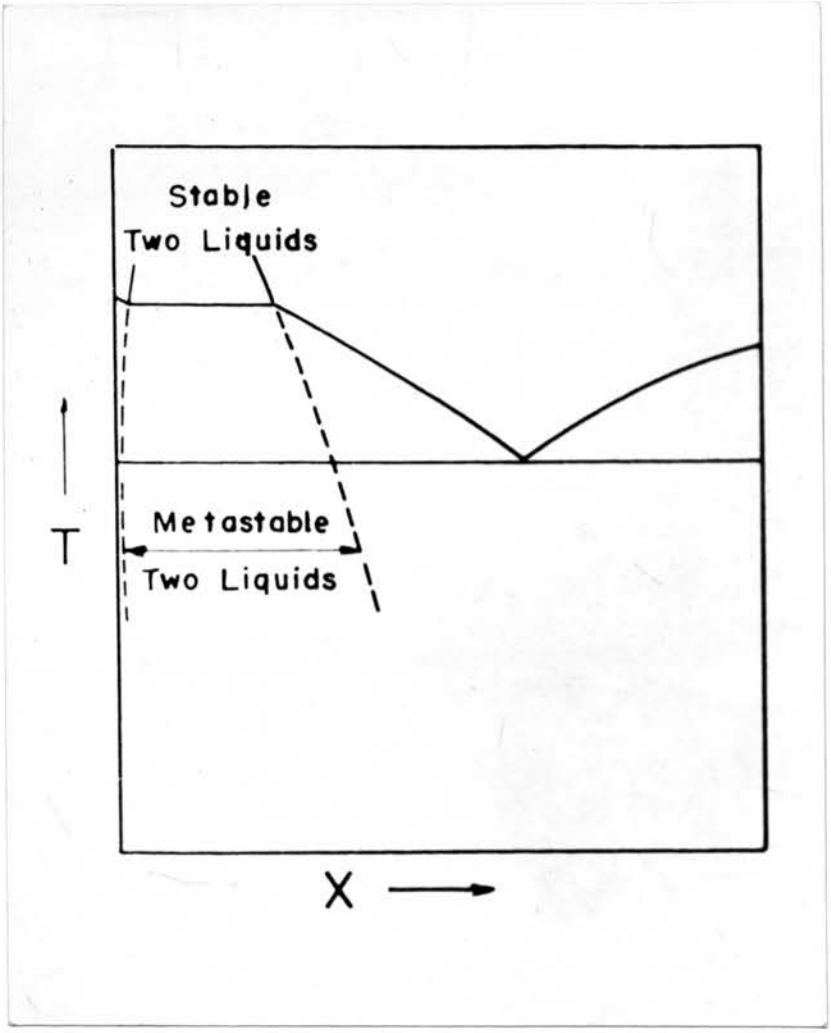

Figure 13. Representation of a simple binary system in which two immiscible glass phases could be separated and exist metastably below the solidus line. (After Roy[37])

melt and ideal order of the crystalline state during the solidification process. The rapid cooling of the melt inhibits the orientation process resulting in this intermediate cluster stage which is a prerequisite for crystallization. They further say that under certain conditions the clusters will come together to form droplets which separate from the matrix glass, forming crystalline-like interfaces. Many electron-microscope pictures of these glassy droplets taken by these authors offer dramatic evidence of their existence. That the formation of these droplets can and must be controlled and is the basic process in any production of glass-ceramics is the summary of these authors.

Ohlberg, et. al.,[35,43] have also made impressive photomicrographs revealing the presence of these immiscible glass droplets. They choose to use the terms "surface nucleation" and "internal nucleation" in order to distinguish the observed phenomena in the devitrification of glasses. They suggest that the more commonly used terms, heterogeneous or homogeneous nucleation can be a source of misunderstanding because it is frequently difficult to establish the presence or absence of foreign nuclei. Surface nucleation means then, merely, that crystallization begins at an external surface, whereas internal nucleation refers to crystallization originating throughout a glass body. This excludes crystallization beginning at bubbles and impurities. Ohlberg, et. al.,[35] showed ample evidence in three different compositions that the glasses were crystallized by virtue of a glass-in-glass droplet separation which internally nucleated them. Their study of a composition in the system $MgO-Al_2O_3-SiO_2-TiO_2$ determined that droplets form spontaneously upon cooling this composition, and reach a 500 Å critical size upon heat-treating, after which a glass-crystal transformation occurred. These crystalline centers formed of the droplets then act as the nucleating agents for the matrix glass. A similar

phenomenon was found in a composition in the Li_2O-CaO-SiO_2-TiO_2 system. Droplets in this composition formed spontaneously to a diameter of 2000-4000 Å. Crystallization at the droplet interface then proceeded inward upon reheating and the crystalline centers then nucleated the matrix.

It can be seen that a wealth of recent evidence has been presented in favor of a glass-in-glass separation mechanism for nucleation of glass-ceramics. Of interest here is the contribution of Turnbull,[44] who has shown that the free energy of nucleation, ΔF, for a liquid-liquid separation is proportional to the cube of the interfacial energy, which is nearly zero for most glasses.

7. Studies on the system SiO_2-MgO-Al_2O_3-Li_2O

The last glass composition to be studied by Ohlberg, et. al., in his previously mentioned paper[35] was the composition 53 percent SiO_2, 19 percent Al_2O_3, 15 percent MgO, and 13 percent Li_2O, by weight. It was because of their paper that this particular composition was chosen for the present study. Glass droplets were not only evidenced in their study, but could be seen with merely a light microscope. Under crossed nicols a thin section of the droplet-laden material appeared as bright, uniform circles against a dark background, with a perfect optic cross in each circle. The size of the droplets ranged from 1 to 30μ, depending on the thermal treatment and slight composition variations. The crystalline phase of the samples was determined by X-ray diffraction to be silica-O[45] when the glass was 58 percent crystalline (after heat-treating for 96 hours at 595° C and 30 minutes at 650° C). On further heat-treatment (650° C for 19 hours) the sample was found to be 85 percent crystalline, the phases being β-spodumene and silica-O. Photomicrographs show that crystallization is initiated at the droplet-matrix interface and then

proceeds inward. Because of this, Ohlberg, et. al.,[35] proposed a new mechanism for spherulite growth, that of radiating inward from the droplet-matrix interface to a common center rather than the conventional theory of radiating outward from single point nucleus. They point out that the glass droplets can easily be distinguished from the crystallized spherulites by the near-perfect shape of the droplet, its lower birefringence, and its lack of radiating structure. As in their studies of other compositions previously mentioned, the crystallized spherulites then served to nucleate and crystallize the matrix glass.

Tashiro, et. al.,[46] studied the effect of a platinum nucleating agent on glasses in the system SiO_2-Al_2O_3-MgO-Li_2O by measuring bending strengths of the nucleated rods. The composition was varied, keeping the Li_2O content at a constant 12 percent in order to obtain glasses with the following properties:

(a) Glass which may be obtained at a melting temperature lower than 1400° C.

(b) Glass which converts into the polycrystalline material without any noticeable deformation during the reheating.

The range in which condition (a) was satisfied was 60-100 percent SiO_2, 0-30 percent MgO; and that of condition (b) was 60-100 percent SiO_2, 0-30 percent Al_2O_3, and 0-20 percent MgO. It is well to note that the composition studies in this thesis meet neither of these requirements since only 53 percent SiO_2 was used.

Sakka, et. al.,[47] studied the effect of heat-treatment on the strength of glass-ceramic materials from the system SiO_2-Al_2O_3-MgO-Li_2O. The composition 62 percent SiO_2, 23 percent Al_2O_3, 15 percent MgO, and 4 percent Li_2O produced the crystalline material with the highest modulus of rupture, that of 1550 kg./cm^2. X-ray analysis of this composition

showed that β-eucryptite crystallized out first at about 850° C and β-spodumene at about 1000° C. Slow heating (less than 5° per minute) was necessary in the 800° to 900° range (where β-eucryptite crystallized) for maximum strength. It was found that the strength also increased with holding temperature.

That this system has many and complex variables to contend with is evidenced from the above review and the fact that when Ohlberg learned of the present study he said that the system had a strong tendency to devitrify and that the immiscibility behavior was sensitive to slight variations in composition. "We never felt we could control or even knew all the variables connected with this metastable state," he said.[48]

III. EXPERIMENTAL PROCEDURE

A. Selecting a Uniform Strength Testing Procedure Using Soda-Lime Glass Cylinders

To the author's knowledge, the diametral loading technique, as such, had not been previously applied to glass. In order to find a method of preparing suitable cylindrical glass specimens, the following steps were taken:

1. Soda-lime glass samples 12 mm. in diameter and 12 mm. in length, the ends of which were ground smooth, flat, and parallel, were obtained from the Corning Glass Works, Corning, New York.

2. The samples were checked for cracks, chips, and other visible imperfections which may have impaired their strength. The number of samples which were not rejected on this basis was about 24.

3. Half of the samples were flame-polished on the ground bases of the cylinders (the round surfaces were already flame-polished). Half of those flame-polished and half of those not flame-polished were then annealed to the point of showing no birefringence under crossed nicols (the unannealed samples displayed a high degree of birefringence).

4. The four groups of samples were then tested on a Tinius-Olson, dual gage, 300,000-lb. capacity compressive loading machine according to the diametral loading technique, at a rate of approximately 6,000 lb./minute. The loading strips were of the wide, blotter paper variety developed and described by Moore.[20]

B. Preparation and Testing of Pyrex Glass Cylinders

Since the glass cylinders to be used for this study were to be made by the author, a satisfactory technique for cutting and truing the flat ends of glass cylinders from glass rod had to be developed. In addition,

a more thorough study of the effect of surface condition on the strength data of diametrally loaded glass cylinders was desired.

One-half inch Pyrex chemical-resistant glass rod from the Corning Glass Works was cut into 10-inch lengths with a circular diamond saw. The 10-inch lengths were then securely held perpendicular to the saw blade by means of a wooden jig and cut into 5/8-inch pieces, rotating the rod slowly while cutting in order to produce cylinders as free from chips as possible.

Twenty-five holes 17/32-inch in diameter were drilled in a 7 inch disc of 3/8-inch aluminum plate. The holes were staggered evenly at radii varying between 1-1/2 and 3 inches. A 1-1/2 inch diameter hole was cut in the center of the disc. The glass cylinders were secured in the holes with "liquid solder" so that 1/8-inch of each of the glass cylinders protruded from each side of the aluminum disc with the cylinder axes perpendicular to the disc. After the liquid solder has set up, the disc was placed on an 8 inch grinding and polishing wheel, where the cylinder faces were ground smooth by feeding water and grit through the larger 1-1/2 inch hole in the center of the disc. The grits used were 120, 240, and 320 silicon carbide and 400 alumina, in that order. The aluminum disc was held with even pressure against the rotating wheel by means of another aluminum disc 1/8-inch thick and 7 inches in diameter, fitted with 2 short bolts that fit into small holes in the glass cylinder-containing disc to keep it from turning with the wheel. A rubber disc 3/16-inch in diameter and 7 inches thick was placed between the two discs to act as a cushion to the cylinders and to allow a more even pressure to be applied on each one. Both the rubber and the 1/8-inch aluminum discs had 1-1/2 inch holes drilled in their centers to allow passage of the

grit and water to the grinding and polishing surface. This grinding process reduced the length of the cylinders to approximately 0.45-inch and eliminated most of the small chips left by the diamond saw. Acetone was used to remove the cylinders from the aluminum disc. Seventy-five discs were prepared in this way; the obviously defective discs (chipped, cracked, etc.) were discarded.

One-third of the Pyrex cylinders were broken without further treatment, using the diametral loading technique. The second one-third of the Pyrex cylinders were scratched lengthwise on their sides and at random on their faces on a 325 grit sandpaper wheel. These cylinders were then broken in diametral compression. The final third of the Pyrex cylinders were etched in an acid solution (24 percent Hf, 24 percent H_2SO_4, and 52 percent H_2O) by dipping them in the solution for 30 to 60 seconds and rinsing in water successively, for a total time in the acid solution of 5 minutes. The etched cylinders were then broken (dry) in diametral compression.

C. Selecting a Glass Composition

Two of the compositions studied by Ohlberg, et. al.,[35] were made up into 200-gram batches. The first was similar in composition to that described by Stookey.[49] The final batch composition, after melting, was calculated to be 56 percent SiO_2, 7 percent TiO_2, 20 percent Al_2O_3, 17 percent MgO, and contained the following raw materials:

SiO_2 - Ottawa Sand (99.95 percent SiO_2), Ottawa Flint Co., Ottawa, Ill.

TiO_2 - Titanox-A CG from the Titanium Pigment Corp.

Al_2O_3 - (anhydrous) Reagent Lot #711119 from Fisher Scientific Co., Fairlawn, New Jersey.

$MgCO_3$ - (light powder) U.S.P. Lot #713541 from Fisher Scientific Co., Fairlawn, New Jersey.

The second composition was 53 percent SiO_2, 19 percent Al_2O_3, 15 percent MgO, and 13 percent Li_2O. (This composition was finally selected for this study.) The raw materials were the same as above with the $LiCO_3$ (N.F. VIII Lot #705441) obtained from the Fisher Scientific Co.

The batches described above were melted in Kyanite crucibles in an electric globar furnace. The temperature limit of this furnace was slightly above 1500° C. The crucibles were obtained from Findlay Refractories, Co.

The ease of melting, viscosity of the melt, melting temperature, crucible erosion, tendency to crystallize on cooling, etc., were examined.

D. Preliminary Heat-Treatment Procedure

In order to determine the effect of heat-treatment on the glass composition 53 percent SiO_2, 19 percent Al_2O_3, 15 percent MgO, and 13 percent Li_2O, rods were formed of the glass by pouring the melted glass into 3/8-inch holes drilled in a carbon block. Short sections of these rods were heat-treated in a small electric, 2-inch alumina tube furnace, in alumina boats, for 96 hours at 595° C. (according to the procedure of Ohlberg, et. al.[35]) and then heat-treated further for various times and temperatures.

E. Making Suitable Molds

Since it was desired to produce cylinders with as smooth a surface as possible, many types of molds in which to pour the fined glass were investigated. (See Appendix C.)

Although carbon molds were avoided in the preliminary search for mold materials, they were the ones finally used for this experiment. A 5-3/16 inch diameter graphite cylinder from National Carbon Co. was cut into 2-3/16 inch lengths. Thirty-six 7/16-inch holes, spaced 11/16-inch apart (center to center) were drilled into each length. Special care was

taken to see that the bit was sharp and aligned, and produced smooth, true holes. Carbon discs 3/8-inch thick were cut from the same 5-3/16 inch diameter stock to act as mold "bottoms". Before pouring, the molds and bottoms were heated to 450° C. in a preheated furnace for 5 to 10 minutes and placed back into this furnace immediately after pouring, to avoid thermal shocking the glass rods. The furnace was then allowed to cool.

F. Specimen Preparation

Four-hundred-gram batches of the selected glass composition were mixed from the raw materials previously mentioned. The batches were mixed in a stainless-steel twin-shell dry blender from Patterson-Kelley Corp., East Stroudsburg, Pa., for 1-1/2 hours with the intensifier bar in operation. The mixed batch was then charged in the preheated Kyanite crucible in the furnace as the temperature was going up between 1100° C. and 1400° C. The glass batch was held constant at 1450° C. and stirred every 15 minutes until it appeared to be thoroughly fined and homogeneous. The glass was then poured into the carbon molds preheated to 450° C., and the filled molds were placed back into the 450° furnace. The furnace was turned off and allowed to cool.

After the glass rods had been pushed out of the cooled carbon molds, those that were cracked or had other internal or surface defects were discarded. The acceptable rods were cut into 5/8-inch cylinders on a circular diamond saw, using the method previously described for Pyrex rods. The cut cylinders were mounted in an aluminum disc and polished in the identical manner described for Pyrex cylinders. All chipped or otherwise visibly defective specimens were discarded or used for purposes other than strength testing. One-hundred-two acceptable specimens were divided into three groups of 34 each. One group of 34 specimens

was broken, using the diametral loading technique without further treatment. They were not annealed because that would constitute heat-treating them.

G. Heat-Treating Specimens

Since the specimens in the remaining two groups were all to be heat-treated to some degree, they were placed on a platinum sheet and heat-treated for 96 hours at 595° C. in an electric globar furnace. The rate of heating and the rate of cooling were both 1° per minute, as controlled by a cam-operated L & N controller. Half of these specimens were then reheated at 1° per minute to 625° C., held for 58 hours, and cooled at 1° per minute to room temperature. The heat-treatments of these two groups are represented by points 1.0 and 2.0 on Figure 14. The other heat-treatments were accomplished by taking three samples of each of heat-treatments 1.0 and 2.0 and heating them at a rate of 1.5° per minute to each of the 3 temperatures, 650°, 750°, and 1000° C., holding 3 hours, and then cooling at 1° per minute to room temperature. These treatments are represented by points 1.1 and 2.1, 1.2 and 2.2, and 1.4 and 2.4, respectively, on Figure 14. In addition, two other heat-treatments, as shown by points 1.05 and 2.3 of Figure 14, were performed, representing 30 minutes at 650° C. and 3 hours at 900° C., respectively, both with heating rates of 1.5° per minute and cooling rates of 1° per minute. Samples from all heat-treatments were broken according to the diametral loading technique.

H. Preparation of Thin-Sections

Samples represented by each of the 10 heat-treatment points of Figure 14 plus a nonheat-treated sample were made into thin sections as follows:

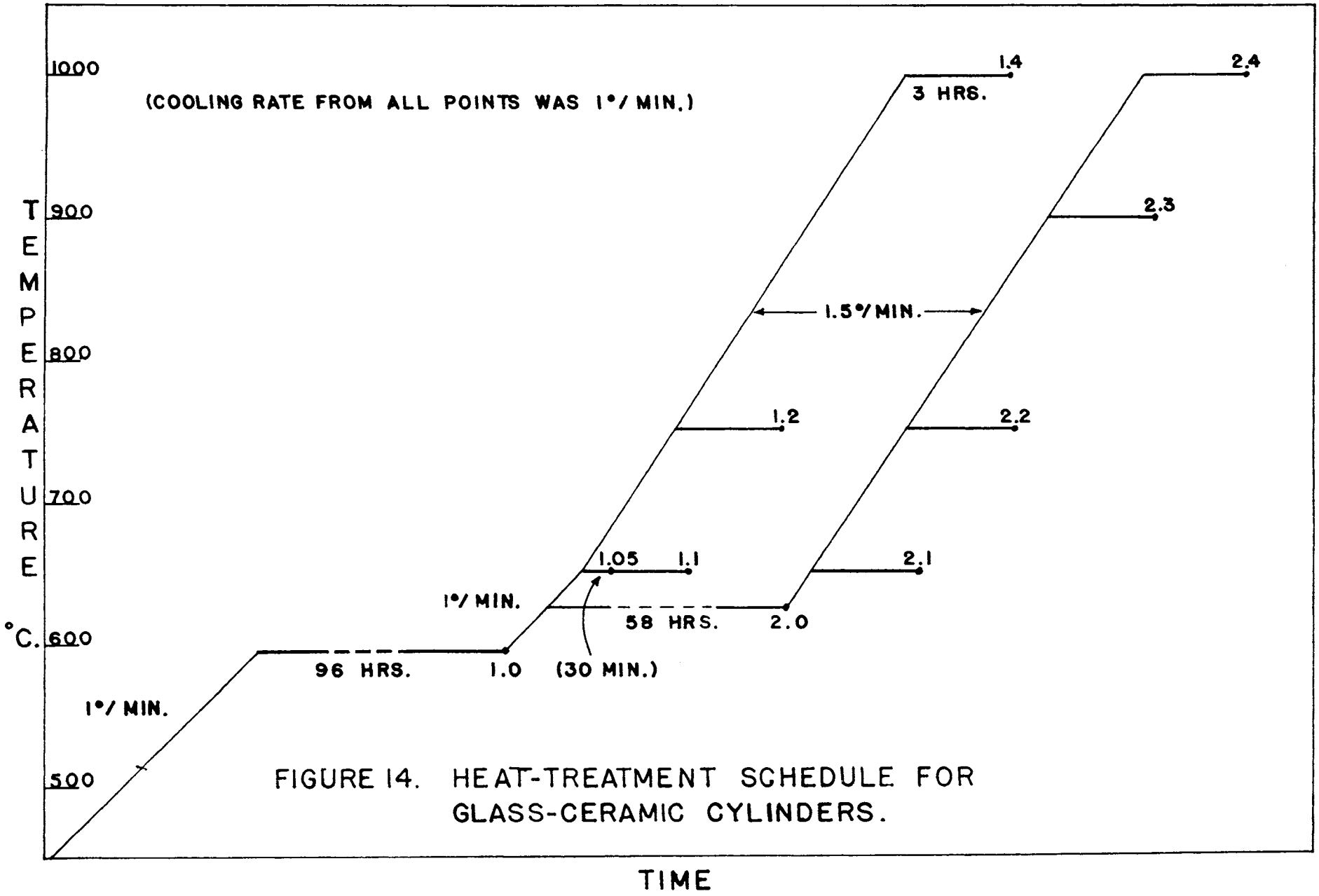

FIGURE 14. HEAT-TREATMENT SCHEDULE FOR GLASS-CERAMIC CYLINDERS.

The samples were polished smooth individually by hand on a grinding and polishing wheel using the same grits as used for grinding the ends of the cylindrical specimens originally. The samples were then dried thoroughly and attached to clean glass slides by means of Canada Balsam which was melted on the slide and allowed to cool while the smooth sample was being held tightly to the slide in the melted balsam. On some samples it was necessary to grind the slide on the grinding wheel with the 400 alumina grit in order to get a strong enough bond between the sample and slide. The sample was cut off with a diamond saw close to the slide and then ground down to the desired thin section thickness on the grinding wheel.

I. Preparation of Polished Sections

Samples representing the various degrees of heat-treatment were also made into polished sections as follows:

Each sample was sanded fairly smooth with 240 grit sand paper and mounted in bakelite using a Buehler bakelite mounting apparatus. The specimens were ground and polished with a Buehler automatic grinding and polishing apparatus (Automet) using 320 and 400 grit Automet abrasive paper, at low speed. The samples remained in the same mounting while they were polished on a Buehler low-nap Metcloth with alumina-A abrasive. A discussion of the Automet and other automatic polishing techniques is given in the ASTM Special Technical Publication No. 285.[50]

The samples were etched by dipping them in a solution of 40 percent H_2O, 40 percent Hf, and 20 percent H_2SO_4 (by volume) for 1 to 5 seconds and washing them off immediately with tap water. This procedure etched the crystalline phase and left the glassy phase essentially in its polished state.

J. Microscope Techniques

The techniques of petrographic, transmitted-light microscopy and of metallographic, reflected-light microscopy were utilized in this study. The thin sections were examined and photographed with transmitted light using a Seitz, binocular, petrographic microscope. Both polarized (crossed nicols) and unpolarized light were used. The bakelite-mounted samples were examined and photographed with transmitted light using a Bausch and Lomb research metallograph. These samples, too, were examined under polarized and unpolarized light.

K. X-Ray Diffraction Analysis

Three powdered samples having been heat-treated corresponding to points 1.0, 2.1, and 2.3 on Figure 14 were chosen for phase analysis by X-ray diffraction on a Norelco diffractometer. They were to be representative of the just-nucleated glass, the partially crystalline glass, and the completely-crystallized glass-ceramic, respectively. An emission spectrograph was also used for qualitative chemical analysis of the crystallized glass.

L. Softening Range

As an indication of the degree of crystallization that had taken place and the effect of heat-treatment on the softening behavior of the glass-ceramic material, dilatometer tests were performed on a sample at each heat-treatment point (Figure 14). The test consisted of placing the sample in a globar furnace with a sapphire rod 15-7/8 inches long and 1/8-inch in diameter resting on the sample with the opposite end of the rod sticking out of the furnace and depressing a dilatometer which was clamped securely to the furnace. As the temperature rose, the expanding sample pushed on the rod which, in turn, moved the dilatometer

dial in a positive direction. When sufficient temperature was reached to soften the sample, the dial began turning in a negative direction. The furnace heating rate for these tests was 5.3° per minute and the load upon the sample was calculated to be 10 pounds per square inch.

IV. EXPERIMENTAL RESULTS AND DISCUSSION

A. Results of Surface Treatment on the Strength of Diametrally Loaded Glass Cylinders

1. Soda-lime glass cylinders

Table I shows the strength data obtained from the soda-lime cylinders tested. It will be noted from this table that the amount of data obtained varied from group to group. This was due mainly to the fact that the technique and the material were new to this author and errors were made in platen alignment, etc., which eliminated some specimens.

Careful examination of the flame-polished specimens showed a "dumbell" effect at the ends of the cylinders. The process of flame-polishing had softened the specimens on the flat faces just enough to cause them to be very slightly larger on the extreme ends. Although this phenomenon was slight, it was felt that flame-polishing was undesirable because (a) the degree of "dumbelling" was somewhat uncontrollable and immeasurable, and (b) even slight deviations from parallel contacts between the specimen and the platens of the loading device would cause serious deviations from the calculated stress distribution (Figure 9).

The stresses shown on Table I were calculated from equation 9 ($\sigma = \frac{2P}{\pi DL}$) which, in this case of constant dimensions is $\sigma = 2.85P$. The fact that the average stress values are tensile stresses is recalled from the theory and Figure 9. Very little difference in average tensile strength can be seen in the various groups of Table I, but a difference in dispersion can be seen between the flame-polished and the not flame-polished specimens.

TABLE I

Strength Data Obtained for Soda-Lime Glass Cylinders Loaded Along a Diametral Plane*

Annealed				Unannealed			
Flame-Polished		Not Flame-Polished		Flame-Polished		Not Flame-Polished	
Load P (lb.)	Stress σ (psi)	Load P (lb.)	Stress σ (psi)	Load P (lb.)	Stress σ (psi)	Load P (lb.)	Stress σ (psi)
3,750	10,700	3,800	10,820	3,600	10,280	4,000	11,400
3,200	9,120	3,560	10,150	4,800	13,690	3,875	11,040
4,650	13,270	4,500	12,820	4,150	11,690	4,000	11,400
4,150	11,820	-	-	5,000	14,260	4,550	12,980
3,750	10,700	-	-	-	-	-	-
Av. 11,115 psi Range - 4,150		Av. 11,267 psi Range - 2,670		Av. 12,504 psi Range - 3,980		Av. 11,703 psi Range - 1,940	

*Received as samples from Corning Glass Works. Dimensions were 12 mm. in diameter and 12 mm. in length.

2. Pyrex glass cylinders

The data obtained from the Pyrex glass cylinders is shown in Table II. Note from this table that the "average" diameter is given instead of the diameter. This term was used because the commercial Pyrex rods used for making these cylinders were not round or uniform in diameter. The diameter of each cylinder varied a total amount of 0.010 to 0.020-inch as it was turned in the micrometer. The lengthwise variation was generally not appreciable on the short cylinders, although it could easily be detected on the long, uncut rods. Another deviation from the ideal glass cylinder was the existence of a tiny capillary-like hole (apparently created by an elongated bubble produced during the drawing of the rod) running the entire length of each cylinder, approximately at its center. These little "bubble holes" varied slightly in size and position. In some specimens there were two, in others they were particularly large, even to the extent of containing grit from the end-polishing operation. In every case tested these specimens (with large holes and two holes) broke at a load value far below that of the other specimens and, therefore, their data were disregarded and do not appear in Table II.

It can be seen from the values of the mean tensile stresses ($\bar{X} = \frac{\sum_{i=1}^{n} X_i}{n}$) on Table II that the scratched specimens yielded the lowest average stress values and the etched specimens, the highest. The range values, however, show that the etched specimens stress range was almost equal to their average stress value, while the ranges for the other specimens were less than half the average stress values. This is indicative of the tendency of acid attack to enlarge large flaws (like large bubble holes, deep scratches, etc.) while it eliminates the small surface

TABLE II

Diametral Loading of Pyrex Glass Cylinders (Annealed)

No surface treatment				Scratched specimens				Etched specimens			
Length L (in.)	Average dia. D (in.)	Break load P (lb.)	Tensile stress σ (psi)	Length L (in.)	Average dia. D (in.)	Break load P (lb.)	Tensile stress σ (psi)	Length L (in.)	Average dia. D (in.)	Break load P (lb.)	Tensile stress σ (psi)
.450	.507	3,400	9,484	.419	.504	3,050	9,193	.406	.493	2,670	8,490
.465	.518	3,720	9,830	.445	.508	3,650	10,277	.455	.494	6,950	19,681
.469	.497	4,280	11,689	.441	.492	2,880	8,449	.444	.485	3,300	9,757
.431	.499	3,700	10,950	.419	.501	2,800	8,492	.462	.497	4,050	11,229
.475	.507	5,050	13,351	.415	.500	2,470	7,578	.415	.496	4,140	12,806
.418	.504	4,250	12,841	.412	.492	3,450	10,835	.417	.505	6,330	19,134
.475	.493	5,050	13,351	.417	.510	3,300	9,877	.457	.497	5,090	14,268
.425	.497	4,600	13,865	.450	.498	4,210	11,959	.418	.496	2,900	8,905
.456	.504	4,250	12,841	.418	.506	3,600	10,836	.416	.492	5,550	17,260
.414	.505	3,450	10,503	.413	.505	2,500	7,630	.409	.490	3,200	10,165
.458	.498	3,550	9,907	.444	.506	3,450	9,774	.421	.495	3,880	11,852
.425	.498	3,160	9,502	.441	.498	2,610	7,566	.420	.492	4,770	14,698
.415	.494	2,900	9,005	.474	.503	3,500	9,346	.406	.502	3,210	10,027
.421	.495	2,990	9,133	.463	.497	3,280	9,075	.452	.503	3,230	9,042
.428	.498	3,670	10,964	.443	.491	3,330	9,746	.442	.489	5,280	15,554
.428	.493	3,270	9,866	.460	.499	3,280	9,098	.405	.499	3,150	9,922
.455	.498	3,750	10,535	.427	.498	3,250	9,732	.439	.496	6,850	20,031
.474	.504	3,480	9,273	.431	.508	3,680	10,702	.452	.495	4,250	12,095
.411	.500	3,760	11,648	.415	.506	3,190	9,670	.424	.500	3,680	11,050
.427	.512	3,240	9,436	.441	.508	2,910	8,270	.421	.503	2,610	7,845
.415	.511	3,620	10,865	.417	.514	2,800	8,318	.441	.489	4,170	12,312
-	-	-	-	.470	.497	3,900	10,628	.470	.493	4,700	12,913
-	-	-	-	-	-	-	-	.464	.488	4,220	11,866
-	-	-	-	-	-	-	-	.453	.491	5,470	15,657
L.....R = 475-411 = 64				L....R = 474-412 = 62				L....R = 470-406 = 64			
D.....R = 518-493 = 25				D....R = 514-491 = 23				D....R = 505-485 = 20			
σ.....R = 13,865-9,005 = 4,860				σ....R = 11,959-7,566 = 4,393				σ....R = 19,681-7,845 = 11,836			
$\bar{X}$ = 10,884 psi				$\bar{X}$ = 9,411 psi				$\bar{X}$ = 12,773 psi			

flaws by etching away the glass to a depth in excess of the small flaw depth. Even though the highest strengths were obtained on the etched cylinders, the great dispersion of strength values was a factor in deciding against etching in this study. It was found that scratching the specimens did not reduce the dispersion appreciably from that of the specimens which were without treatment and that scratching uniformly and consistently was difficult. Scratching future specimens, therefore, was also eliminated.

B. Comparison of Diametral Loading Strength Results

A comparison of Tables I and II shows the average stress values to be approximately the same for the soda-lime and the Pyrex cylinders. The ranges of the Pyrex specimens (unetched) are approximately double those of the soda-lime specimens which were not flame-polished, and approximately equal to the flame-polished soda-lime specimens. In each case, the greater scatter can be attributed to visible defects, i.e., the "dumbelling" and the "bubble holes". The tensile strength and the range of strength values for these two glasses seem to correlate very well.

Comparison of the work done by Kenny[23] will now be made with the preliminary work done in this study. Even though Kenny did not do a strength study on glass, as such, in his data for his surface energy study, enough information is given to calculate the tensile stress attained on his cylinders at the point of fracture. His data, with the stress calculations according to the diametral loading theory and equation (9), as computed on the LGP-30 digital computer of the Missouri School of Mines Computer Center, are given in Table III.

Caution must be used in comparing Kenny's results with those in this study. Without the use of loading strips, the maximum tensile stress

TABLE III

Strength Data From Report on Surface Energy of Crushed Pyrex Cylinders*

Cylinders crushed on-the-round			
Large Diameter .498" Length .499"		Small Diameter .365" Length .355"	
Load P (lb.)	Tensile stress σ (psi)	Load P (lb.)	Tensile stress σ (psi)
2,290	5,867	1,810	8,893
3,500	8,966	2,050	10,072
1,810	4,637	1,330	6,534
1,330	3,407	1,570	6,534
2,050	5,252	1,570	7,714
1,810	4,637	1,810	7,714
1,570	4,022	1,450	8,893
2,050	5,252	1,450	7,124
1,680	4,304	1,940	7,124
-	-	1,330	9,532
-	-	1,080	5,306
-	-	1,570	7,714

*Stress calculated on the basis of diametral loading theory of stress distribution.

may not always be measured. Since the load is applied directly to a very small area on the glass surface by the hardened steel platens, cracking could easily result, causing premature breaks. Also, variables such as loading rates, etc., which were not of particular importance in Kenny's study are not known and, therefore, make comparison difficult. It is, however, expected that his values would average somewhat lower than those in this study, as they do. It will be noted, also, that the maximum tensile stresses in Kenny's study are near the average stress values determined in this study. Taking into consideration the difference in technique and purpose, the work done by Kenny seems to correlate reasonably well with the present work.

The glass fragments and products resulting from breaking the specimens will be mentioned here and discussed further in succeeding sections. The products from the soda-lime and Pyrex glass cylinders broken in this study were similar to those described by Kenny when he said that the specimens failed suddenly with a loud report and were reduced immediately to a fine powder. If any large fragments did fly from the "exploding" specimens, they hit the wall and protection shield with such force that they may have broken at this time. In any case, very few fragments of any size were found after breaking. Not too infrequently, the thin diametral plane along which the specimen was loaded remained after breaking. It was thinner than that described by Moore[20] on Figure 10, and seemed to be a single plane rather than being split in the center.

C. Selection of a Glass Composition for Study

The first of the batch compositions melted and described in the experimental procedure was found to be very difficult to melt at 1500° C. (the furnace maximum temperature). When finally melted, the high viscosity

at that temperature prevented satisfactory fining in reasonable time periods. This composition was, therefore, not used for further study.

The second composition, namely 53 percent SiO_2, 19 percent Al_2O_3, 15 percent MgO, and 13 percent Li_2O was found to be sufficiently fluid at 1450° C. to reach apparent homogeneity in fairly short time periods (approximately 2 hours). Although it did have a tendency to erode crucibles quite rapidly, Kyanite crucibles seemed to be fairly satisfactory for melting. This composition had several things in its favor as far as being able to see changes (such as droplet separation, etc.) by ordinary light microscopy methods, as discussed in the literature survey.

D. Preliminary Heat-Treatment Results

The first heat-treatment given the small sections described in the procedure (after the 96 hours at 595° C. treatment which was given to all specimens) was 625° C. for 30 minutes, after the procedure of Ohlberg, et. al.[35] The glass didn't seem to be nucleated sufficiently from this treatment, as reported by Ohlberg, so a group of samples were heated to 625° C and one was taken out every few hours to determine a suitable schedule for droplet formation. It was found that the samples would have to be treated at 625° C. in excess of 50 hours for large, clear droplets to be reasonably plentiful, although octahedral crystals also formed during this process. The samples were opaque at this point. Some of these samples were later completely crystallized at 700° C. for 3 hours.

In addition to those small samples, a larger rod (3/8-inch in diameter by 2-1/2 inches long) was placed in an alumina boat and heated to 750° C. for 3 hours and cooled. This sample was completely crystallized but showed very unusual growth appendages protruding from the side of the rod. Also, the surface of the rod, although still possessing its smooth

appearance (with the exception of the appendaged portions), had peaks and valleys in a wave-like manner around its surface. Further discussion of this phenomenon will appear later in this report.

E. Mold Selection

The carbon molds did not produce the smooth surfaces that the steel molds were capable of producing, but proved to be the most satisfactory considering all the desired features of glass rods, i.e., homogeneity, smooth surface, uniform diameter, absence of cracks and bubbles, etc.

F. Nonheat-Treated Specimen Strength Results

The results of breaking the nonheat-treated specimens appear on Table IV. The stresses were calculated from equation (9) and the standard deviation from Std. Dev. $= \sqrt{\frac{\sum_{i=1}^{n} (X_i - \bar{X})^2}{n}}$ using the LGP-30 digital computer, with a floating-point program for the former and a fixed-point program for the latter.

It can be seen that the tensile stress required to break these specimens was somewhat lower than that required for the commercial glasses. The products remaining after breaking also differed from those of the commercial glasses (see Figure 15). Note that the manner of fracture is nearly identical to that observed on porcelain cylinders and described by Moore (Figure 10). It will also be noted that the stress values obtained for the glass under study are near the values obtained by Moore for porcelain. These lower values themselves can account for the breaking into large fragments as has been previously explained.

Several factors may be involved in the reason for the apparent lower tensile strength of this glass as compared to the other glasses studied. For one, the carbon molds did not leave as smooth a surface on these

TABLE IV

Strength Data for Nonheat-Treated Glass Cylinders*

Length (inches)	Diameter (inches)	Load (pounds)	Tensile stress (psi)
.406	.433	1,600	5,794
.403	.432	2,200	8,045
.397	.431	1,600	5,953
.403	.435	1,300	4,721
.399	.434	1,550	5,698
.396	.436	1,350	4,978
.384	.435	1,350	5,145
.398	.433	1,550	5,726
.390	.434	1,750	6,582
.413	.435	1,800	6,378
.403	.434	1,450	5,278
.396	.432	1,600	5,954
.414	.430	2,300	8,225
.400	.435	1,800	6,586
.400	.433	1,850	6,800
.403	.432	1,200	4,388
.382	.435	1,500	5,746
.413	.432	1,800	6,432
.396	.435	2,100	7,761
.397	.435	1,800	6,635
.419	.434	1,800	6,302
.398	.431	1,550	5,752
.382	.435	1,750	6,704
.394	.433	1,850	6,903
.382	.433	1,750	6,735
.378	.434	2,000	7,761
.386	.432	2,200	8,399
.399	.434	1,600	5,882
.384	.434	1,450	5,539
.395	.433	1,000	3,722
.406	.435	1,800	6,488
.396	.431	2,100	7,833
.383	.430	2,100	8,118
.398	.434	1,300	4,791

*Composition of cylinders - 53% SiO_2, 19% Al_2O_3, 15% MgO, 13% Li_2O.

Std. Dev. = 1139 = 18.4% $\bar{X}$

$\bar{X}$ = 6286.7 psi

R = 4677

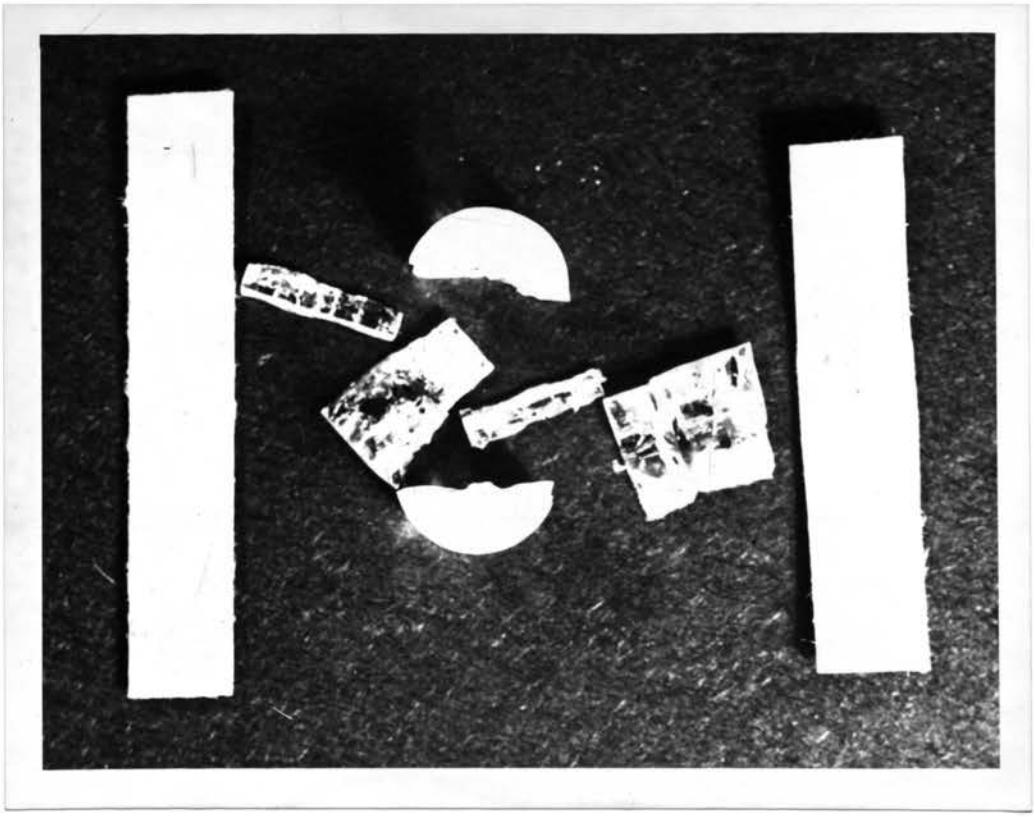

Figure 15. Nonheat-treated SiO_2-Al_2O_3-MgO-Li_2O glass cylinder after breaking by the diametral loading technique, shown with loading strips.

cylinders as the fire-polished surface on the commercial glass. In order for the diametral loading technique theory to hold, the specimens must be loaded evenly along a diametral plane. A rough surface may cause deviations from the theoretical stress pattern and give birth to extreme stress concentrations in localized regions leading to premature failure. It is suspected that the homogeneity of this glass may not be optimum. This factor, too, could cause the stress pattern to deviate from ideality.

G. Results of Heat-Treating

The samples heat-treated to point 1.0 (Figure 14) were very slightly milky. The surface of these specimens had a wave-like appearance with peaks and valleys as seen on the rod in the preliminary heat-treatment study. The 1.05 and 1.1 heat-treatment samples were even more milky (but still transparent) and the wave-like surface was even more pronounced. The 1.1 specimens were partially transparent and partially opaque. All other heat-treatments produced specimens which were not transparent at all. The specimens with the 2.0 heat-treatment had a greenish-white opaque appearance.

As heat-treatment of the specimens proceeded to higher temperatures the specimens went from a greenish-white, opaque to a solid-white crystalline appearance. Figure 16 shows specimens at various heat-treatment stages. The wave-like appearance can be seen on all but the nonheat-treated cylinder. The bright spot on the nonheat-treated specimen is a chip, making this particular specimen ineligible for strength tests. It can be seen from Figure 14 that the heat-treatments "branched" into two sections. One section utilized only the preliminary heat-treatment used by Ohlberg (595° for 96 hours). This is designated as the 1.x heat-treatment series on Figure 14 (where x indicates the maximum holding

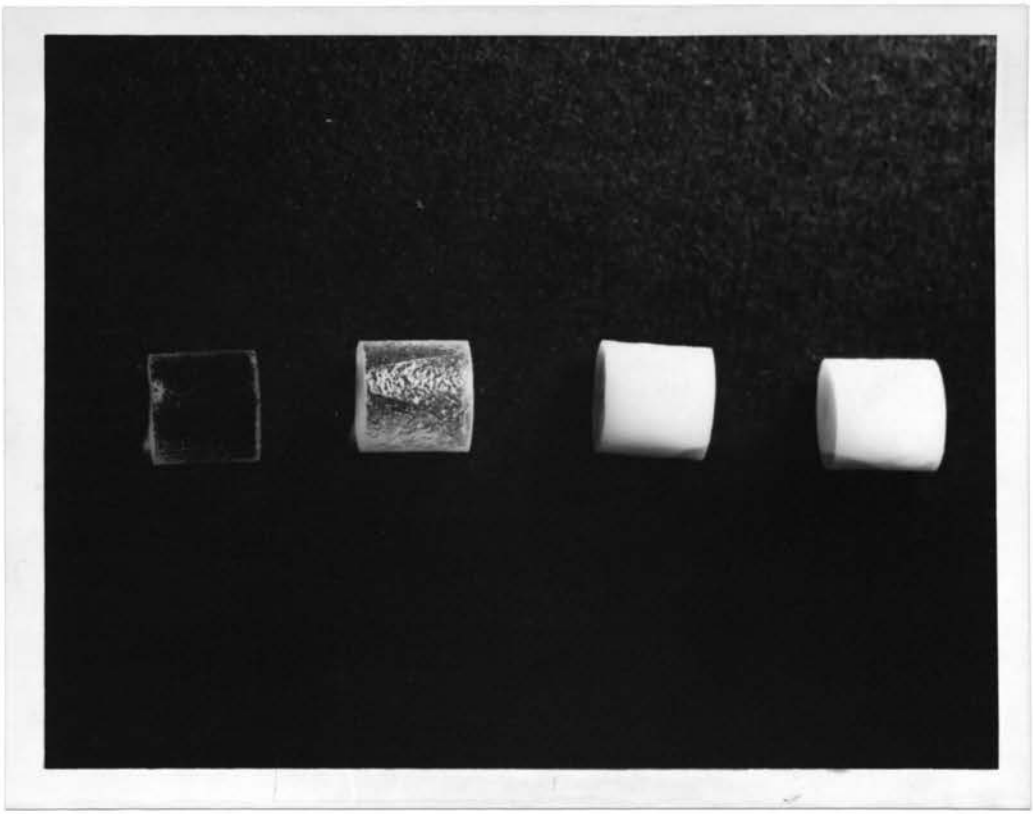

Nonheat-treated 1.0 2.0 2.4

Figure 16. Glass-ceramic cylinders at four different stages of heat-treatment. (See Figure 14.)

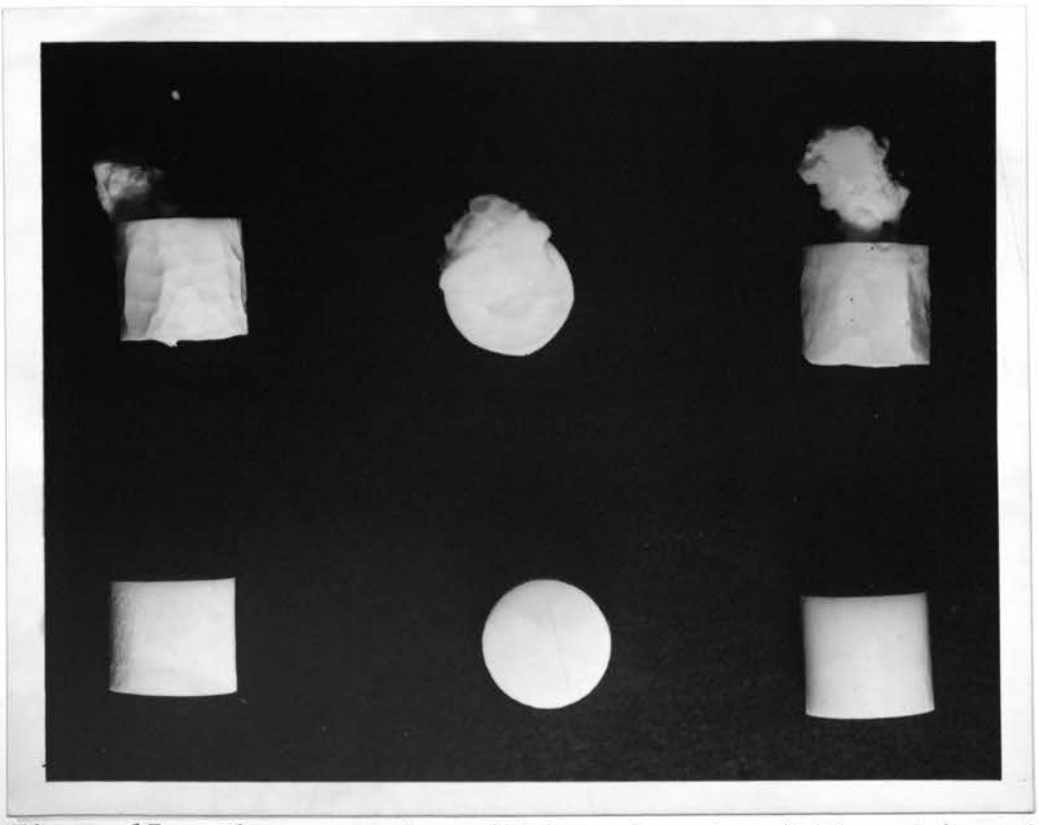

1.2

2.2

Figure 17. Glass-ceramic cylinders from two different branches of the heat-treatment schedule (Figure 14). (Treatments 1.4 and 2.4 are identical in appearance.)

temperature). The other section added an additional "nucleation treatment" of 625° C. for 58 hours. This is designated as the 2.x series on Figure 14. Subsequent treatments along these two branches were nearly identical.

The crystallization behavior at the higher temperatures of these two branches was strikingly different. An example of this difference is illustrated on Figure 17. The top set of specimens was from the 1.2 heat-treatment, and the bottom set from the 2.2 heat-treatment. The peculiar growth appendage mentioned in the preliminary heat-treatment study can be seen as it again appeared here in the 1.2 specimens. Note also the extreme degree of "wave-like", "peak and valley" surface in the 1.2 specimens, also mentioned in previous work. An identically similar picture could have been taken of the 1.4 and 2.4 specimens. For this reason the need for a 1.3 heat-treatment was decided to be unnecessary and was not done and, therefore, does not appear in Figure 14. It will be noted that these growth appendages always grew from the bottom of the specimen, i.e., the face which was in contact with the platinum sheet in the furnace. In the preliminary study of heat-treatment the rod from which the first appendage grew was not in contact with platinum but was touching the alumina boat on the side of the rod where the appendage grew. Further examination of the rod and boat used in that study showed that growths had occurred all along the bottom of the rod where the rod was touching the boat.

It appears from these observations that two things effect the anomalous growth behavior seen here. First, and apparently most important, is the degree of nucleation that has taken place, due to prior treatment prior to heating the specimen above 650° C. Second is the contact of the specimen with other materials. To iterate, if insufficient

nucleation has taken place, anomalous external appendages will appear at points of contact with other material, as in heat-treatments 1.2 and 1.4 (Figure 17). On the other hand, when the specimen is well-nucleated prior to higher temperature treatment, no anomalous growth appendages occur, regardless of contact with other materials.

Tables V and VI show the results of the strength tests of the heat-treated specimens. It can be seen from Table V that the maximum strength in the 1.0 heat-treatment series (see Figure 14) was more than double that of the maximum strength of an untreated specimen (Table IV). The average strength value was 50 percent greater than the average of the untreated specimens. Figure 18 shows the average strengths of all specimens as a function of heat-treatment temperature. The numbers at the experimental points correspond to the points on the heat-treatment schedule. Even though the strength increased up to the 1.0 point, it sharply decreased on further treatment on both branches of the heat-treatment schedule. The specimens from the 1.x branch of the schedule lost their strength entirely as the appendage growth occurred (points 1.2 and 1.4, Figure 18). This growth left these specimens very porous and, therefore, weak. The specimens from the 2.x branch of the heat-treatment schedule, however, increased in strength at the higher temperature levels (points 2.3 and 2.4 of Figure 18). This rise apparently corresponds to the final stages of crystallization, but the weakening effect of the 2.0 and 2.1 stages of treatment were so great that the final strength didn't reach the original strength of the glass.

H. Results of Observations Through Thin-Sections of the Glass-Ceramic Cylinders With a Research Petrographic Microscope

The various stages of droplet and crystal growth were studied by petrographic means. Under crossed nicols immiscible droplets appeared as

TABLE V

Heat-Treatment 1.0*

Length (inches)	Diameter (inches)	Load (pounds)	Tensile stress (psi)
.412	.435	2,500	8,880
.415	.435	2,100	7,400
.408	.435	5,630	20,200
.400	.436	3,700	13,500
.405	.435	2,250	8,130
.405	.435	1,820	6,570
.405	.436	3,200	11,560
.420	.440	1,800	6,200
.387	.436	1,570	5,940
.405	.437	3,100	11,150
.408	.435	3,350	12,000
.393	.438	1,630	6,020
.410	.436	1,620	5,770
.414	.435	1,540	5,410
.408	.435	4,000	14,340
.413	.440	2,450	8,600
.415	.435	3,280	11,580
.390	.438	1,730	6,440
.415	.437	4,400	15,420
.414	.437	3,050	10,710
.413	.434	3,580	12,710
.385	.438	1,120	4,340

*See Figure 14.

$\overline{X}$ = 9,539 psi
R = 15,860

TABLE VI

Strength of Heat-Treated Samples

Treatment No.	Length (in.)	Diameter (in.)	Load (lbs.)	Stress (psi)
1.05	.422	.435	2,750	9,530
1.1	.420	.435	950	3,310
1.2	.405	.435	0.00	0.00
1.4	.410	.438	0.00	0.00
2.0	.420	.438	480	1,660
	.430	.436	440	1,490
	.387	.438	350	1,310
	.385	.438	450	1,690
	.405	.437	860	3,090
	$\bar{X}$ = 1,848 psi		R = 1,780	
2.1	.412	.438	400	1,410
2.3	.393	.440	950	3,500
	.420	.434	670	2,340
	$\bar{X}$ = 2,920 psi		R = 1,160	
2.4	.395	.436	1,400	5,180
	.406	.438	1,230	4,400
	$\bar{X}$ = 4,790 psi		R = 780	

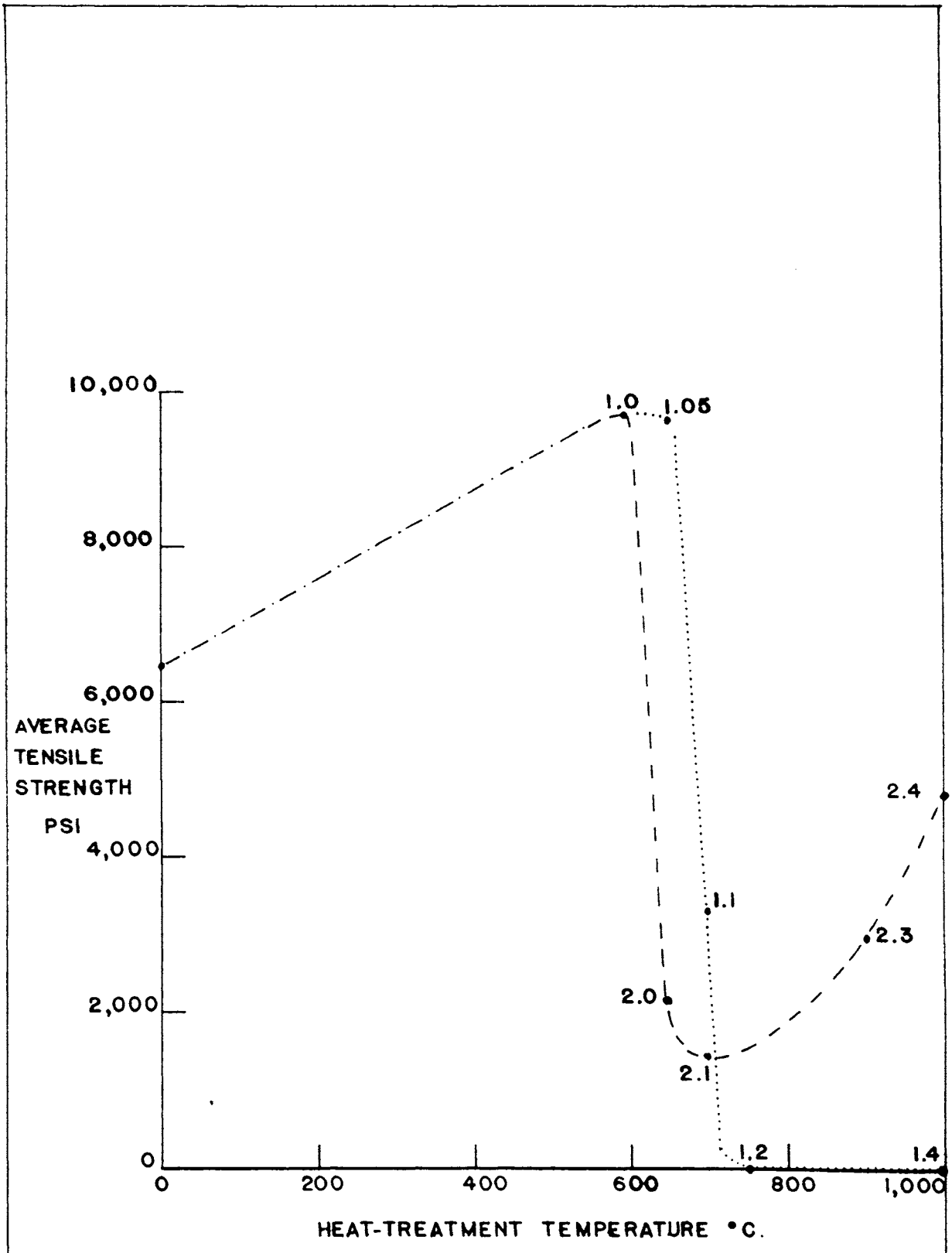

FIGURE 18. STRENGTH OF GLASS-CERAMIC CYLINDERS VS. HEAT-TREATMENT

light, usually gray circles with a black optic cross in the center. They show no birefringe like near-by crystals. These optic crosses remained stationary with respect to the cross-hairs of the microscope, upon rotation of the stage, as described by Dayton.[51] This phenomenon is usually associated with looking down the optic axis of uniaxial crystals. Dayton's explanation of the theory of the formation of these crosses is, clearly, evidence of the spherical and glassy nature of the droplets (see Appendix D). Figure 19 shows a photomicrograph of a section of the glass-ceramic that had been heat-treated to point 1.0. This picture shows several different aspects of the devitrification process. The common surface nucleation and crystallization is illustrated by the string of crystals running along the bottom of the picture. A droplet is seen next to the surface in the lower part of the picture. Just to the right of center is a birefringent octahedron. To the extreme left is seen an octahedron twin. A closer view of this picture is seen in Figure 20. The dark line running through the octahedron is a crack that was seen easily under uncrossed nicols. The crack seemed to be associated in part with this crystal.

Between the droplet and the octahedron is seen a more disorderly form of crystallization. More of this variety of the nucleation and crystallization process is seen in Figure 21, where droplets can be seen in various stages of crystallization.

Two different mechanisms in which droplets serve as nuclei for crystallization are seen in Figure 22. First, concerning the amorphous droplet on the right, crystallization was initiated at the glass-droplet - glass-matrix interface; the droplet served as a nucleus, crystallizing the matrix while remaining glassy itself. The crystalline phase around the droplet is highly birefringent, while the droplet is still gray.

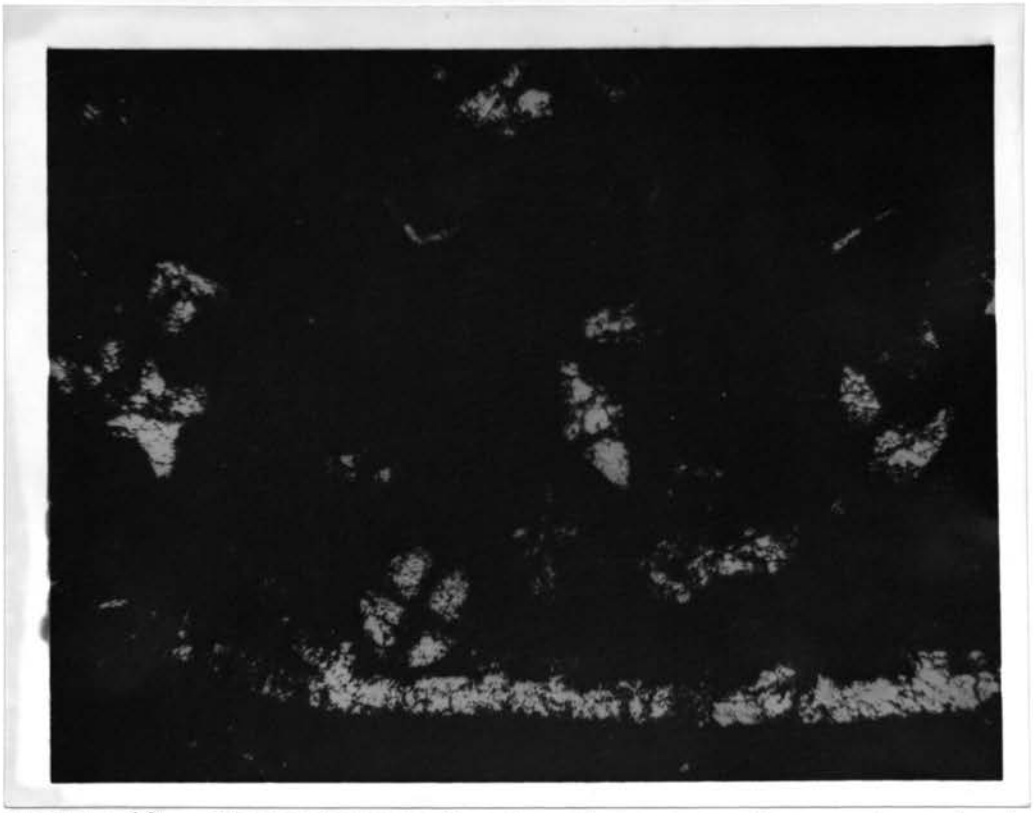

Figure 19. Photomicrograph of a glass-ceramic specimen heat-treated according to point 1.0 (Figure 14) viewed with transmitted light under crossed nicols. 16X

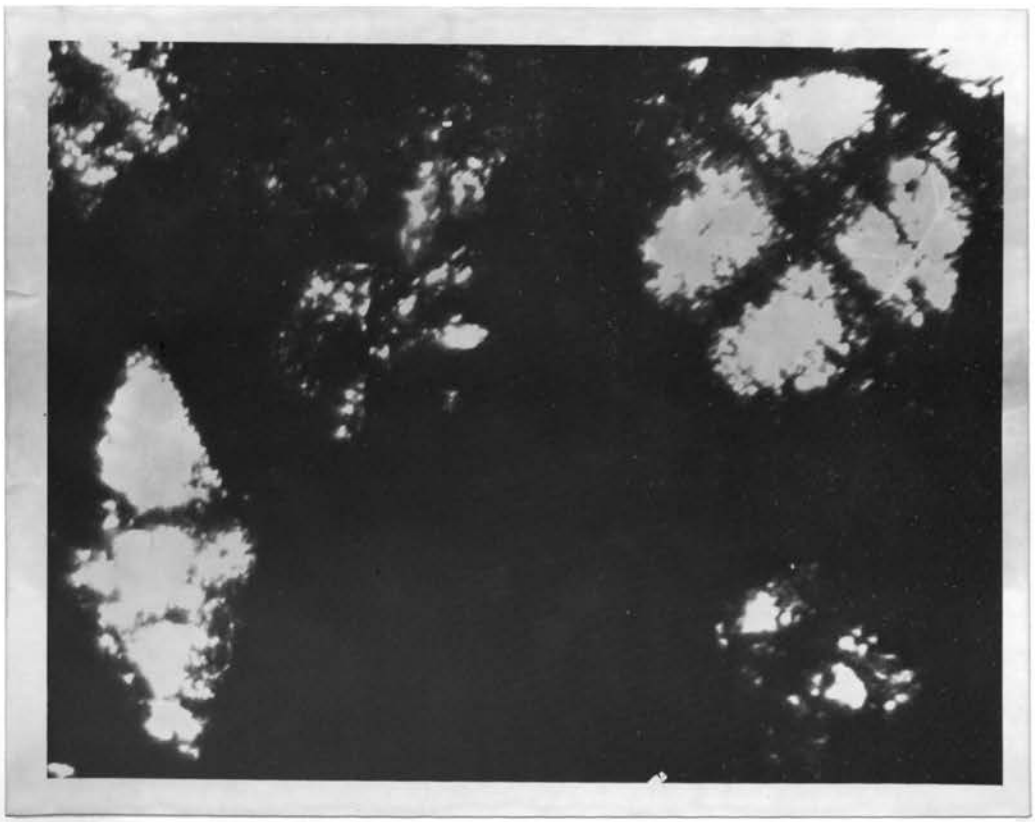

Figure 20. Photomicrograph of a glass-ceramic specimen heat-treated according to point 1.0 (Figure 14) viewed with transmitted light under crossed nicols. 54X

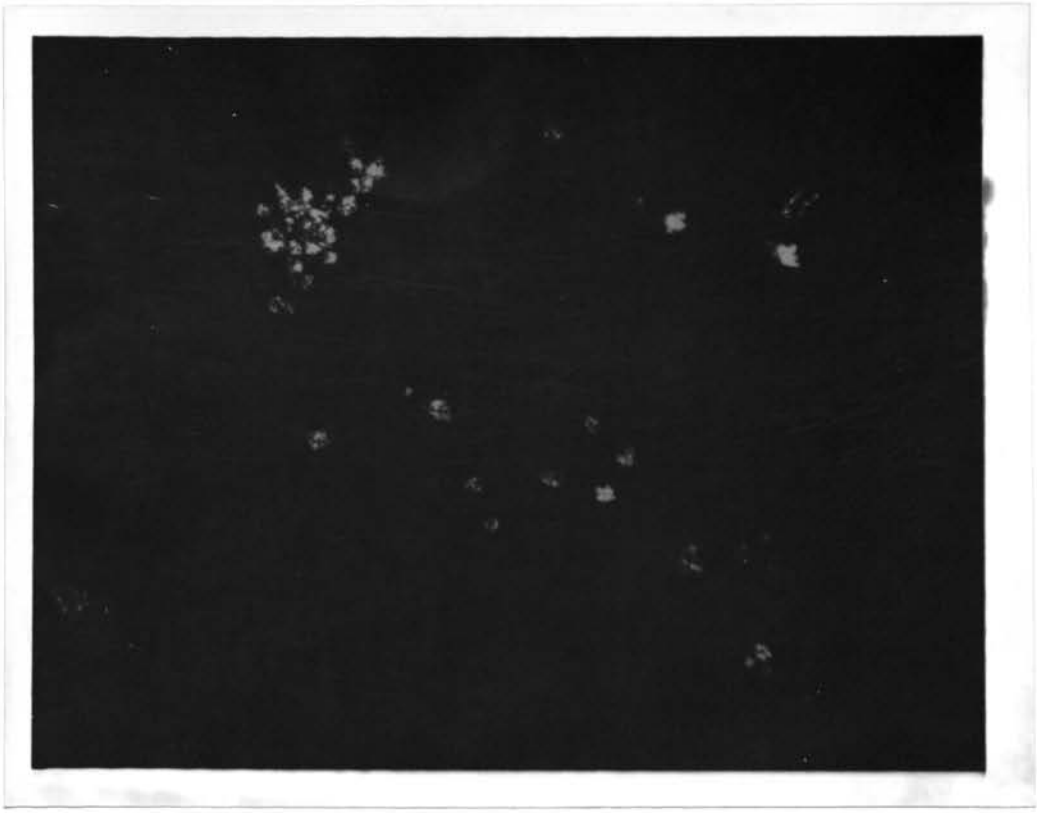

Figure 21. Photomicrograph of a glass-ceramic specimen heat-treated according to point 1.05 (Figure 14) viewed with transmitted light under crossed nicols. 20X

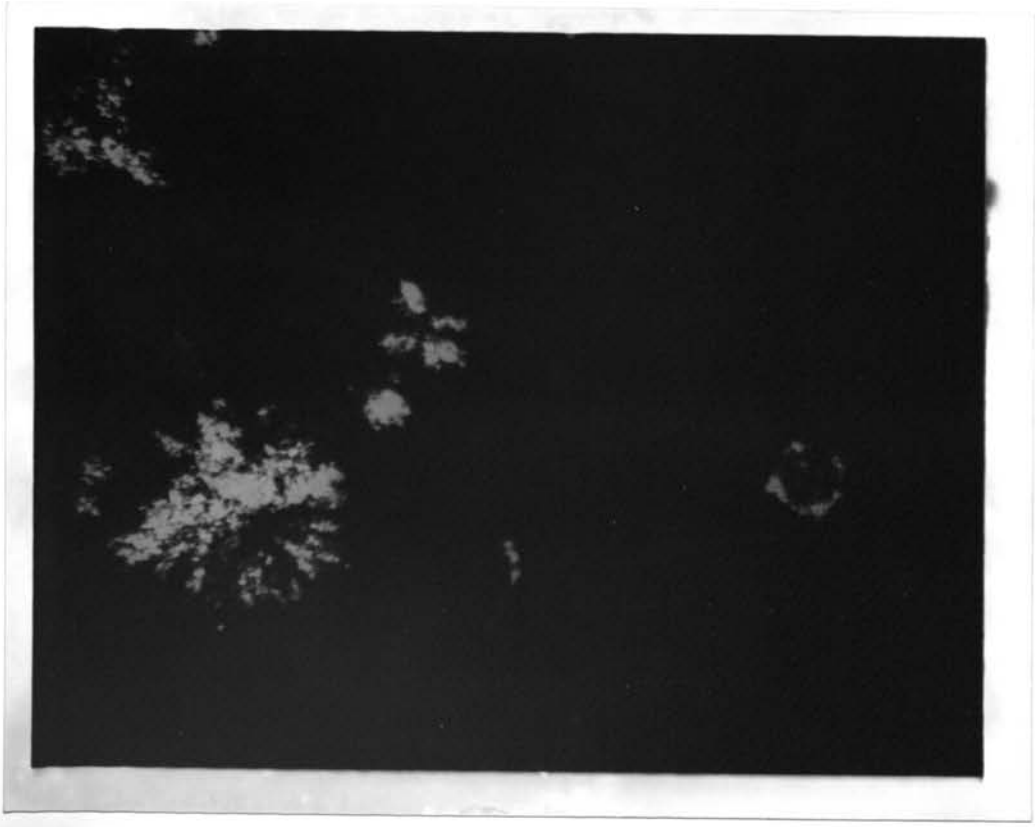

Figure 22. Photomicrograph of a glass-ceramic specimen heat-treated according to point 1.1 (Figure 14) viewed with transmitted light under crossed nicols. 20X

Second, concerning the droplet in the second quadrant center, this droplet has undergone crystallization itself; then, acting as the nucleus, it served to crystallize the surrounding matrix. The remanent cross can still be seen indicating this originally was a droplet. This is an example of a phenomenon also observed by Ohlberg[35] where the droplet crystallized from the glass-glass interface, radially inward, and then acted as a nucleus for the matrix. Droplets in more detailed steps of this process were observed but all steps could not be photographed.

The case first mentioned in the discussion of Figure 22 was not mentioned in Ohlberg's study of this system and is of particular interest here. Figure 23 is a picture of these glassy droplets still existing at further heat-treatment stages. They appeared gray in an essentially crystalline matrix which displayed the usual birefringence. The same view with uncrossed nicols is seen in Figure 24. Here the droplets appear as clear circles in colored surroundings. The circles in the upper right-hand corner are bubbles in the balsam. Note the extensive cracking in the matrix. It can easily be seen why the 2.0 heat-treatment specimens were so low in strength (Figure 18). Closer views of these droplets are shown in Figures 25 and 26, with still greater magnification shown in Figures 27 and 28. The spherical and amorphous nature of these droplets, and their crystalline surroundings may be clearly visualized in these photographs.

The second case seen on Figure 22 can also still be seen after further heat-treatment. Figures 29 and 30 show examples of this case. In the upper left-hand corner of Figure 29 is a droplet which appears, judging from its shape, to have crystallized while the matrix was still glassy. In the upper right-hand corner of Figure 30 is a crystallized droplet which

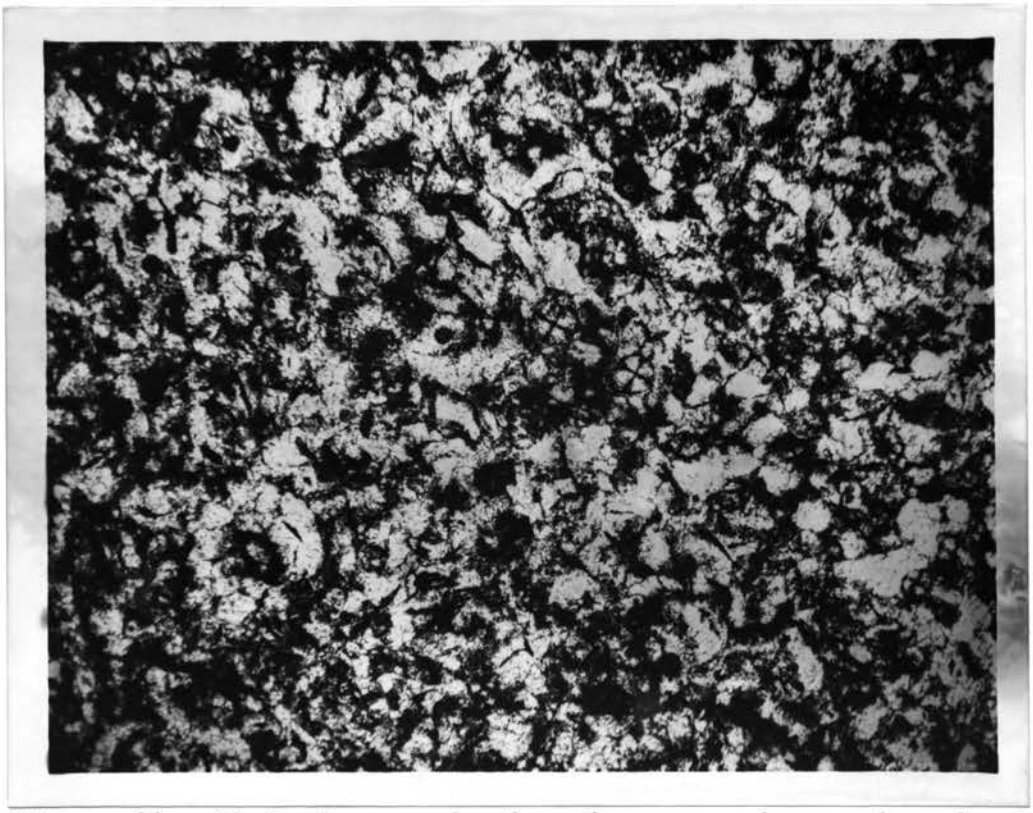

Figure 23. Photomicrograph of a glass-ceramic specimen heat-treated according to point 2.0 (Figure 14) viewed with transmitted light under crossed nicols. 16X

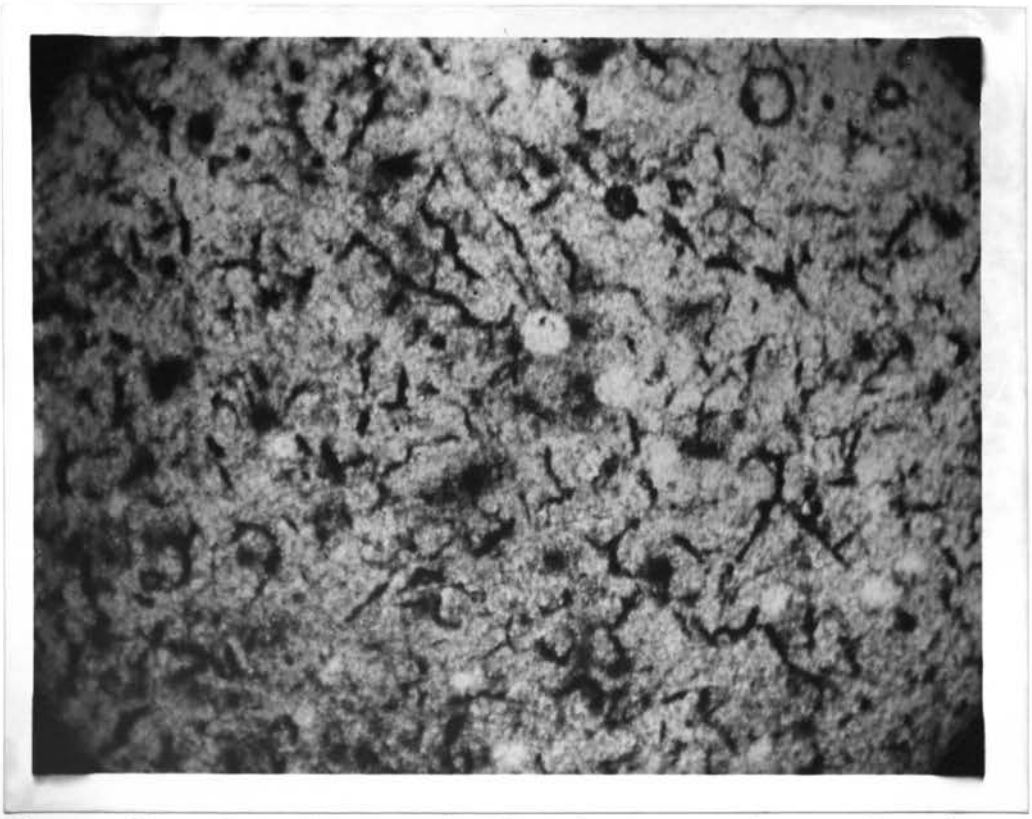

Figure 24. Photomicrograph of a glass-ceramic specimen heat-treated according to point 2.0 (Figure 14) viewed with transmitted light under uncrossed nicols. 16X

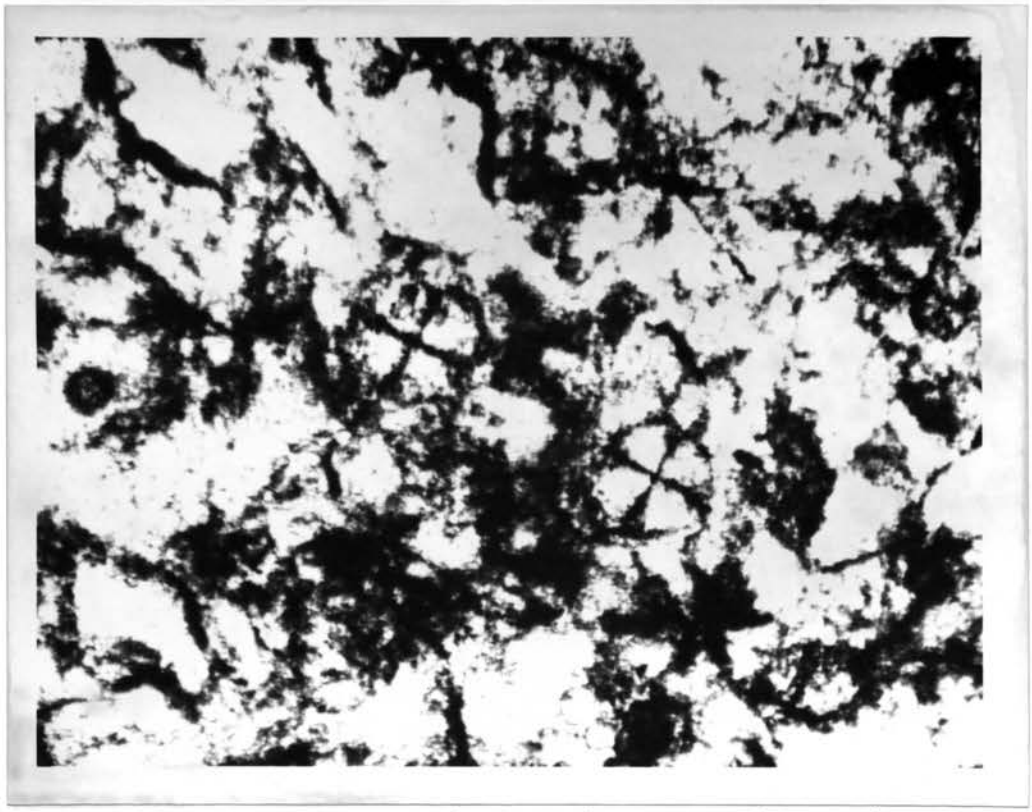

Figure 25. Photomicrograph of a glass-ceramic specimen heat-treated according to point 2.0 (Figure 14) viewed with transmitted light under crossed nicols. 54X

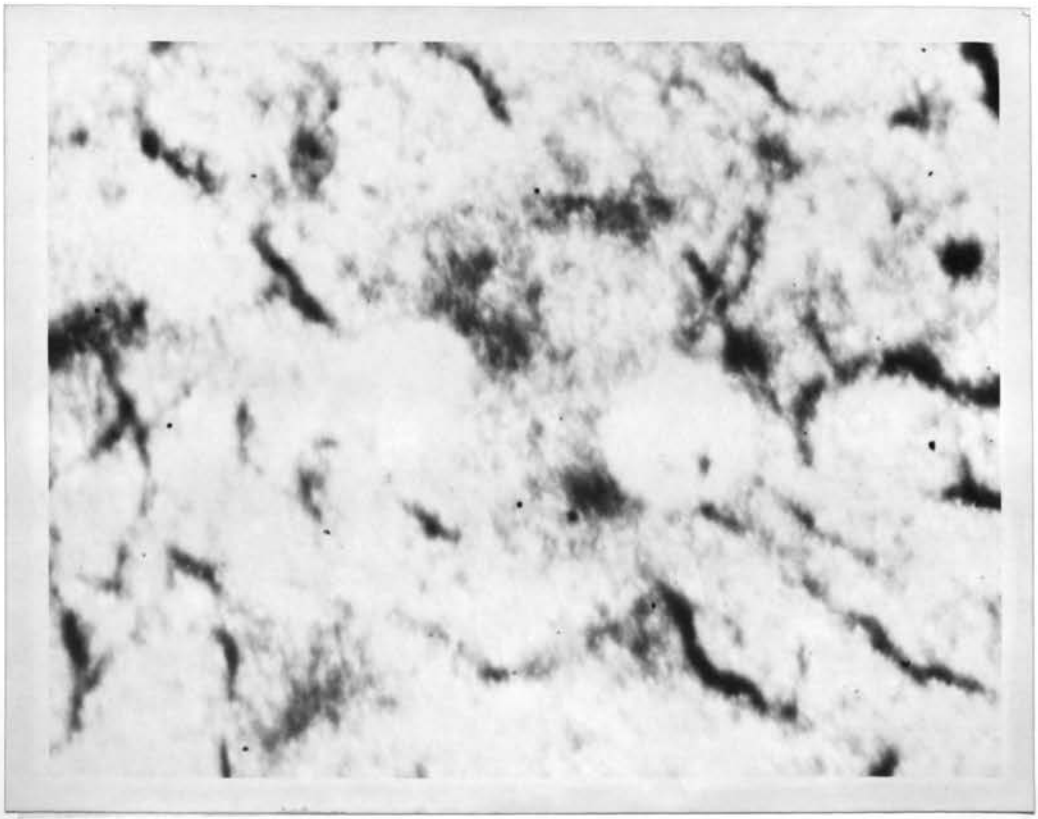

Figure 26. Photomicrograph of a glass-ceramic specimen heat-treated according to point 2.0 (Figure 14) viewed with transmitted light under uncrossed nicols. 54X

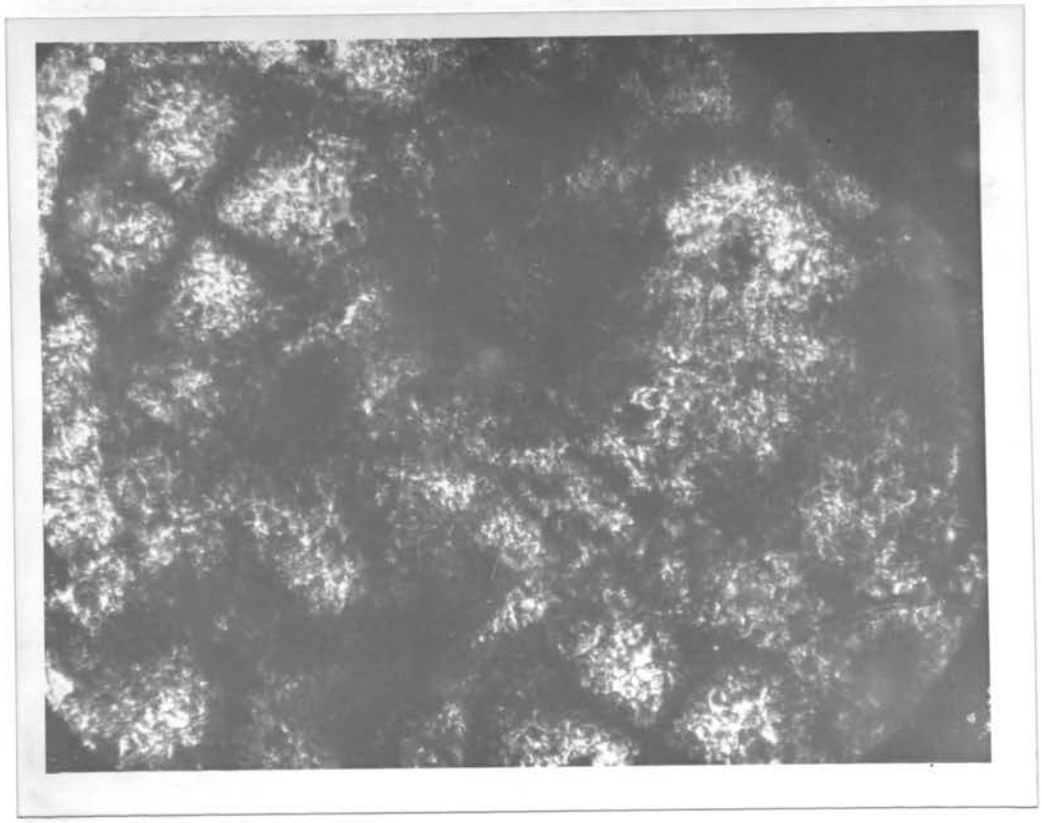

Figure 27. Photomicrograph of a glass-ceramic specimen heat-treated according to point 2.0 (Figure 14) viewed with transmitted light under crossed nicols. 300X

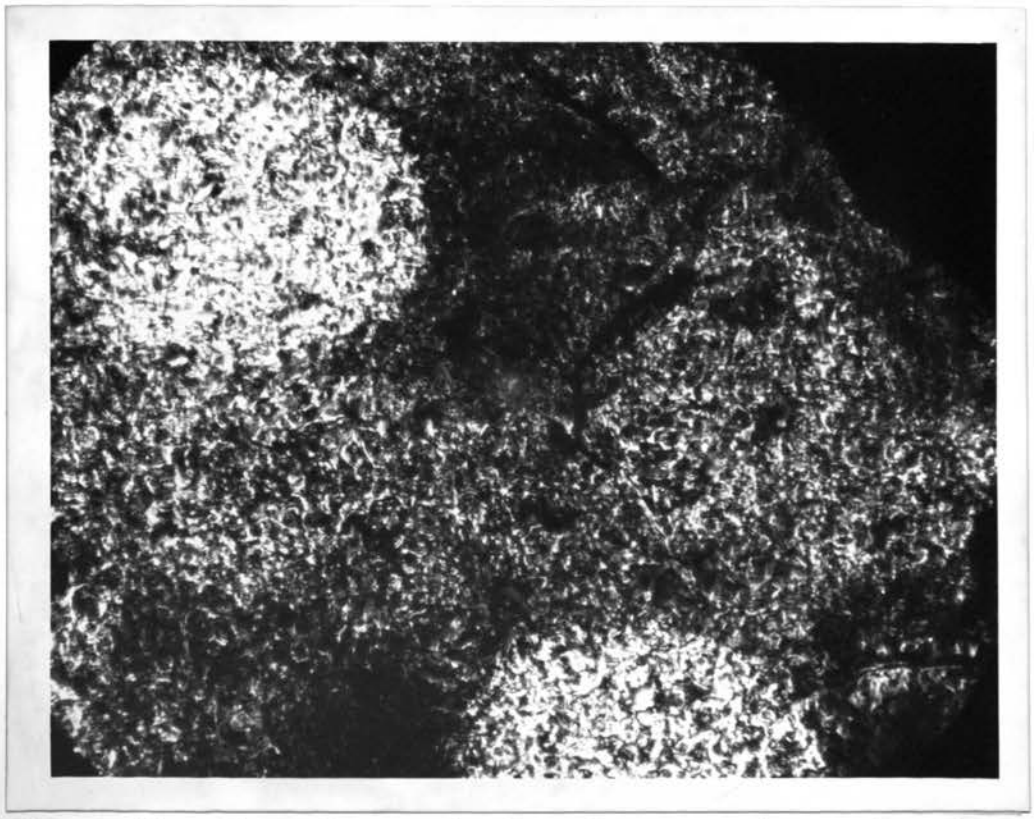

Figure 28. Photomicrograph of a glass-ceramic specimen heat-treated according to point 2.0 (Figure 14) viewed with transmitted light under uncrossed nicols. 300X

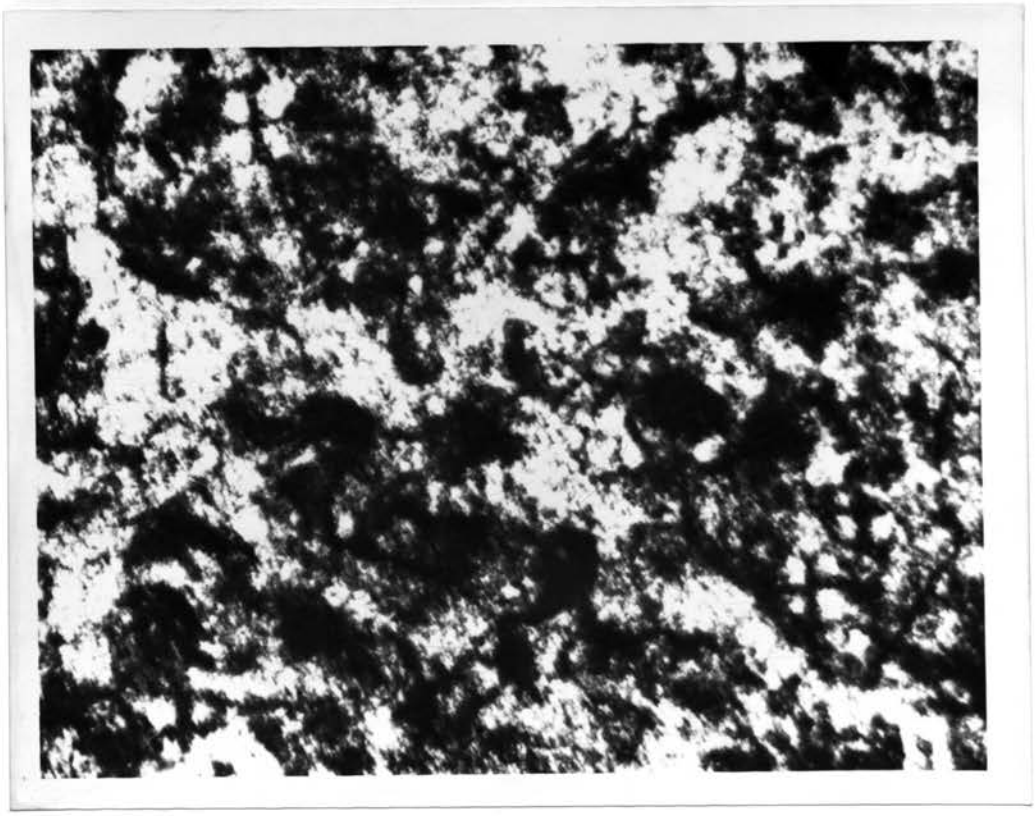

Figure 29. Photomicrograph of a glass-ceramic specimen heat-treated according to point 2.0 (Figure 14) viewed with transmitted light under crossed nicols. 39X

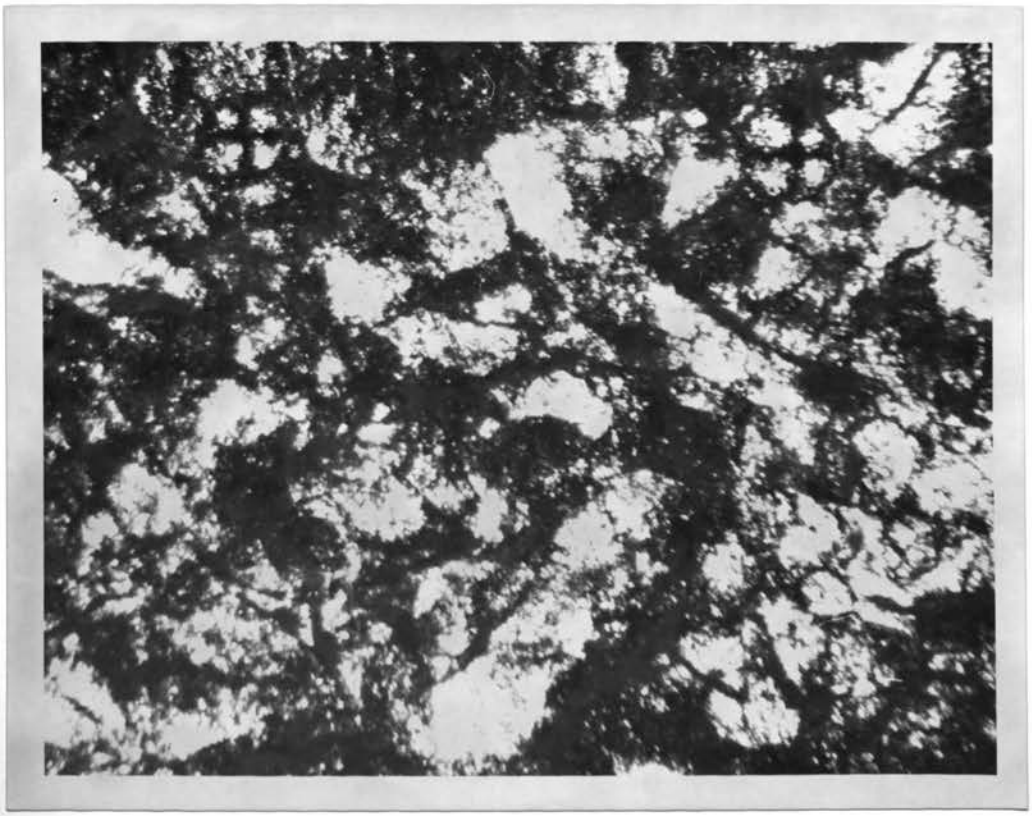

Figure 30. Photomicrograph of a glass-ceramic specimen heat-treated according to point 2.1 (Figure 14) viewed with transmitted light under crossed nicols. 37X

remained glassy slightly longer (note its more spherical shape). Another example of this can be seen in the first quadrant near the center in Figure 29. The droplet in the upper left-hand corner of Figure 30 appears to have remained glassy until nearly complete crystallization of the matrix had occurred.

Both of these cases illustrate and support Ohlberg's[35] new theory of spherulite growth, as previously discussed. The classical theory as discussed by Morse and Donnay[52] may also be supported in this study. Reference to the large structure in Figure 22 is made. Said Morse, et. al., "The first idea that naturally comes to mind is that a spherulite must grow by simultaneous crystallization of fibers radiating from a common center in all directions with equal speed." The large structure referred to appears to be formed by a mechanism allied to the one Morse described. Both mechanisms may be possible and may even occur side by side in the same sample.

Figure 31 shows the glass-ceramic near complete crystallization with crystallized droplets still visible but more difficult to distinguish. The cracks are still widespread but look somewhat "healed".

No thin-sections (or polished sections) were made of the 1.2 or 1.4 specimens because of their high porosity and crumbly nature.

I. Observations of Polished Specimens by Reflected-Light Microscopy

The metallograph was of great value in seeing the cause of cracking and the resulting weakness in the glass-ceramic cylinders. It also provided further enlightenment as to the nature of the crystalline phases which developed.

Even after the most preliminary heat-treatment, where the strength values were the highest, cracks can be seen initiating from octahedra and droplets (see Figure 32). The stress of the nucleation and growth

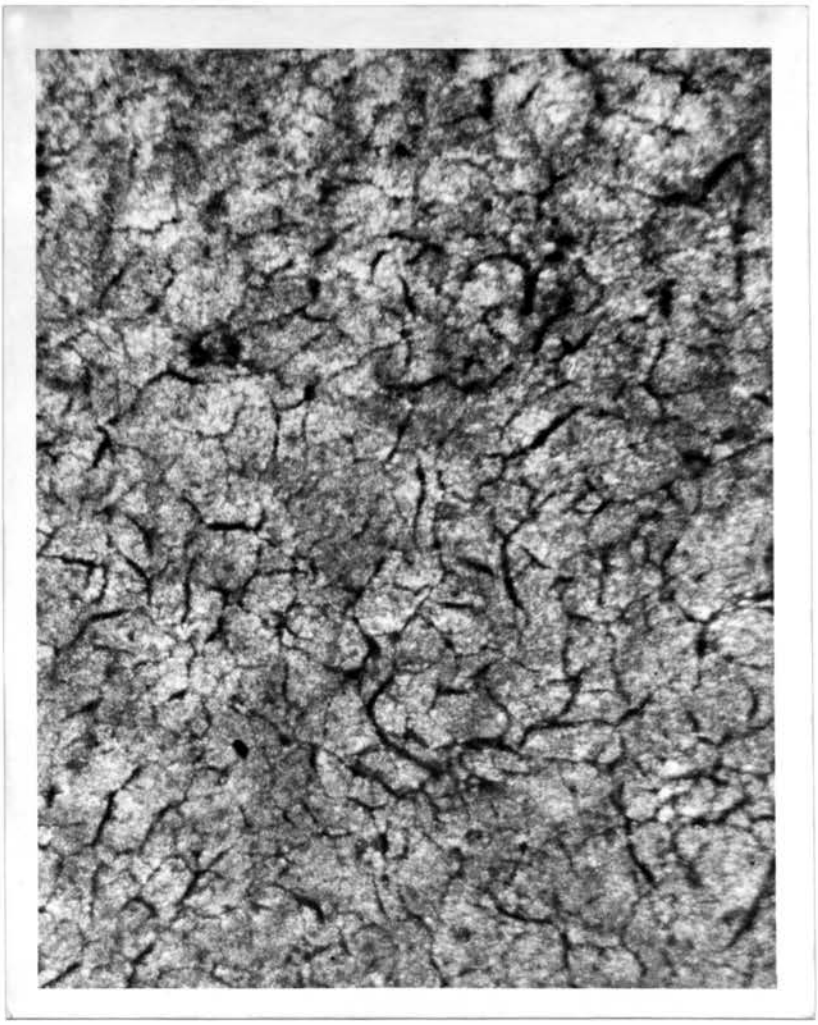

Figure 31. Photomicrograph of a glass-ceramic specimen heat-treated according to point 2.3 (Figure 14), viewed with transmitted light under uncrossed nicols. 27X

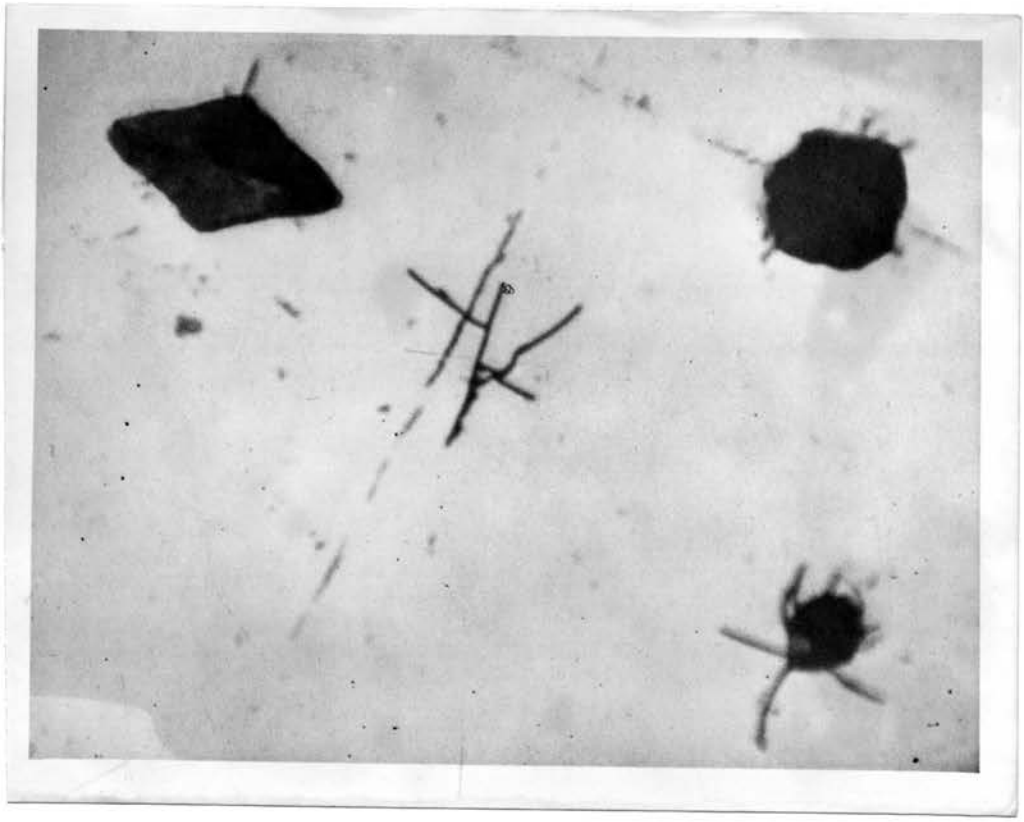

Figure 32. Photomicrograph of a glass-ceramic specimen heat-treated according to point 1.0 (Figure 14) viewed with reflected light under uncrossed nicols. 305X

process evidently was great enough to propagate flaws (whether at the interfaces or elsewhere) into visible cracks. The droplets seen here were probably crystalline since they were preferentially etched as were the other crystalline phases. Further heat-treated samples showed the cracks extending to link crystals together forming a crack network (see Figure 33).

The white areas are regions of high stress. Of interest also are the hexagonal crystals co-existing with the familiar octahedra in the glassy matrix. Figure 34 is a view of the same area using polarized light and focused below the polished surface. High birefringence is seen along the cracks. Other large crystals are made visible that were not visible on the surface, and appear as light, ghost-like octahedrons. The pinacoidal crystals radiating inward from the surface can be seen on Figure 35. Cracks connecting these crystals to a large distorted octahedron can be seen. From the other branch of the heat-treatment schedule a more nearly crystallized sample can be viewed (Figure 36). The only glassy regions left are the large white "islands" shown. It is interesting to see crystallization proceeding inward from the major cracks. Note that the well-defined crystalline forms visible in the glass are hexagonal. This crystalline habit seems to have replaced the octahedrons of the lower temperatures. A closer view of the same surface is seen in Figure 37.

Some very small glass droplets were made visible through the reflected light technique that could not be seen by transmitted light. Careful inspection of Figure 38 shows a small ring of white "dots" near the specimen surface, close to a surface crack. A closer view of these dots is revealing, for in Figure 39 the dots are seen to be very small

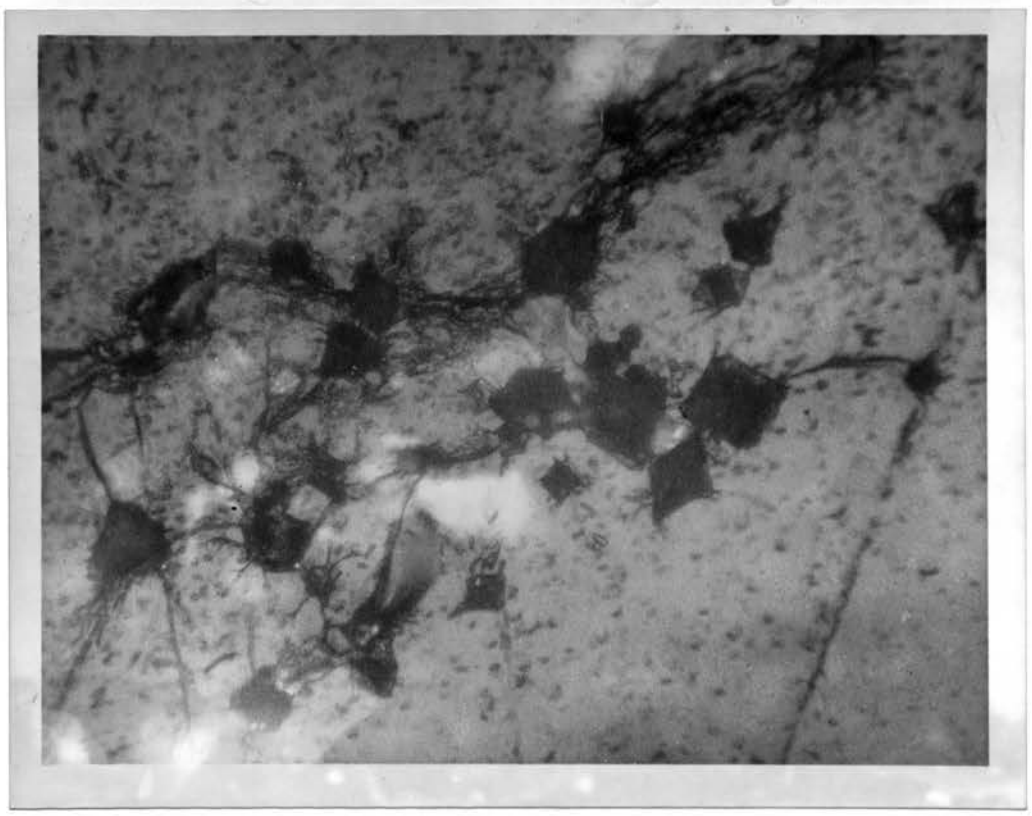

Figure 33. Photomicrograph of a glass-ceramic specimen heat-treated according to point 1.05 (Figure 14) viewed with reflected light under uncrossed nicols. 170X

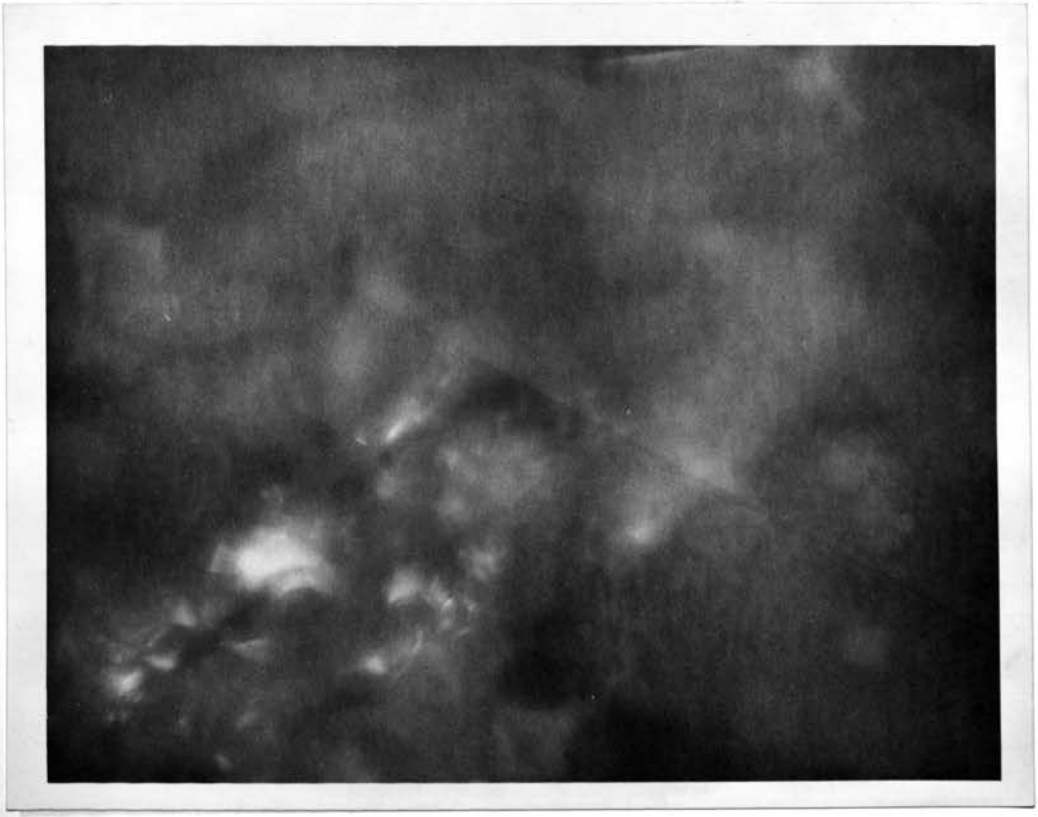

Figure 34. Photomicrograph of a glass-ceramic specimen heat-treated according to point 1.05 (Figure 14) viewed with reflected light under crossed nicols. 170X

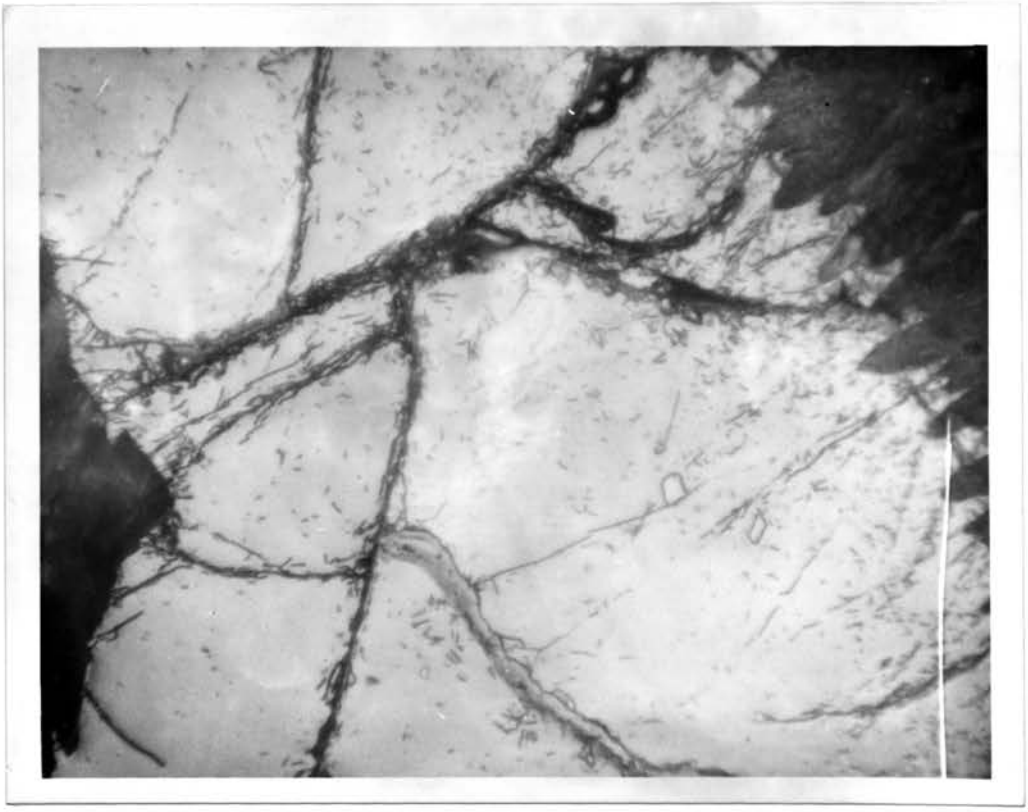

Figure 35. Photomicrograph of a glass-ceramic specimen heat-treated according to point 1.1 (Figure 14) viewed with reflected light under uncrossed nicols. 148X

Figure 36. Photomicrograph of a glass-ceramic specimen heat-treated according to point 2.1 (Figure 14) viewed with reflected light under uncrossed nicols. 60X

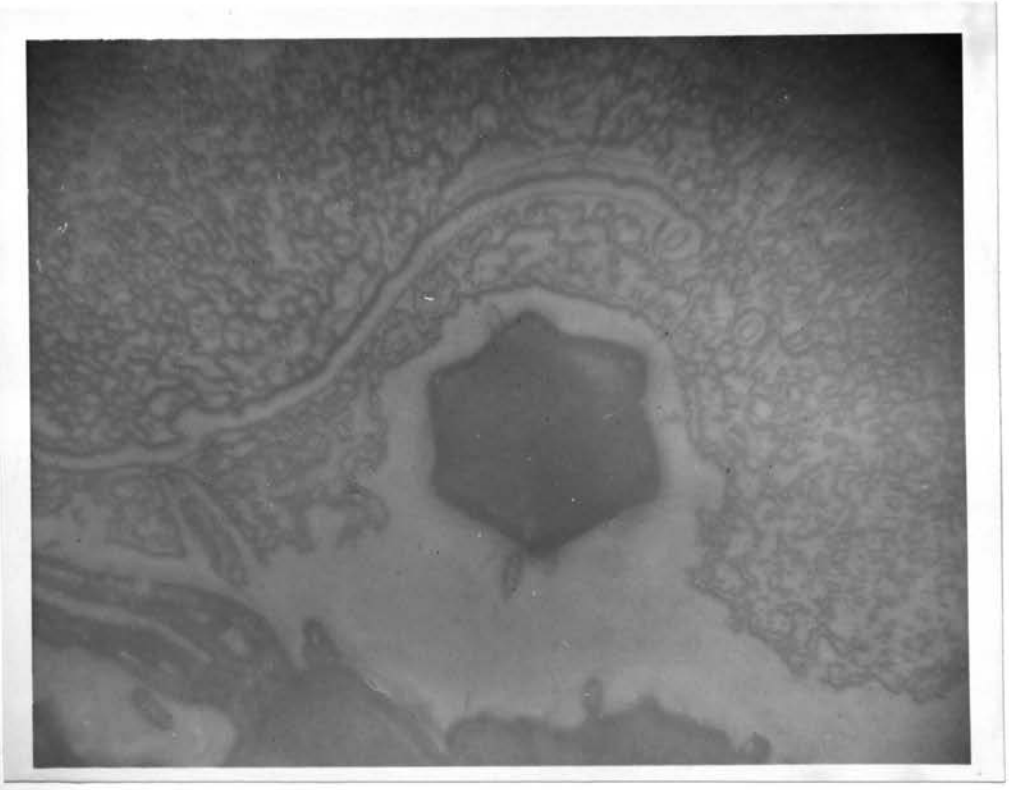

Figure 37. Photomicrograph of a glass-ceramic specimen heat-treated according to point 2.1 (Figure 14) viewed with reflected light under uncrossed nicols. 970X

Figure 38. Photomicrograph of a glass-ceramic specimen heat-treated according to point 2.0 (Figure 14) viewed with reflected light under crossed nicols. 72X

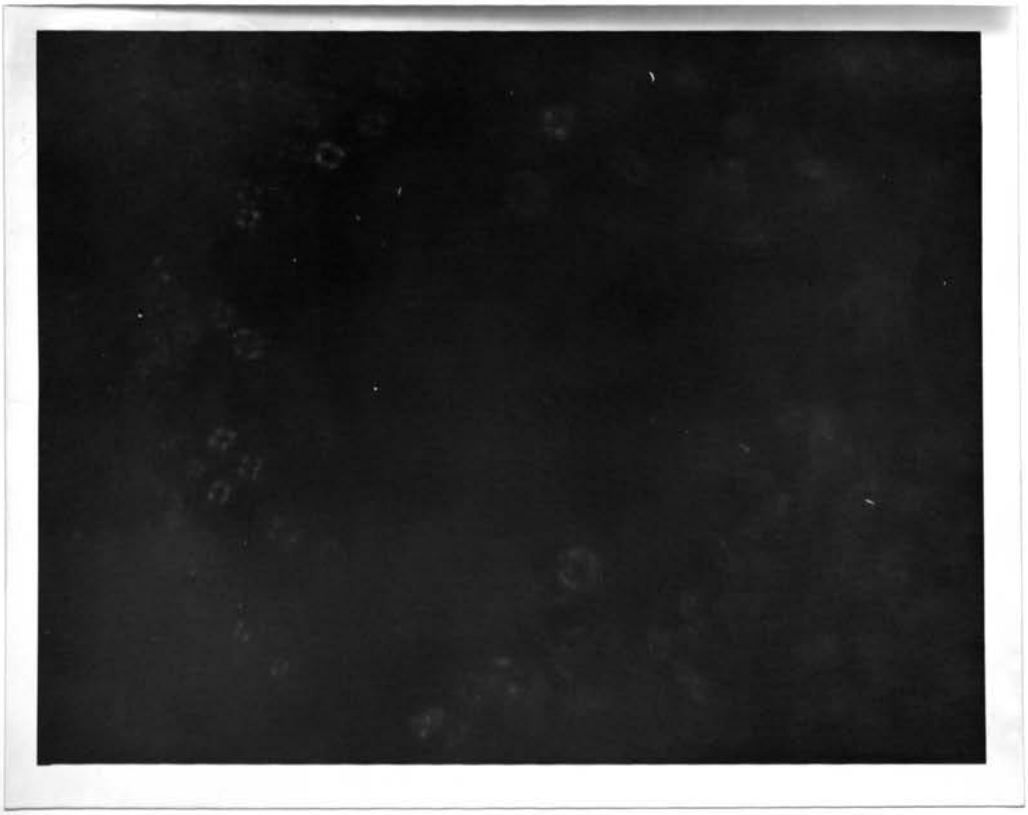

Figure 39. Photomicrograph of a glass-ceramic specimen heat-treated according to point 2.0 (Figure 14) viewed with reflected light under crossed nicols. 1100X

glass droplets complete with optic crosses still existing in the crystalline phase. It would be interesting to know the cause of the ring. It looks as if it may have been a larger droplet at lower heat-treatment stages.

Figure 40 shows a crack extending inward from the surface. These large cracks were seen on specimens which had been heat-treated less than the specimen in this figure. They appeared to have been getting smaller as the treatment went to higher temperatures.

J. Phase and Chemical Analyses

X-ray diffraction analysis identified no crystalline phases existing in the 1.0 powdered specimen. A broad, diffuse peak indicative of glass was all that was seen on the pattern. The patterns for the 2.1 and 2.3 specimens were qualitatively identical. They corresponded to the data given by Roy, et. al.,[53] for β-spodumene (negative). These data could not be found elsewhere and are given in Appendix E. β-spodumene has been assumed to have a tetragonal crystal habit on the basis of the "ditetragonal dipyramids" formed above 500° C. by Hatch[54] and Roy, et al.,[55] but, as yet, it has not been indexed on the basis of the tetragonal system. Gruner[56] suggested that β-spodumene has a quartz derivative structure like β-eucryptite. This indicates that β-spodumene is hexagonal If it is, in fact, hexagonal the photomicrographs indicate that in this study a polymorphic phase change takes place in the phase at higher temperatures to its more stable form

Ohlberg[35] identified a "silica-O" phase at the lower heat-treatment temperatures of his work by X-ray diffraction. Silica-O[45] refers to a family of phases and is the end member of a series based on the β-eucryptite structure. This phase was not identified in this study.

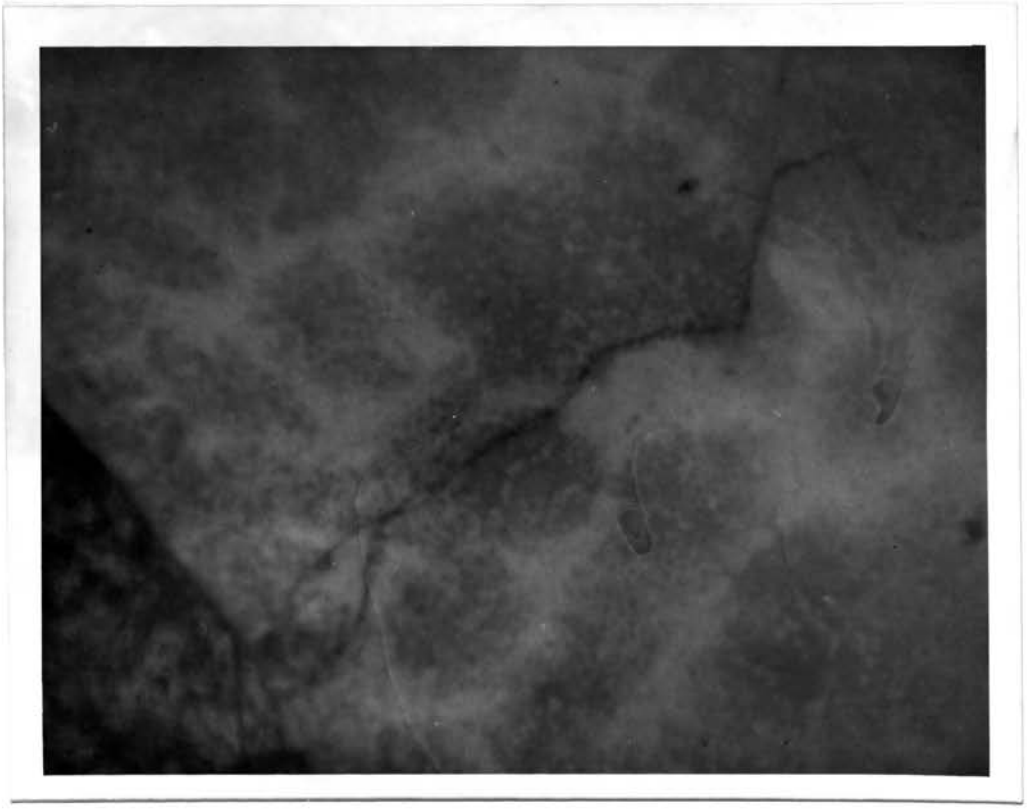

Figure 40. Photomicrograph of a glass-ceramic specimen heat-treated according to point 2.3 (Figure 14) viewed with reflected light under crossed nicols. 170X

The spectrograph merely identified the metal elements Si, Al, Mg, and Li.

K. Dilatometer Test Results

Further insight into the nature of the glass-ceramic material at the various heat-treatment stages can be gained from Figure 41. The ordinate on this figure is arbitrary for each curve in order that the curves may be distinguished from each other. This information is valuable in setting up heat-treating schedules to avoid deformation of specimens by too-rapid heating. These samples from the 1.x series all softened by 650° whereas the 2.x series softened about 1,075° C.

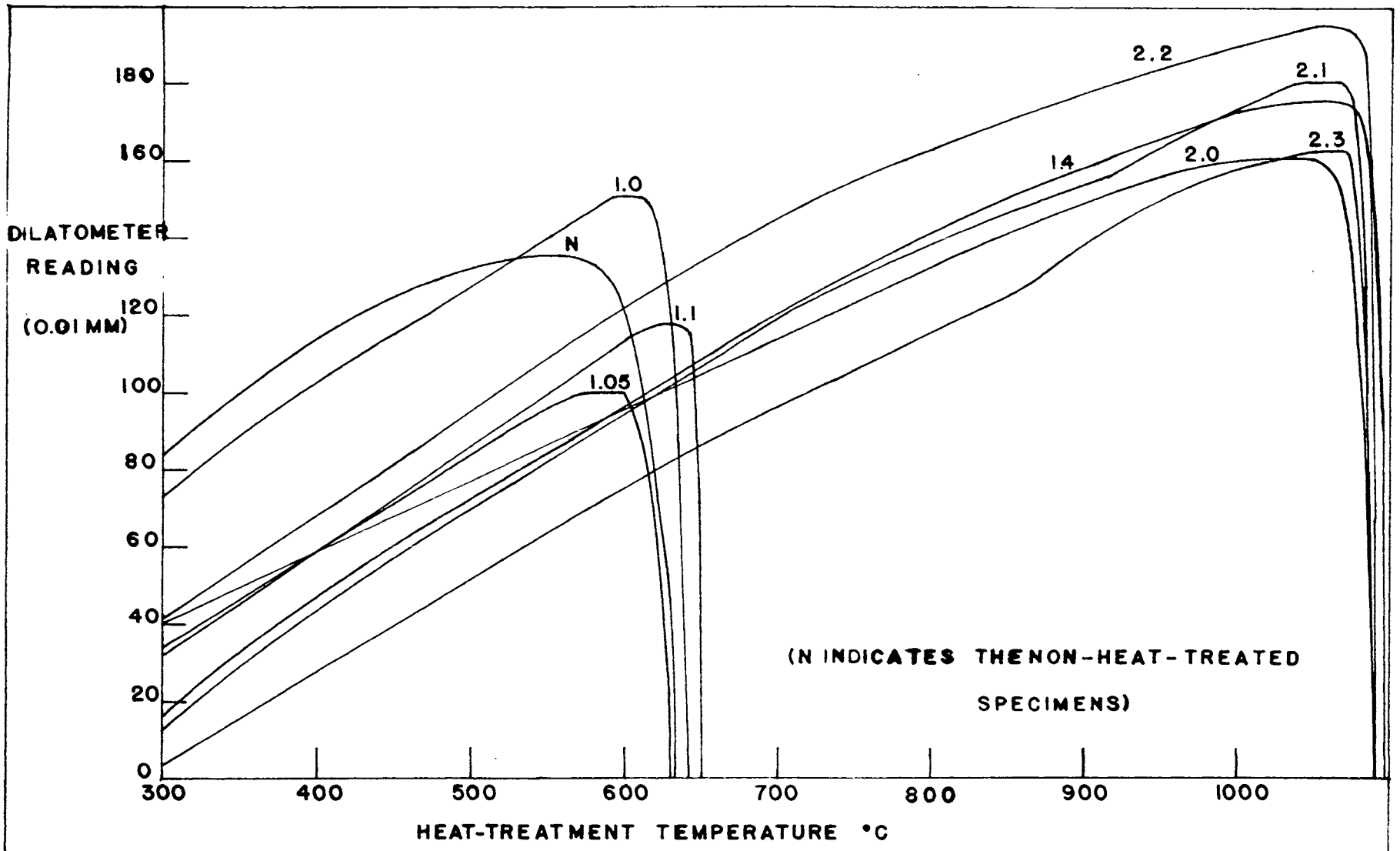

FIGURE 41. SOFTENING BEHAVIOR OF HEAT-TREATED CYLINDERS

V. SUMMARY AND CONCLUSIONS

The following conclusions were made from the results of this study:

1. Insight was gained into the anomalous growth behavior producing appendages which protruded from the main body of the glass-ceramic specimen. It was found that these appendages were not a function of the maximum heat-treatment temperature but rather of the preliminary, low-temperature, nucleation portion of the heat-treatment process. When specimens were insufficiently nucleated these anomalous external appendages occurred, apparently initiating at those areas which were in contact with other material. Well-nucleated specimens showed no such growth at the identical higher heat-treatment temperatures.

Further investigation should now be made of these appendages and the factors concerning their initiation and growth should be more precisely determined.

2. The strength of the glass-ceramic specimens was found to increase after the most preliminary stage of heat-treatment, but subsequent treatment caused a great decrease in strength. Although the considerable initial increase is not completely understood, the sharp decrease was concluded to be due to an extensive crack network which was set up by the nucleation and growth of crystalline octahedra and glass droplets, some of which crystallized.

The more thoroughly nucleated specimens then exhibited a trend toward increasing in strength at the higher heat-treatment temperatures as the final stages of crystallization were approached. This was apparently due to the healing effect of a sintering process in operation at the higher temperatures.

The less thoroughly nucleated specimens, on the other hand, continued to decrease until their strength vanished. It was concluded that this was due to the high porosity of the specimens resulting from the anomalous appendage growth carrying a good deal of the material from the inside of the specimen out with it.

3. The crystallization of the glass studied was found to proceed through three discreet mechanisms. Each of these mechanisms could be clearly seen in operation by the techniques of microscopy. First, the more common phenomenon of surface nucleation and consequent crystallization was observed from the earliest stages of heat-treatment. These nuclei grew as pinacoidal crystals radiating inward. After the crack network was set up creating new surfaces, this type of pinacoidal, surface-nucleated crystals was again observed growing inward from and perpendicular to the cracks. Second, internally nucleated glass-in-glass droplets could be seen even from the most preliminary of heat-treatments. Conclusive evidence of the important role played by those droplets in the crystallization process was recorded on photomicrographs. Third, internally nucleated, well-developed crystals, existing as octahedra in the primitive stages of heat-treatment and possessing hexagonal crystalline habit in the advanced stages were observed.

Of particular significance is the fact that none of these mechanisms seemed to play a dominant role in the nucleation and crystallization processess. Each seemed, however, to play an important role in the crystallization of the specimens and in their strength behavior at each stage of development.

4. The optional crystallization characteristics exhibited by the glass-droplets are worthy of note. Some droplets could choose to crystal-

lize and then choose to act as nuclei for crystallizing the matrix glass or remain isolated and let the matrix crystallize by other means; other droplets could choose to remain amorphous and then act as nuclei to crystallize the matrix or let the matrix crystallize independently while they still maintained their amorphous character. The factors which control the "choices" made by these droplets would be interesting for future work.

5. Evidence which served as the bases for both theories of spherulite growth was given.

6. Nucleation-induced stresses which increased during the growth of the nuclei to the point of initiating visible cracks were an important observation of this report. These and other stresses seemed to contribute to further nucleation.

It would be of interest to study further these phenomena of nucleation-induced stress and stress-induced nucleation in this system, and correlate the results with similar studies on other systems.

7. The β-spodumene phase observed in this study was seen to undergo a polymorphic phase transformation from the tetragonal to the hexagonal crystal systems.

8. Extremely small (1 - 4μ) glass droplets existing at higher heat-treatment temperatures in an otherwise crystalline specimen were observed These haven't been reported before in this system and would be an interesting area of future study.

In addition to those already mentioned, the following recommendations are made for future study:

1. The crystal system of β-spodumene should be identified from the published, X-ray diffraction data.

2. A study should be made of the exact stage of nuclei and crystal development in which cracks begin to appear at given heat-treatment rates and temperatures. This might be done using sonic means by measuring the damping coefficients of the material.

3. The substantial increase in strength of the specimens studied in this report on preliminary heat-treatment was not expalined herein. Although other studies on glass-ceramics have shown an increase in strength on crystallization, no strength increase has been reported at such an early stage in the heat-treatment process. Investigation in this area may prove of great value in our understanding of observed glass strengths.

BIBLIOGRAPHY

1. B. E. Warren, H. Krutter, and O. Morningstar, "Fourier Analysis of X-ray Patterns of Vitreous SiO_2 and B_2O_3," J. Am. Ceram. Soc., 19 (7) 202-06 (1936).

2. W. H. Zachariasen, "Atomic Arrangement in Glass," J. Am. Chem. Soc., 54 (10) 3841-51 (1932).

3. G. W. Morey, Properties of Glass, 2d ed., Reinhold Publishing Corp., New York, 1954. 561 pp.

4. M. Polanyi, Z. Phys., 7 (1921) 323.

5. E. Orowan, "Energy Criteria for Fracture," Welding J., 34 (1955) 1575-78.

6. R. Houwink, Elasticity, Plasticity and Structure of Matter, 2d ed., Harren Press, Washington, D. C.

7. A. A. Griffith, "Phenomena of Rupture and Flow in Solids," Phil. Trans. Roy. Soc. London, A221 (1920) 163-98.

8. F. O. Anderegg, "Strength of Glass Fiber," Ind. Eng. Chem., 31 (1939) 290-98.

9. C. E. Inglis, "Stresses in a Plate Due to the Presence of Cracks and Sharp Corners," Proc. Inst. Naval Arch., 55 (1913) 219.

10. B. Epstein, "Statistical Aspects of Fracture Problems," J. Appl. Phys., 19 (1948) 140-47.

11. J. C. Fisher, and R. J. Charles, Conference on Non-Crystalline Solids, John Wiley and Sons, Inc., New York (1959).

12. M. Watanabe and T. Moriya, "A Consideration on Relation Between Mechanical Behavior of Glasses and Their Internal Structure," Rev. Elect. Common Lab., 9 (1 & 2) 50-71 (1961).

13. C. H. Phillips, Glass - Its Industrial Applications, Reinhold Publishing Corp., New York (1960). 252 pp.

14. M. Watanabe, H. Hoake, and T. Aiba, "Electron Micrographs of Some Borosilicate Glasses and Their Internal Structure," J. Am. Ceram. Soc., 42 (12) 593-99 (1959).

15. T. Moriya, "The Constitution of Glass," J. Japanese Ceram. Assoc., 55 and 56 (1947 and 1948) 60, 87, 134, and 4.

16. M. Watanabe, R. V. Caporali, and R. E. Mould, "The Effect of Chemical Composition on the Strength and Static Fatigue of Soda-Lime Glass," Physics and Chemistry of Glasses, 2 (1) 12-23 (1961).

17. S. Spinner, "Elastic Moduli of Glasses at Elevated Temperatures by a Dynamic Method," J. Am. Ceram. Soc., 39 (3) 113 (1956).

18. H. T. Jessop and F. C. Harris, Photoelasticity - Principles and Methods, Dover Publications, Inc., New York (1960). 184 pp.

19. P. J. F. Wright, "Comments on an Indirect Tensile Test on Concrete Cylinders," Magazine of Concrete Research, 7 (20) 87-96 (1955).

20. R. E. Moore, Statistical Analysis of Fracture Stresses of Triaxial Porcelain Bodies, Thesis, Missouri School of Mines and Metallurgy (1962). 163 pp.

21. W. J. Kenny and E. L. Piret, "Slow Compression Crushing of Single Particles of Glass," A. I. Ch. E. J., 7 (2) 199-202 (1961).

22. F. Carneiro, "Une Nouvelle Methode d'Essai Pour Determiner la Resistance a la Traction du Beton," Reunion des Laboratoires d'Essai de Materiaux, Paris, France (1947).

23. W. J. Kenny, Energy - New Surface Relationship in the Crushing of Solids, Thesis, University of Minnesota, Microfilm, (1957).

24. S. D. Stookey, Fundamentals of Glass-Ceramics, Corning Glass Works, Corning, New York. (1958).

25. M. Watanabe, R. V. Caporali, and R. E. Mould, "The Effect of Heat Treatment on the Strength and Abrasion Resistance of a Glass-Ceramic Material," pp. 23-28 in Symposium on Nucleation and Crystallization in Glasses and Melts, American Ceramic Society, 1962.

26. M. Reaumur, Memoires de L'Academie des Sciences, Paris, France (1939) 370-88.

27. S. D. Stookey, "Ceramics Made by Nucleation of Glass - Comparison of Microstructure and Properties With Sintered Ceramics," pp. 1-4 in Symposium on Nucleation and Crystallization in Glasses and Melts, American Ceramic Society, 1962.

28. W. D. Kingery (editor), Ceramic Fabrication Processes, The Technology Press, Massachusetts Institute of Technology, and John Wiley and Sons, Inc., New York (1960). 235 pp.

29. R. E. Mould and R. D. Southwick, "Strength and Static Fatigue of Abraded Glass Under Controlled Ambient Conditions: I. General Concepts and Apparatus," J. Am. Ceram. Soc., 42 (11) 542-47 (1959).

30. R. E. Mould and R. D. Southwick, "Strength and Static Fatigue of Abraded Glass Under Controlled Ambient Conditions: II. Effect of Various Abrasions and the Universal Fatigue Curve," J. Am. Ceram. Soc., 42 (12) 582-92 (1959).

31. R. E. Mould, "Strength and Static Fatigue of Abraded Glass Under Controlled Ambient Conditions: III. Aging of Fresh Abrasions," J. Am. Ceram. Soc., 43 (3) 160-67 (1960).

32. R. E. Mould, "Strength and Static Fatigue of Abraded Glass Under Controlled Ambient Conditions: IV. Effect of Surrounding Medium," J. Am. Ceram. Soc., 44 (10) 481-91 (1961).

33. S. D. Stookey, Method of Making Ceramics and Product Thereof, Japanese Patent SHOWA 32-5080 (1957).

34. W. D. Kingery, Introduction to Ceramics, John Wiley and Sons, Inc., New York and London, p. 314 (1960).

35. S. M. Ohlberg, H. R. Golob, and D. W. Strickler, "Crystal Nucleation by Glass in Glass Separation," pp. 55-62 in Symposium on Nucleation and Crystallization in Glasses and Melts, American Ceramic Society, 1962.

36. S. D. Stookey, "Catalyzed Crystallization of Glass in Theory and Practice," V. Internationaler Glaskongress (Fifth International Congress on Glass), Glastech. Ber., 32K (1959) v/1-8.

37. R. Roy, "Metastable Liquid Immiscibility and Subsolidus Nucleation," J. Am. Ceram. Soc., 43 (12) 670-71 (1960).

38. W. B. Hillig, "A Theoretical and Experimental Investigation of Nucleation Leading to Uniform Crystallization of Glass," pp. 77-89 in Symposium on Nucleation and Crystallization in Glasses and Melts, American Ceramic Society, 1962.

39. W. Vogel and K. Gerth, "Catalyzed Crystallization in Glass," pp. 11-22 in Symposium on Nucleation and Crystallization in Glasses and Melts, American Ceramic Society, 1962.

40. J. W. Greig, "Immiscibility in Silicate Melts, I-II," Ceram. Abstr., 6 (4) 157 (1927).

41. B. E. Warren and A. G. Pincus, "Atomic Consideration of Immiscibility in Glass Systems," J. Am. Ceram. Soc., 23 (10) 301-04 (1940).

42. R. Roy, "Phase Equilibria and the Crystallization of Glass," pp. 39-45 in Symposium on Nucleation and Crystallization in Glasses and Melts, American Ceramic Society, 1962.

43. S. M. Ohlberg, H. R. Golob, and C. M. Hollabaugh, "Fractography of Glasses Evidencing Liquid-in-Liquid Colloidal Immiscibility," J. Am. Ceram. Soc., 45 (1) 1-4 (1962).

44. D. Turnbull, "Transient Nucleation," Trans. Am. Inst. Mining Met. Engrs., 175 (1948) 744-83.

45. R. Roy, "Silica-O, a New Common Form of Silica," Z. Krist., 111 (3) 185-89 (1959).

46. M. Tashiro, S. Sakka, and M. Wada, "Mechanical Strength of Polycrystalline Materials Produced from Platinum Containing Glasses," J. Ceram. Soc. Japan, 68 (778) 223-30 (1960); Abstract, Physics and Chemistry of Glasses, Soc. of Glass Tech., 3, April 1962.

47. S. Sakka, M. Wada, and M. Tashiro, "Effects of Heat Treatment on the Strength of Polycrystalline Material Produced from Glass of the System Li_2O-MgO-Al_2O_3-SiO_2," Yogyo Kyokai Shi, 69 (782) 35-43 (1961); Abstract, J. Am. Ceram. Soc., 45 (6) 137, June 1962.

48. S. M. Ohlberg, Personal communication to D. E. Day, Advisor (1962).

49. S. D. Stookey, Method of Making Ceramics and Product Thereof, U.S. Patent 2,920,971. Ceram. Abstr., p. 142a (1960).

50. R. L. Anderson, "The Automatic Polishing of Metallographic Specimens," pp. 58-77 in Symposium on Methods of Metallographic Specimen Preparation, ASTM Sp. Tech. Publ. No. 285, 1960.

51. R. W. Dayton, "Theory and Use of the Metallurgical Polarization Microscope," Trans. Am. Inst. Mining Met. Engrs., 117, 145-48 (1935).

52. H. W. Morse and J. D. H. Donnay, "Optics and Structure of Three-Dimensional Spherulites," Am. Mineralogist, 21 (7) 391-426 (1936).

53. R. Roy, D. M. Roy, and E. F. Osborn, "Compositional and Stability Relationships Among the Lithium Alumina Silicates: Eucryptite, Spodumene, and Petalite," J. Am. Ceram. Soc., 33 (5) 155,157 (1950).

54. R. A. Hatch, "Phase Equilibrium in the System Li_2O-Al_2O_3-SiO_2," Am. Mineralogist, 28, 471-96 (1943); Ceram. Abstr., 23 (1) 26 (1944).

55. R. Roy and E. F. Osborn, "The System Lithium Metasilicate-Spodumene Silica," J. Am. Chem. Soc., 71, 2086-95 (1949).

56. J. W. Gruner, "Progress in Silicate Structures," Am. Mineralogist, 33 (11/12) 679-91 (1948).

57. W. Weibull, "A Statistical Theory of the Strength of Materials," Ing. Vetenskaps Akad, Handl., 151. "The Phenomenon of Rupture in Solids," Ibid, 153.

58. C. H. Greene, "Flaw Distributions and the Variation of Glass Strength With Dimensions of the Sample," J. Am. Ceram. Soc., 39 (2) 66 (1956).

59. T. A. Kontorova, J. Tech. Phys., USSR, 10 (1940) 886.

60. J. J. Frenkel and T. A. Kontorova, "A Statistical Theory of the Brittle Strength of Real Crystals," J. Tech. Phys., USSR, 7 (1943) 108.

61. J. D. Fisher and J. H. Hollomon, Trans. Am. Inst. Mech. Engrs., 121 (1947) 546.

62. S. Kase, "A Theoretical Analysis of the Distribution of Tensile Strength of Vulcanized Rubber," J. Polymer Sci., 11 (1953) 425-31.

63. S. Timoshenko, Theory of Elasticity, 1st ed., McGraw-Hill Book Co., Inc., New York and London, pp. 104-108 (1934).

64. M. M. Frocht, Photoelasticity, vol. 2, John Wiley and Sons, Inc., New York, pp. 121-129 (1948).

65. Hoyt and Scheil, "Use of the Polarizing Microscope in the Study of Inclusions in Metals," Trans. A.I.M.E., 116 (1935) 405.

APPENDIX A

APPENDIX A

SUMMARY OF STATISTICAL THEORIES OF FRACTURE

The following is a summary of statistical theories of fracture taken from the work of Epstein[10,11]:

(1) Let the underlying probability distribution of flaw strengths $\underline{s}$ be $\underline{f(s)}$, so that the probability that the strength of a given flaw lies between s_1 and s_2 is $\int_{s_1}^{s_2} f(s)ds$.

(2) The associated cumulative distribution, giving the probability that the strength of a given flaw is less than $\underline{s}$, then is $F(s) = \int_{-\infty}^{s} f(s)ds$.

(3) The probability distribution of the strength of a sample containing $\underline{n}$ flaws then is $g_n(s) = nf(s)[1 - F(s)]^{n-1}$, for which,

(4) The associated cumulative distribution function is $G_n(s) = \int_{-\infty}^{s} g_n(s)ds = 1 - [1 - F(s)]^n$.

(5) (When $\underline{n}$ is sufficiently large, the probability distribution of the strength of a sample containing $\underline{n}$ flaws simplifies to $g_n(s) \approx nfe^{-nF}$, and the cumulative distribution to $G_n(s) \approx 1\text{-}e^{-nF}$, where f and F stand for f(s) and F(s).)

(6) The most probable strength of a sample containing $\underline{n}$ flaws corresponds to the maximum of $g_n(s)$. It is S_n^* in the relationship,

$$(n-1)[f(S_n^*)]^2 = f'(S_n^*)[1-F(S_n^*)]$$

(7) Most statistical theories of fracture differ from one another only in the form of the distribution function f(s) that is assumed.

On the basis of Epstein's treatment, it is convenient to classify statistical theories of fracture according to the various sorts of distribution laws f(s) that are assumed to relate the probability of failure of a flaw to the stress.

(1) Weibull[57] and more recently Greene[58] assume $f(s) = ks^m$. When their data cannot be fit with so simple a law, Weibull used $f(s) = k(s-s_o)^m$, and Greene uses $f(s) = \sum_{i=o}^{\infty} {}_i k_i s^{m_i}$. Weibull fits the experimental fracture strengths of glazed porcelain, portland cement, Indian cotton fibers, cotton yarn, cotton fabric strips, green spruce, a mixture of stearic acid and plaster of Paris, aluminum die castings, malleable iron castings, and valve spring wire. Greene fits the strengths of glass samples of various sizes.

(2) Kontorova[59] does not assume a form of f(s) directly but instead says that the important flaws are cracks that fail according to Griffith's formula, $s = Ac^{-1/2}$ (s is the fracture stress, A a constant, c the crack diameter). The crack sizes are assumed to be distributed according to the probability law $p(c) \sim e^{-\beta(c-c_o)^2}$.

(3) Frenkel and Kontorova[60] assume $f(s) \sim e^{-a(s-s_o)^2}$.

(4) Fisher and Hollomon[61] assume that the important flaws are cracks that respond to stress according to Griffith's formula, and that the crack diameters are distributed according to the probability law $p(c) = \lambda e^{-\lambda c}$, with λ a constant. For hydrostatic tension, the corresponding f(s) is $f(s) = (2s_o^2/s^3)e^{-s_o^2/s^2}$, with s_o a constant; and for other stress combinations f(s) is a more complicated function. These workers fit the strengths of glass samples of various sizes.

(5) Kase[62] assumes that the important flaws are cracks, but that the tensile stress is reduced by a flaw of area A according to the equation $s = s_o(1-aA)$, where s_o and a are constants. Assuming the flaw areas to be distributed according to the law $f(A) = \lambda e^{-\lambda A}$, he obtains $F(s) = d^{-e^{\beta(s-s^*)}}$, with β and s^* constants, as the cumulative distribution law for the strength of samples containing many flaws, and fits the experimental data for samples of rubber.

Different as these several forms of f(s) may be, they all can be made to fit at least a portion of the experimental data. They all predict that larger samples will be weaker, and that the distributions of fracture stresses will be skewed toward smaller stresses, as is observed. These observations do not enable the selection of any one of the proposed forms of f(s) as most nearly correct, but they do suggest that the idea of randomly distributed flaws has merit.

APPENDIX B

APPENDIX B

DERIVATION OF STRESSES IN A DIAMETRALLY LOADED CYLINDER

A. Introduction

A new test has been introduced by Fernando Carneiro[22] of Brazil, in which a compressive load is applied to a cylinder along two opposite generators. This condition sets up a uniform tensile stress over the diametral plane containing the applied load, and fracture occurs along this plane. The test is carried out in a compression testing machine, strips of packing material normally being placed between the specimen and the platens of the machine. An attractive feature of the test is that it enables similar specimens, and the same testing machine, to be used for both tensile and compressive strength tests.

B. The Distribution of Stress in a Diametrally Loaded Disc

It has been shown by mathematical analysis[63,64] that a compressive load applied perpendicularly to the axis of a cylinder and in a diametral plane gives rise to a uniform tensile stress over that plane. A simplified treatment of this problem as described by Frocht[64] is given below. The theory is based on two fundamental conditions of stress distribution, which can both be deduced by mathematical analysis.

The first basic stress distribution is that due to a concentrated force P (Figure 42) acting on the edge of a plate of thickness t bounded by one straight edge but otherwise unlimited in extent. Assuming the material to obey Hooke's law that stress is proportional to strain, and assuming a condition of plane stress (i.e., no stresses perpendicular to the plane of the plate), the stress components on the element shown are:

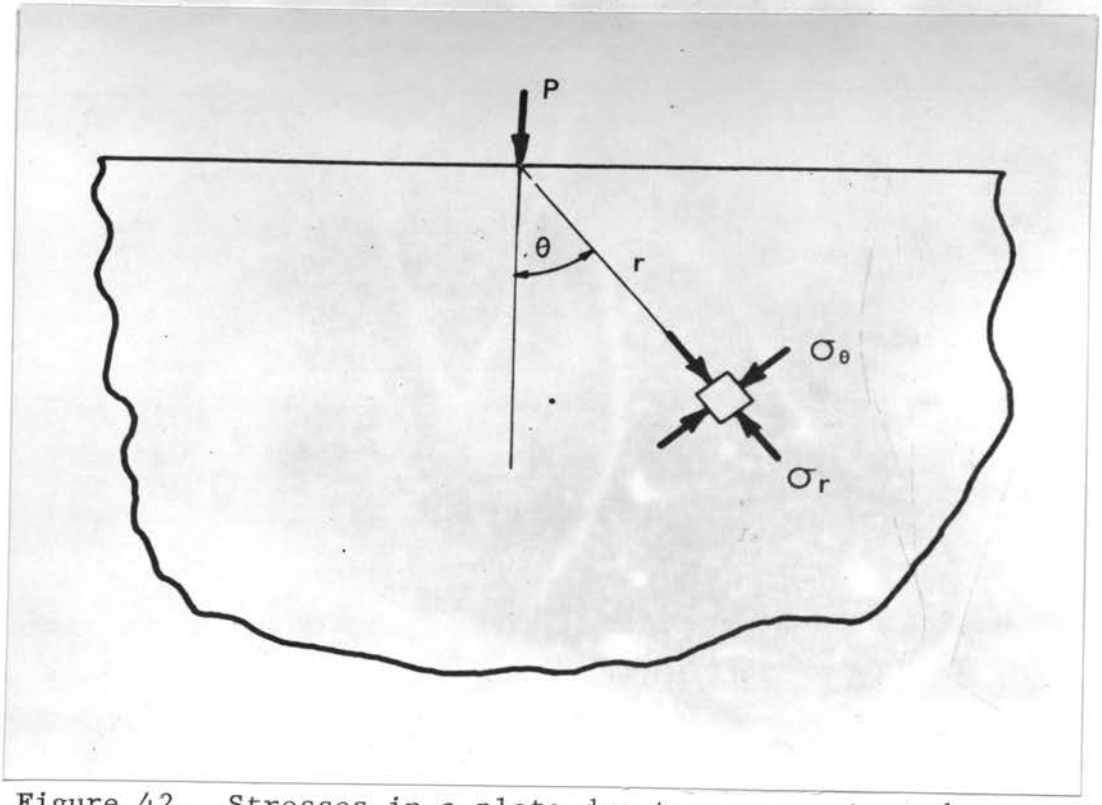

Figure 42. Stresses in a plate due to a concentrated load P_1 applied to an edge.

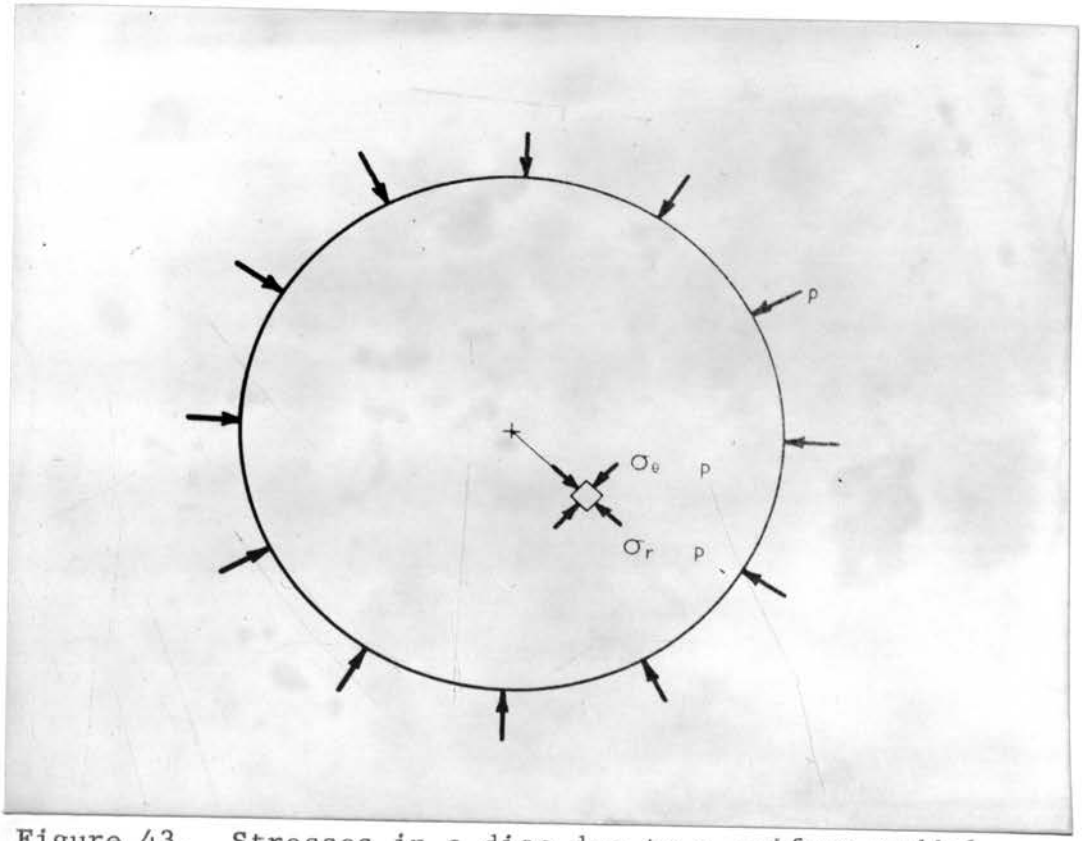

Figure 43. Stresses in a disc due to a uniform radial pressure P.

radial stress, towards the point of application of the load	$\sigma_r = \frac{2P}{\pi t} \frac{\cos \theta}{r}$
circumferential stress, perpendicular to σ_r	$\sigma_\theta = 0$
shear stress	$\tau_{r\theta} = 0$

Thus a concentrated load gives rise to a radial compression which decreases as r increases and as θ increases.

The second basic stress distribution is that in a circular disc subjected to a uniform pressure p round the edge (Figure 43). Making the same assumptions as previously, the stress in any direction and at any point is equal to the applied pressure p, and there is no shear.

$$\sigma_r = p$$
$$\sigma_\theta = p$$
$$\tau_{r\theta} = 0$$

In Figure 44 is shown a circular disc subjected to a concentrated load P, the disc being considered as part of the plate in Figure 42. At any point on the circumference there is a stress $\frac{2P}{\pi t} \frac{\cos \theta}{r}$ acting towards O, and, from the geometry of the figure, $r/d = \cos \theta$. Therefore,

$$\sigma_r = \frac{2P}{\pi t} \frac{1}{d}$$

Let the circular area be removed from the plate (Figure 45) and such stresses, q, be applied to the circumference as will maintain the same conditions of stress within the disc; i.e., let stresses be applied exactly equal to those exerted by the surrounding area of the plate. Considering the equilibrium of the element ABC,

$$\frac{2P}{\pi td} BC = qAC$$

Therefore

$$q = \frac{2P}{\pi td} \frac{BC}{AC} = \frac{2P}{\pi td} \cos\theta$$

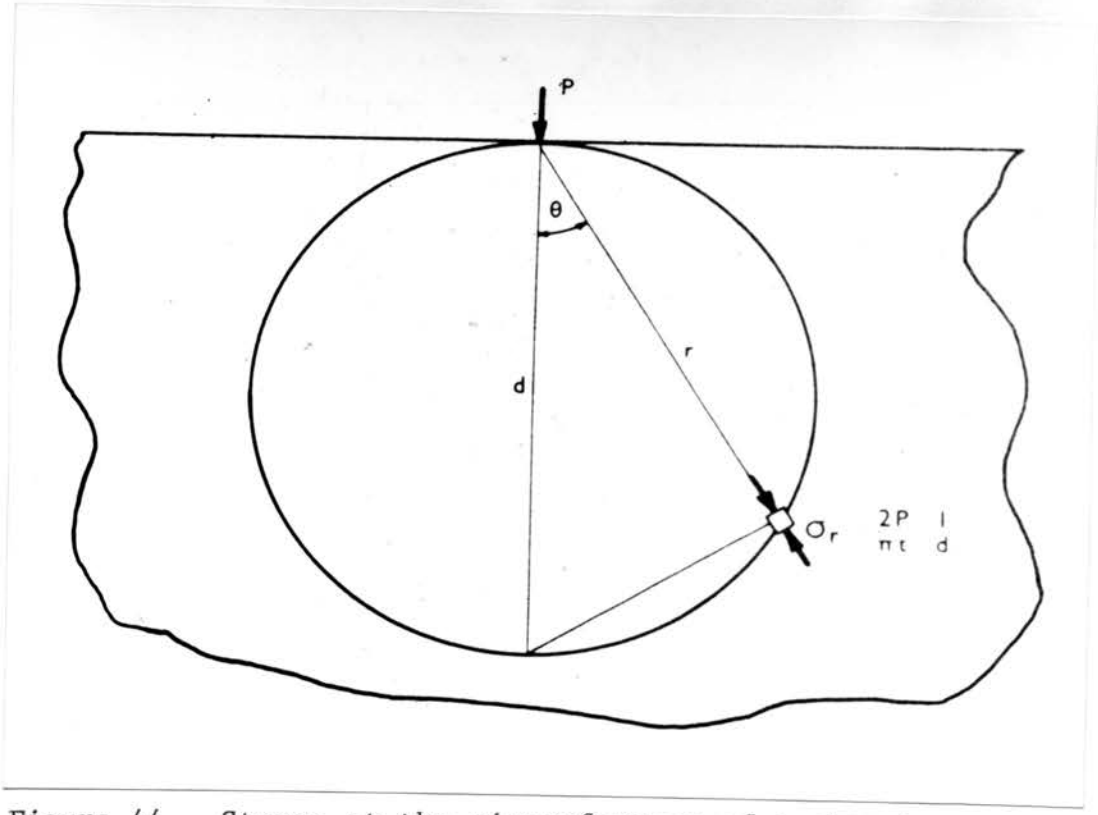

Figure 44. Stress at the circumference of a circular area of the plate shown in Figure 42.

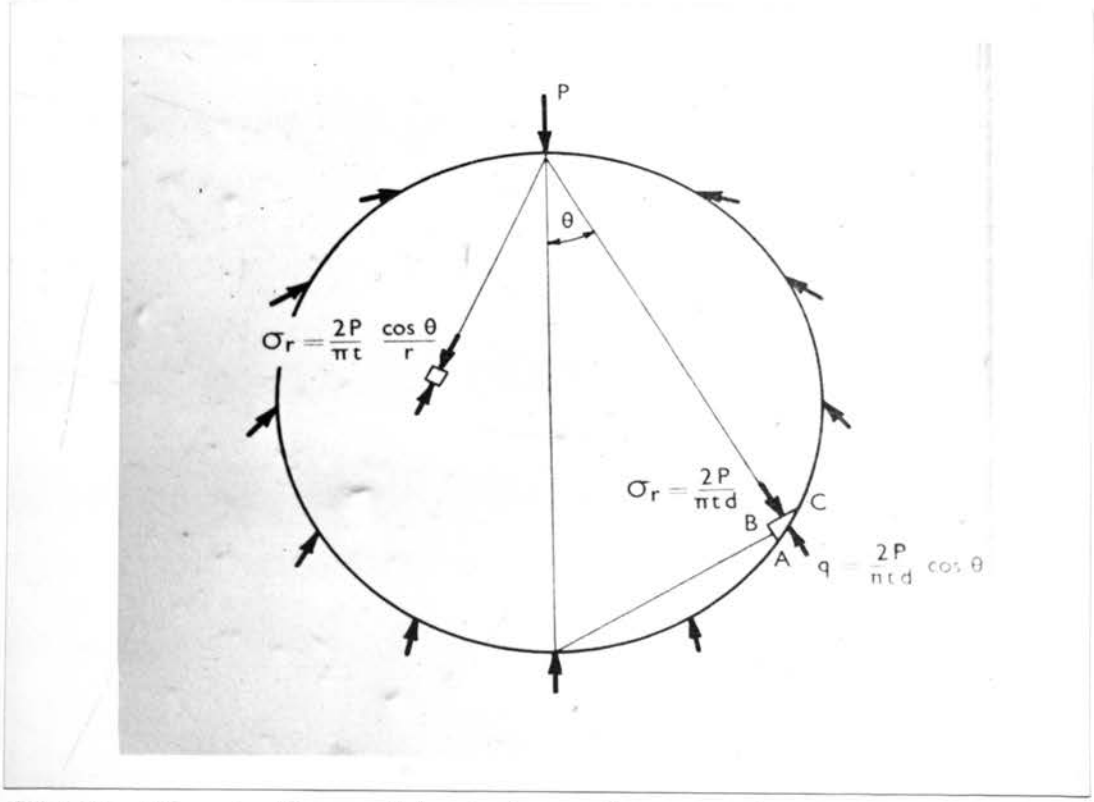

Figure 45. A disc subjected to the same loading as the circular area of the plate in Figure 44.

There are no forces in the direction BC. The stress at any point within the disc is still $\frac{2P}{\pi t}\frac{\cos\theta}{r}$.

The conditions would be similar if the force P acted on the bottom of the disc, and, therefore, upon the system of stresses already described, a similar system inverted may be superimposed (Figure 46). We now have a disc subjected to two opposite forces P acting along a diameter, and two sets of stresses, acting on the circumference, of magnitude $\frac{2P}{\pi td}\frac{r}{d}$ along AO and $\frac{2P}{\pi td}\frac{r_1}{d}$ along AO_1. These two external stresses are proportional to AO and AO_1 and may therefore be represented by these lines in a parallelogram of stresses. The resultant is clearly $AB = \frac{2P}{\pi td}$, which is constant and passes through the center. Thus the two systems together are equivalent to a uniform radial compression of magnitude $\frac{2P}{\pi td}$. Any element within the disc is now subject to two radial stresses.

Let us now superimpose a uniform radial tension of magnitude $\frac{2P}{\pi td}$ acting on the circumference of the disc. The resultant distributed loads now vanish, and we are left with the conditions of the problem; i.e., a disc subjected to two opposite forces acting along a diameter (Figure 47). Also, this uniform tension gives rise to a tensile stress $\frac{2P}{\pi td}$ at all points in the disc and in any direction. Any element A is therefore subject to the two compressive stress components $\frac{2P}{\pi t}\frac{\cos\theta}{r}$ and $\frac{2P}{\pi t}\frac{\cos\theta}{r_1}$, as indicated, and a tensile stress $\frac{2P}{\pi td}$ in all directions. The exact stresses at any point can thus be calculated readily. In particular, on the vertical diameter,

$$\theta = \theta_1 = 0$$

Thus the vertical stress component (compressive)

$$= \frac{2P}{\pi t}\frac{1}{r} + \frac{2P}{\pi t}\frac{1}{d - r} - \frac{2P}{\pi td}$$

$$= \frac{2P}{\pi td}\left(\frac{d}{r} + \frac{d}{d - r} - 1\right)$$

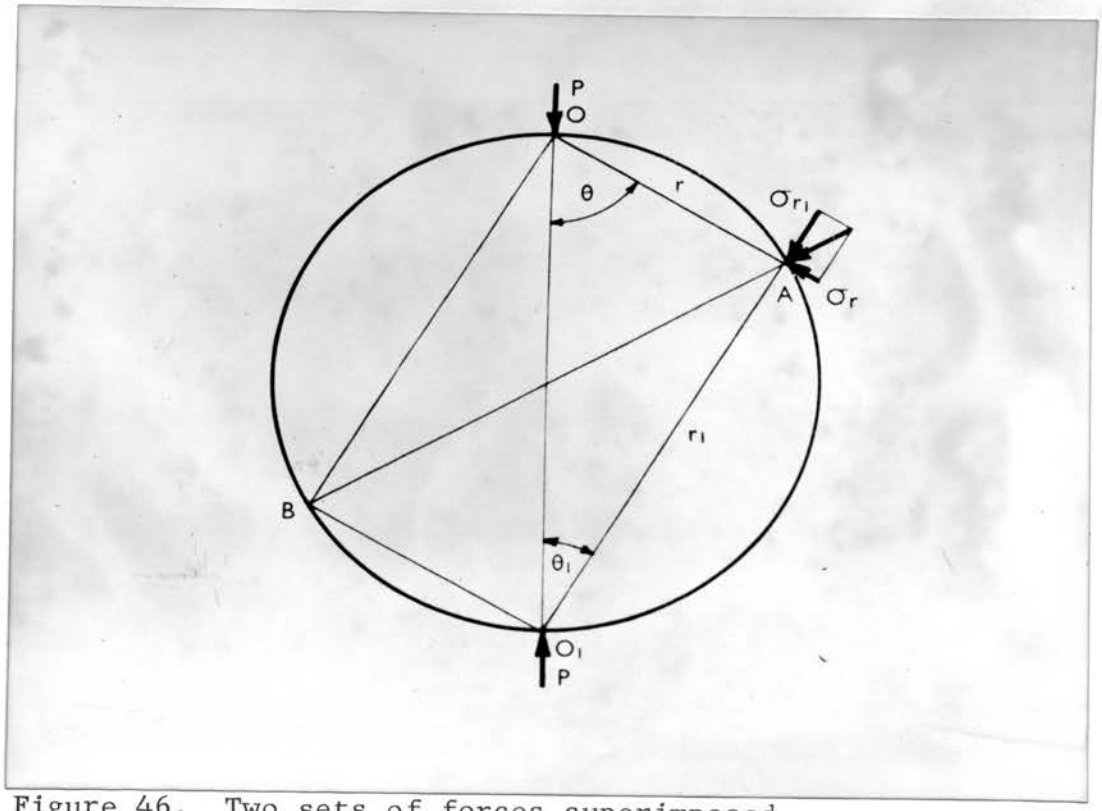

Figure 46. Two sets of forces superimposed.

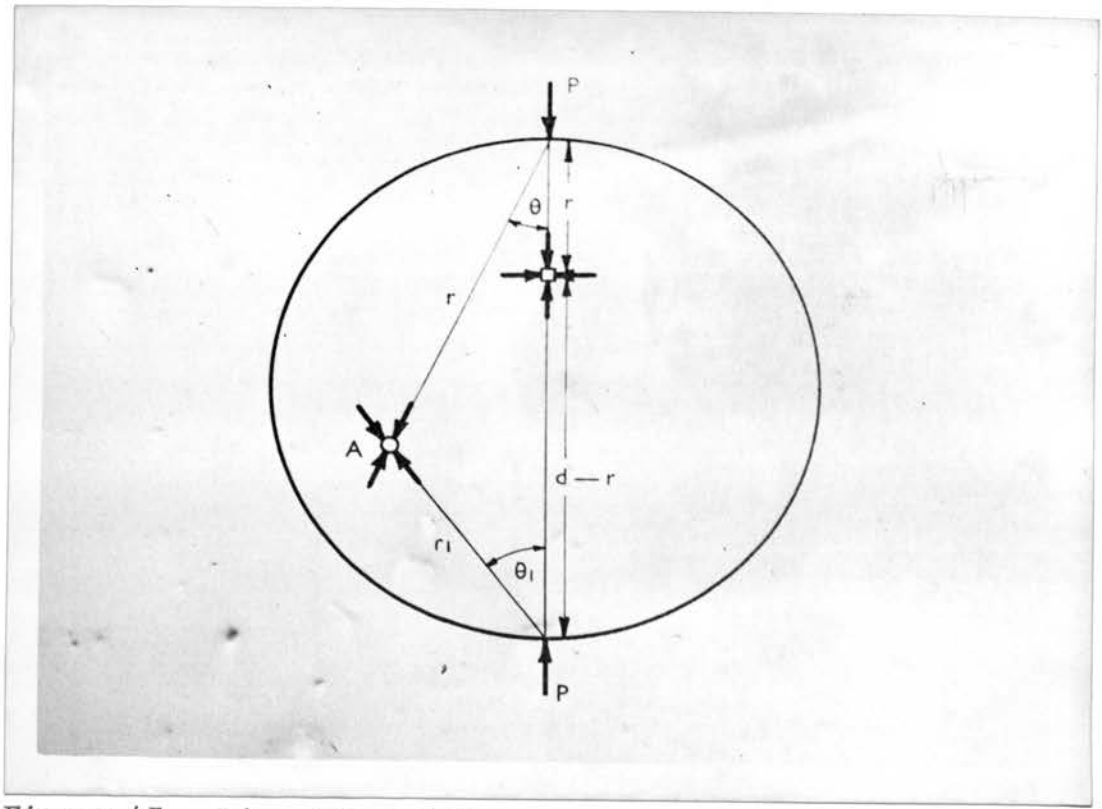

Figure 47. Disc subjected to two concentrated forces only.

and the horizontal stress component (tensile)

$$\sigma = \frac{2P}{\pi td}$$

By considering a cylinder of concrete as a number of such discs, we see that a uniform tensile stress is developed over the vertical diametral plane, and the value of this stress is $\frac{2}{\pi}\frac{P}{DL}$ where D and L are the diameter and length of the cylinder.

APPENDIX C

APPENDIX C

INVESTIGATION OF TYPES OF GLASS MOLDS FOR STUDY ON GLASS-CERAMICS

A. Steel Molds

A cylindrical steel mold was machined 4 inches long and 2 inches in diameter with a 5/8-inch hole in the center. The hole was drilled, reamed, and honed until a very smooth, shiny surface was produced on the walls of the hole.

After melting and fining the glass in one furnace, the steel mold, set on a steel plate, was placed in another furnace preheated to 500° C., and allowed to heat to that temperature (about 10 minutes). The mold was then removed from the furnace and the melted glass was poured into it. Then the mold was placed back in the 500° C. furnace, the glass rod was pushed out with a fused silica rod, and the mold was taken out for another pouring. In order to eliminate trapping bubbles in the glass while pouring, rods were poured in the mold while it was at angles ranging from straight up, standing on its end (90°) to lying nearly flat, on its side (0°). For pourings to be possible at low angles either a platinum spout had to be fitted in the end of the mold or a notch (half of the mold cut away along a diameter for 3/4-inch to 1 inch along its length) had to be machined in the mold at one end. Various mold lengths and pouring speeds were also tried in order to find a successful method of producing smooth, bubble-free glass rods which would consistently release from the mold and would not experience thermal cracking.

The steel molds created a very smooth-surfaced cylinder, but several serious drawbacks prevented their use for this study. For reasons not

completely understood, it was very difficult to pour the fined, molten glass into the steel molds without trapping air bubbles in the glass as it solidified. The best results with steel molds, in this respect, were obtained when the mold was lying at a very low angle, but the bubbles still could not consistently be eliminated.

Another major drawback of the steel molds was that, notwithstanding the precautions taken to avoid thermal shocking and cracking the cooling glass rod, this did occur frequently. When the glass rod cracks in the steel mold, it expands and is so tight in the mold that it cannot be taken out except by the tedious and mold-damaging process of beating it out with a hammer and steel rod. This process scars the inside surface of the mold so badly that it must be rehoned before it can be used again, which is not only time-consuming, but increases the size of the mold hole and, therefore, the diameter size of the finished glass rod.

Making stainless-steel molds of similar design was attempted by the Missouri School of Mines Research Center machine shop, but proved unsuccessful. The reaming operation (after drilling) apparently pushed the hard filings into the side of the hole wall, making it impossible to be honed smooth.

B. Vacuum Mold Techniques

In an attempt to solve the trapped air bubble problem, various devices were devised and experimented with which would draw the glass up into the mold from the crucible by means of a vacuum pump and glass and rubber tubing. The trial molds consisted of steel and stainless-steel tubing.

The vacuum mold devices which were attempted were essentially failures. The reasons for failing to find a successful vacuum mold technique

were, perhaps, legion. Some of these causes for failure were (a) the degree of vacuum could not be controlled with sufficient sensitivity to slowly draw the glass up to the desired point and hold it there until it was solid, (b) the steel tubing used did not act as a sufficient heat sink to draw away the heat from the melt fast enough to prevent the mold from "burning up" (oxidizing and melting), and (c) the level of the glass could not be seen or easily and safely determined.

APPENDIX D

APPENDIX D

THEORY OF OPTICAL CROSS AND CONCENTRIC CIRCLES[51]

In a discussion on oxide in copper, mention was made of the appearance of a dark cross and dark concentric circles. The cross has been noticed in almost all of those inclusions; the rings appear less frequently and are less contrasted.

Hoyt and Scheil[65] have observed this phenomenon; Figure 3 of their paper is an excellent example of a well developed pattern in a glassy silicate. They found that the cross remains stationary with respect to the cross hairs in the microscope when the stage is rotated. In other words, the orientation of the inclusion does not affect the production of the pattern. At any rate, it would not seem possible for a glassy silicate to possess directional properties; any explanation of the phenomenon must therefore not depend on anisotropic effects. Hoyt and Scheil also find that when these round inclusions are elongated by rolling the pattern is no longer developed.

These facts are therefore known: (1) The phenomenon does not depend upon the orientation of the inclusions; (2) isotropic substances such as cuprous oxide can also develop the pattern; (3) the shape of the inclusion is a determining factor. Globular inclusions produce the effects other shapes do not. Development of the theory has demonstrated that the cross and the concentric circles are produced by independent mechanisms.

The formation of the cross is directly dependent upon the focusing effect of a spherical surface for its production. For simplicity, a hemispherical shape of inclusion was selected. This inclusion is embedded in the surface of the metal, on which the microscope is focused. Figure 48

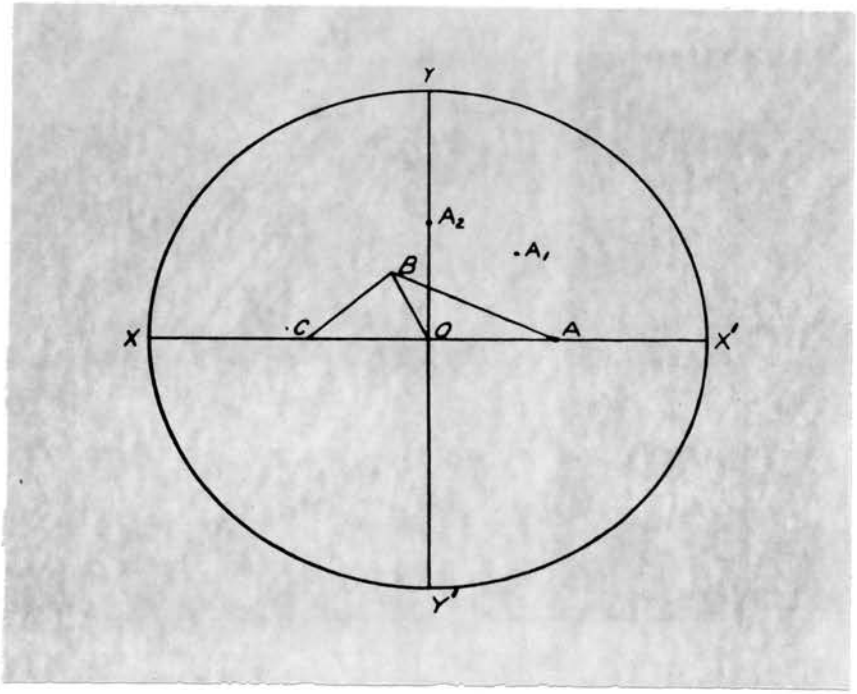

Figure 48. Surface of hemispherical, transparent inclusion in surface of metal.

represents a view of the inclusion as it is seen from above. O is the center of the figure; A represents a point chosen at random on the surface and is a point under observation on the surface. It is desired to find where on the surface the light that illuminates A can enter. BA is any ray of light reaching A and thus participating in the illumination of that point. B is the point at which the light is reflected from the metal-inclusion surface. OB is a normal from O to the point of reflection. The plane of reflection is therefore OAB. As the plane of incidence is always the same as the plane of reflection, the incident ray also lies in the plane OAB. Therefore, whether the light has suffered one, two, or more reflections from the bottom surface of the inclusion, the planes of incidence and reflection are always the same as OAB. When the light is traced backwards to the point at which it entered the surface, that point is on the trace of plane OAB on the surface of the inclusion, the line XOX'. The only light that can ever reach A must enter along the diameter on which A is located. If the particular ray BA had had only one reflection, it might have entered along the path CB.

In accordance with the theory of the formation of elliptically polarized light, the azimuth angle is the angle between the plane of incidence and the plane of polarization. If the azimuth angle is 0° or 90°, no elliptically polarized light can be formed regardless of the phase difference introduced between the parallel and perpendicular components by a reflection, because in these cases there is only one component. When the azimuth angle is 45°, the maximum amount of ellipticity is introduced by any phase difference.

If the plane of polarization is XOX', the light emitted from A or A_2 will still be plane polarized and will be absorbed by the analyzer.

A and A_2 will be relatively dark. A_1, with an azimuth angle of 45°, will be relatively bright.

Selecting points all over the surface, we find that those on XOX' and YOY' are dark; those between are in varying shades of lightness. The lightest are those at 45° to these directions. The resulting figure is the cross, which is observed.

Any roughness of the reflecting surface results in the partial or total destruction of the effect because of the random reflections introduced by this roughness. In the case of a void or gas pocket, the roughness would be greatest because the crystallization of the metal would be least interfered with. This would explain why the optical cross was not observed in voids. An inclusion that solidified above the melting point of the metal would result in the smoothest reflecting surface and the greatest clearness of the cross. Cuprite, which solidifies about 200° above the melting point of copper, gives very distinct optical crosses. An inclusion that solidified below the melting point of the metal would hinder the free crystallization of the metal less and might have a roughened reflecting surface after reflection, resulting in a milky appearance of the inclusion under crossed nicols. This might be the cause of the effect attributed by Hoyt and Scheil to calcium oxide or fluoride.

APPENDIX E

APPENDIX E

X-RAY DATA FOR β-SPODUMENE AND β-EUCRYPTITE*

β-Spodumene (positive)		β-Spodumene (negative)		β-Eucryptite	
d value	Relative Intensity	d value	Relative Intensity	d value	Relative Intensity
4.60	1	4.52	2	4.55	2
3.96	1	3.86	1	3.92	1
3.46	10	3.48	10	3.53	10
3.156	0.2	-	-	-	-
2.921	0.2	-	-	-	-
2.604	1	2.604	1	2.627	1
2.322	0.2	2.328	0.5	2.373	0.5
2.254	1	2.254	1	2.275	1
2.080	1.5	2.083	1	2.110	1
1.932	0.2	-	-	-	-
1.880	6	1.882	6	1.914	6
1.738	0.5	1.734	1	1.760	0.5
1.694	0.3	1.703	0.5	1.728	0.25
1.673	0.2	-	-	-	-
1.628	5	1.627	4	1.644	5
1.540	0.3	-	-	-	-
1.528	0.5	-	-	-	-
1.505	1	1.501	1	1.515	1
1.475	0.15	-	-	-	-
1.448	4	1.443	4	1.460	3.5
1.417	5	1.413	5	1.443	5
1.380	0.2	-	-	-	-
1.348	0.2	-	-	-	-
1.319	3	1.315	3	1.334	2
1.291	2.5	1.300	3	1.311	3
1.260	0.25	-	-	-	-
1.240	2.5	1.242	2	1.261	2
1.217	4	1.219	5	1.232	4
1.206	2.5	1.203	3	1.229	
1.182	0.25	-	-	-	-
1.167	0.20	-	-	-	-
1.156	0.15	-	-	-	-
1.136	3	1.136	2	-	-
1.126	1.5	1.125	2	-	-
1.062	0.5	1.062	1	-	-
1.057	2	1.057	3	-	-
1.033	0.3	1.032	0.25	-	-
1.015	1	1.014	2.5	-	-
1.007	0.5	1.007	0.5	-	-

*The values are in kX units.

VITA

Paul Darrell Ownby was born in Salt Lake City, Utah, on November 9, 1935. After receiving elementary school training at the Emerson public school, he attended the Roosevelt Jr. High School, and graduated from the East High School in 1954.

In April 1953, while still in high school, he joined the Utah Air National Guard, serving for eight years as a reservist in this and other Air Force Reserve units. He received his honorable discharge from the United States Air Force in March 1961.

During the year 1954-1955 he studied Chemical Engineering at the University of Utah. Re-entering the University of Utah in January 1958 after serving as a "Mormon" missionary in South Texas for two years, he continued his studies in Chemical Engineering until September 1959, at which time he changed his major to Ceramic Engineering. He received the Bachelor of Science Degree in Ceramic Engineering in June 1961.

From June 1959 to June 1960 he worked part-time and summers at Electro-Ceramics, Inc. (Salt Lake City, Utah), where he did the research work for his B.S. thesis. He worked as a Ceramic Engineer in the research laboratories of the Sprague Electric Company, North Adams, Mass., from June through August 1961. In September of that year he entered the graduate school of the University of Missouri, School of Mines and Metallurgy, as the Kaiser Aluminum and Chemical Corporation's Ceramic Research Fellow.

He is a member of the American Ceramic Society, Keramos, Sigma Gamma Epsilon, and an associate member of the Society of the Sigma Xi.